MODELING OF ICE-STORAGE SYSTEMS

by

TODD BRYANT JEKEL

A thesis submitted in partial fulfillment
of the requirements for the degree of

MASTER OF SCIENCE
(Mechanical Engineering)

at the

UNIVERSITY OF WISCONSIN -- MADISON

1991

Abstract

The work documented in this thesis presents the modeling of a static ice-on-coil ice-storage tank and a method of minimizing the cooling load for a constant air volume air-conditioning system. The ice-storage model is based on basic heat transfer relationships and analysis. Both the charging and discharging periods of tank operation are modeled and compared with manufacturer's performance data. The agreement for the charging period is within 12% and the discharging period is within 10% of the manufacturer's performance data. In addition, an effectiveness method for both the latent charging period and discharging period of tank operation was presented as a function of tank flow rate, capacity, and inlet brine temperature.

The minimization of the air-conditioning load for a constant air volume system was accomplished by mixing some of the relatively warm return air flow rate with the outlet from the cooling coil to reduce the sensible reheat. Although the air-conditioner must operate at a lower temperature (and coefficient of performance) in order to meet both the sensible and latent loads on the space a decrease in air-conditioner power is still realized. Rules for selecting the fraction of the return air flow that should be mixed with the outlet from the cooling coil is a function of the total space load, the sensible heat ratio

of the space load, the space set-point, and the circulation flow rate of air were determined.

The combination of the variable flow system and ice-storage was investigated and compared to the variable flow system without ice-storage and the convention system with and without ice-storage. The result was that the systems with ice-storage required smaller chillers and less peak time energy use than the systems without storage, and the variable flow systems required smaller chillers than the corresponding constant air volume systems.

Acknowledgements

This is the day I've been waiting for since I started writing: THE LAST DAY! The past few weeks have been awful: finishing up class work _and_ my thesis; explaining to Lisa that I won't be home tonight; and explaining to my dog, Indy, that I can't play fetch with him. This is the time to thank all of the people that I neglected in the past month. Thank you Lisa for the love and support that you gave me, I couldn't have done it without you. Thank you Mom and Dad for the opportunities you have given me. And thank you Indy for always being excited to see me when I came home.

I also would like to thank my advisors: Sanford Klein and John Mitchell. Thanks for the advice and encouragement you gave me when everything seemed so insignificant and insurmountable. Thanks also to Chuck Dorgan, who brought insight into how things are done in the "real world."

And to everyone I have met at the Solar Lab: Thank you! You have all contributed to this thesis. Thanks especially to Dean Tompkins and Doug Reindl, both of whom spent countless hours listening and giving advice. Thanks also to the Beckman's and Klein's for the wonderful parties and hospitality.

v

Table of Contents

Chapter One

Introduction

Chapter 2

Ice-Storage Tank Model Description and Characteristics

Chapter 3

Minimization of Air-conditioning Cooling Load

Chapter 4

Simulations and Results

Chapter 5

Conclusions and Recommendations

List of Tables

List of Figures

Chapter One

Chapter Two (continued)

Chapter Three

Chapter Three (continued)

Chapter Four

Nomenclature

Roman Symbols

Symbol	Definition
A	area
AR	ratio of actual to unconstrained area
C_p	specific heat at constant pressure
C_v	specific heat at constant volume
COP	coefficient of performance
D	diameter
f	correction factor for constrained heat conduction
f	fraction of nominal chiller capacity
$FEHT$	finite element heat transfer program
h	heat transfer coefficient
i	enthalpy
k	thermal conductivity
L	length

Roman Symbols (continued)

Symbol	Definition
m	mass
$\dot{m}$	mass flow rate
MBD	mean bias difference
N_{ice}	number of hours to charge the ice-storage tank
N_{load}	number of hours of space load
N_{tube}	number of tubes in ice-storage tank
NCC	nominal chiller capacity
Nu	Nusselt number
$NMBD$	normalized mean bias difference
$NRMSD$	normalized root mean square difference
Pr	Prandtl number
$\dot{Q}$	heat transfer rate
Ra	Rayleigh number
Re	Reynolds number
$RMSD$	root mean square difference
t	time
t	thickness
T	temperature
T_{amb}	ambient temperature
T_s	surface temperature
TB	blended outlet temperature

Roman Symbols (continued)

Symbol	Definition
$TRNSYS$	transient simulation program
$u_{i,f}$	latent heat of fusion
U	total internal energy
U_{tot}	total conductance
UA	conductance-area product
UA_{tank}	conductance-area product of the ice-storage tank
x	position along length of tube

Greek Symbols

Symbol	Definition
ε	effectiveness
Δ	change
ρ	density
ω	humidity ratio

Subscripts

Symbol	Definition
a	air
act	actual
b	brine

Subscripts (continued)

Symbol	Definition
circ	circulation
crit	intersection of advancing ice or water formations
i	ice
i	in, inside
L	latent
lm	log-mean
o	out, outside
RH	reheat
S	sensible
sat	saturated
set	set-point
sup	supply state
t	tube
t	tank
t-w	tube to water
tot	total
vent	ventilation
w	water
w-i	water to ice
x	position

Superscripts

Symbol	Definition
(1)	new estimate
(0)	old estimate

Chapter One

Introduction

The use of ice-storage systems for air-conditioning applications is of extreme importance due to the increase in peak load power from residential and industrial air-conditioning. Utility companies are beginning to offer variable rate structures that discourage energy use during peak times of the day. These structures make ice-storage systems more economically feasible.

1.1 Scope of study

A mechanistic model was developed to simulate the time dependent performance of the static ice-on-coil ice-storage tank . The buildup of ice on the outside of the tubes of an ice-on-coil storage tank dictates that the performance of the tank is a function of the resident storage capacity and thus a function of time. The model utilizes basic heat transfer relationships and analysis to solve for the rate of heat transfer. Both the charging and discharging periods of tank operation were modeled and compared with manufacturer's performance data.

The reduction of the cooling load by minimization of sensible reheat will be developed and integrated with the sizing of ice-storage systems. A controller was developed to determine the optimum fraction of circulation flow that should be processed

by the air-conditioner. The minimization of reheat requires that the outlet temperature of the cooling coil be lower than for the conventional system. The effect that these lower temperatures have on the sizing of the ice-storage tank will be investigated.

1.2 Ice-storage tank configurations

There are several configurations of the ice tank and chiller loop, the first is the parallel configuration of the tank and the chiller, the second is the series configuration with the chiller downstream of the ice tank, and the third is the series configuration with the chiller upstream of the ice tank [1].

The parallel configuration connects the chiller and ice tank in parallel. Since the inlet to the chiller is at the return state from the cooling coil, the operating temperature, and correspondingly the coefficient of performance (COP), is relatively high. The disadvantage is the complexity of piping and control. The parallel configuration is shown in Fig. 1.1.

The series configuration with the chiller downstream is shown in Fig. 1.2. The disadvantage of this configuration is that the chiller is required to operate at relatively low temperatures (ice tank outlet temperature). These low temperatures reduce both the capacity and the COP of the chiller.

The series configuration with the chiller upstream (shown in Fig. 1.3) will be considered throughout this work because of the advantage of operating the chiller at a relatively higher temperature and utilizing the low temperature of the ice tank to bring the brine temperature down to the desired temperature. Although the parallel configuration of the chiller and ice tank also takes advantage of the higher operating temperature, the piping and control is more complicated than the series configuration.

Temperature
controlled
valve

Flow rate
of air

Pump

Flow Direction

Chiller

Heat
Exchanger

Ice
Storage
Tank

Fig. 1.1 Parallel configuration of chiller and ice tank.

Pump

Chiller

Flow rate
of air

Flow Direction

Temperature
controlled
valve

Heat
Exchanger
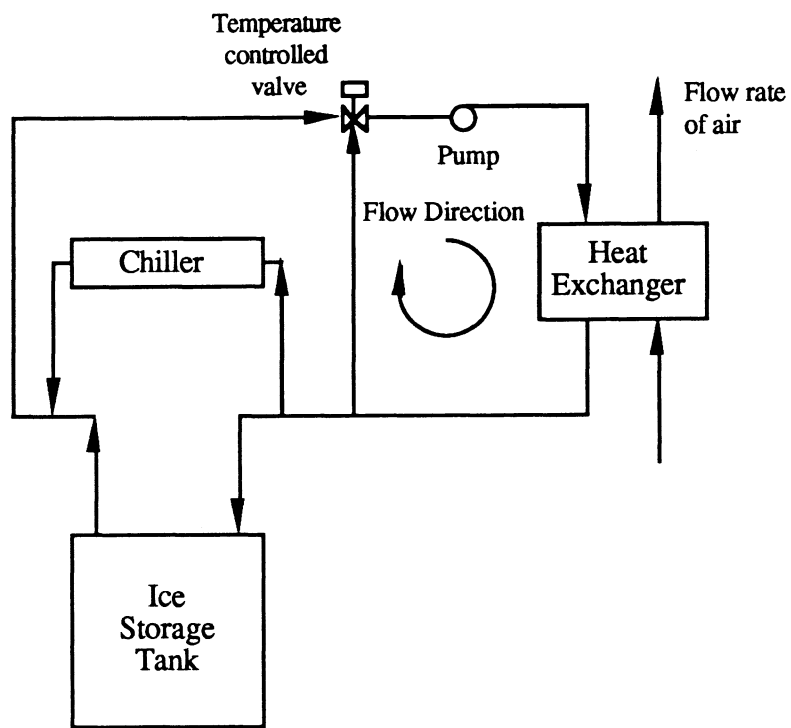
Ice
Storage
Tank
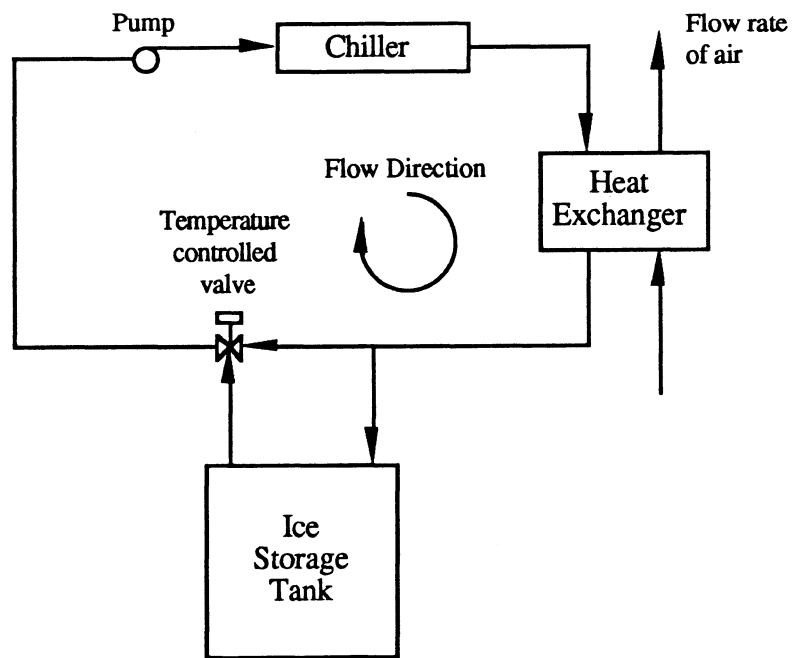
Fig. 1.2 Series configuration of chiller and ice tank with the chiller downstream.
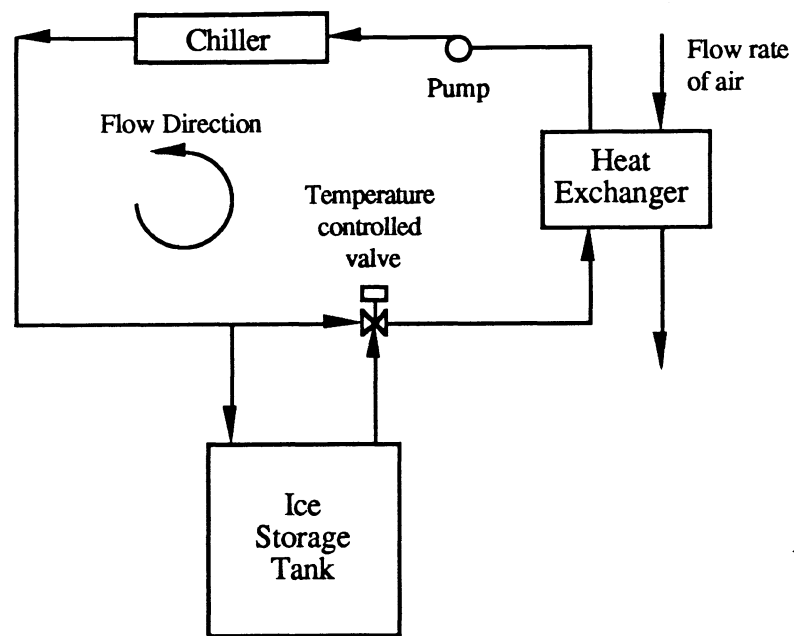
Fig. 1.3 Series configuration of chiller and ice tank with the chiller upstream.

1.3 Ice-storage tank control strategies

There are two major control strategies for the discharging of the ice tank: the partial storage and the full storage strategy. The partial storage control strategy utilizes the ice tank to meet the portion of the load that the chiller cannot meet and the full storage control strategy utilizes the ice tank for the entire cooling load.

The load profile for the partial storage control strategy is shown in Fig. 1.4. During the day the chiller is run at its maximum capacity and the ice tank load fluctuates to meet the rest of the cooling load. If the cooling load is less than or equal to the capacity of the chiller, the chiller is used to meet the entire cooling load; the use of the chiller in this way is called chiller priority. During the night the chiller is used to charge the ice-storage tank. The chiller size is determined such that on the design day the loads can be met during the day and the ice-storage tanks can be charged at night.
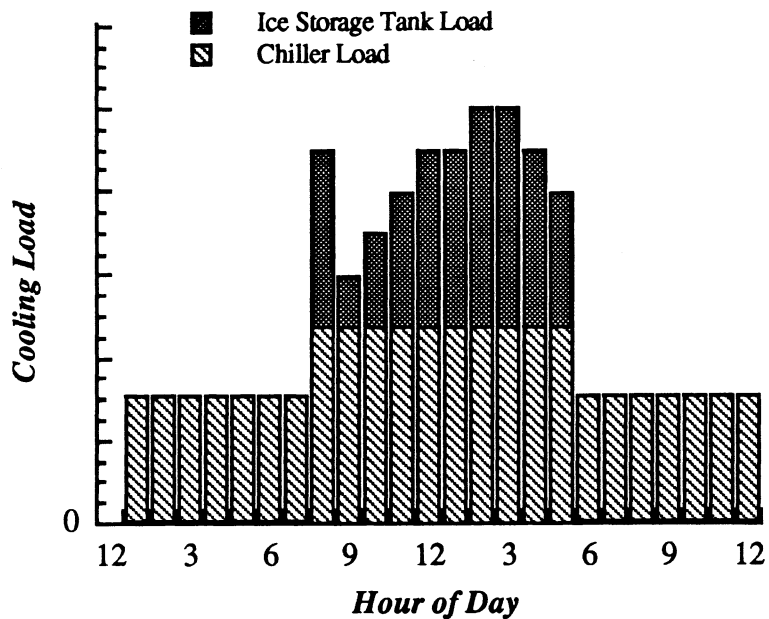
Fig. 1.4 Loads on the ice tank and chiller for partial storage strategy.
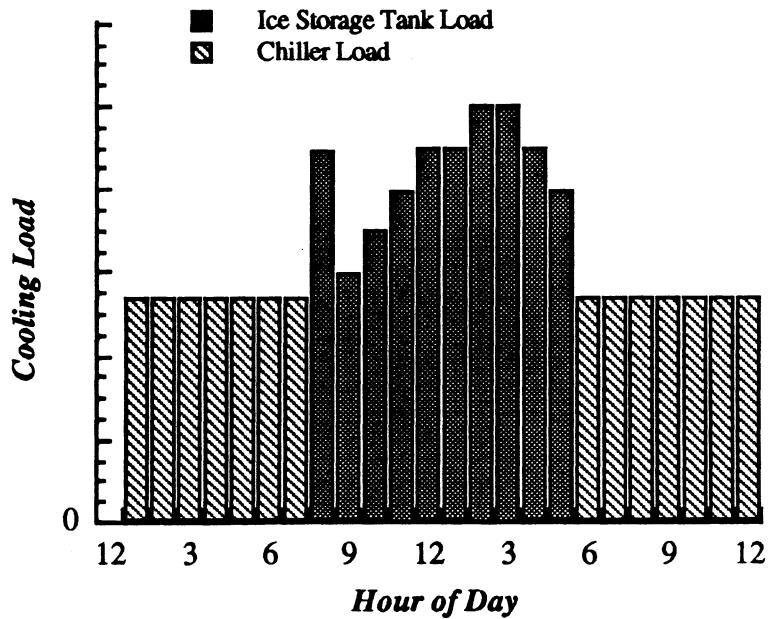
Fig. 1.5 Loads on the ice-storage tank and chiller for full storage strategy.

The load profile for the full storage control strategy is shown in Fig. 1.5. This strategy uses the ice tank to meet the entire load on the space during the day. The required chiller size is larger than the partial strategy but smaller than the conventional system, and the number of ice-storage tanks is larger than the partial storage system.

The partial storage strategy with chiller priority will be used throughout this work because of the advantage of reduced chiller size and number of ice-storage tanks.

1.4   Conventional air-conditioning systems

The basic conventional constant air volume (CAV) air-conditioning system consists of a cooling coil, a reheat coil, and a load. The system is shown in Fig. 1.6. A fraction of the return air flow rate from the space is recirculated through the system and the rest is exhausted to the ambient. The ventilation air flow rate is mixed with the recirculated return air and cooled to the supply state (S) required by the space loads.
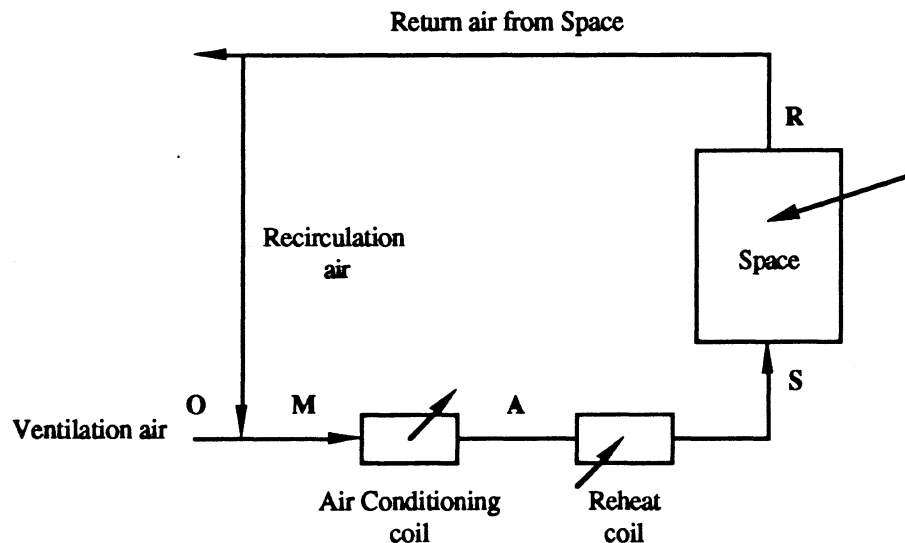
Fig. 1.6 The conventional CAV air-conditioning system.

The latent load on the space usually requires a lower outlet temperature from the coil than the sensible load. Therefore, if the latent load is met, the CAV system usually requires large amounts of sensible reheat in order to deliver the required supply temperature to the space.

The variable air volume (VAV) air-conditioning system eliminates the reheat by varying the circulation flow rate. The VAV system is identical to the CAV system shown in Fig. 1.6 except there is no reheat coil on the VAV system. The amount of mass flow rate through the system is determined from the space set-point, the sensible load on the space, and the desired supply temperature [2].

$$\dot{m}_{circ} = \frac{\dot{Q}_{sens}}{C_{p,a}(T_{set} - T_{sup})}$$
(1.1)

Since the desired supply temperature and the space set-point temperature are chosen in the design of the system and the sensible load determines the mass flow rate through the system, there is the potential that the latent load may not be met. In other words, the humidity of the space will float. The VAV system is not an option if both the sensible and latent loads on the space must be met.

Since the VAV system does not require that both the sensible and latent loads be met, it will not be considered in this work. The CAV system will be investigated and methods for minimizing the reheat will be presented.

1.5 Organization

The main body of the thesis is presented in Chapters 2 through 4. The mechanistic modeling and validation of the ice-storage tank is presented in Chapter 2. The methods for reduction of cooling coil load is presented in Chapters 3. Chapter 4

investigates the sizing of conventional and ice-storage systems with the load reduction techniques described in Chapter 3, and integrates the ice-storage tank model and the reduction of cooling load control to investigate the effect on the sizing of ice-storage systems.

References 1

1. *Levload Ice Bank Performance Manual*, Product Literature, Calmac Manufacturing Corporation, Englewood, New Jersey, April 1987.

2. Mitchell, J. W., *Energy Engineering*, John Wiley & Sons, New York, 1983.

Chapter Two

Ice-Storage Tank Model Description and Characteristics

A model was developed for static ice-storage tanks for both charging and discharging periods using basic heat transfer analysis. This chapter describes the assumptions used in the modeling, presents the characteristics of the charging and discharging periods, and validates the model with performance data. The model was used to develop an effectiveness model for the discharging period of tank operation.

2.1 Tank description

The tank model simulates the charging and discharging of an internal melt, ice-on-coil tank, with a working fluid with finite capacitance (e.g. aqueous solutions of ethylene glycol (brine)). The ice-on-coil tank incorporates a large number of small tubes to effectively transfer the heat from the storage medium (ice) to the transport fluid (brine) and provide a large surface area per ton of storage. During the charging period, cold brine is circulated through the tubes and ice is built on the outside of the tubes. During the discharging period, relatively warmer brine is circulated through the same tubes and ice is melted around the tubes, thus the name internal melt. The large number of small tubes allows the ice-storage tank to be fully charged with ice.

2.2 Tank modeling

The governing differential equations and heat transfer modeling of the tank are presented for the charging and discharging periods of tank operation. The assumptions and the method of solution will be presented for each period of tank operation.

2.2.1 The governing equations

The governing equations for the ice-storage tank considered are derived from an energy balance on the contents of the tank and the heat transfer rate equations. The system is defined as the water and ice in the tank. An energy balance on the system produces the following differential equation.

$$\dot{Q}_b + \dot{Q}_{gain} = \frac{dU}{dt} = m\frac{\partial u}{\partial t} + u\frac{\partial m}{\partial t}$$

(2.1)

$\dot{Q}_b$ is the heat transfer rate from the brine to the system, $\dot{Q}_{gain}$ is the heat transfer rate from the ambient to the system, and U is the total internal energy of the ice and water in the tank. The rate of change of the internal energy of the storage media can be broken down into the sum of three terms (Eq. (2.1a)): 1) the latent internal energy change due to the phase change, 2) the sensible internal energy change of the ice, and 3) the sensible internal energy change of the water.

$$\dot{Q}_b + \dot{Q}_{gain} = -u_{i,f}\frac{dm_i}{dt} + m_i C_{v,i}\frac{dT_i}{dt} + m_w C_{v,w}\frac{dT_w}{dt}$$

(2.1a)

The heat transfer rate is positive into the system. The conductance area product of the tank is assumed constant; therefore, the heat transfer rate from the ambient to the tank is the following:

$$\dot{Q}_{gain} = UA_{tank}(T_{amb} - T_t)$$

(2.2)

where T_t is the temperature of the storage media, and T_{amb} is the ambient temperature. The gain from the ambient is assumed to effect the ice growth on each tube.

The internal energy change of the system is the sum of the latent and sensible change in the ice and the sensible change in the water. The latent change of the ice is the product of the heat of fusion of the water, $u_{i,f}$, and the rate of change in the mass of the ice, dm_i/dt. The sensible change of the ice is the product of the mass of the ice, m_i, the specific heat of the ice, $C_{v,i}$, and the rate of change of the temperature of the ice, dT_i/dt. The sensible change of the water is the product of the mass of water, m_w, the specific heat of the water, $C_{v,w}$, and the rate of change of the temperature of the water, dT_w/dt.

An energy balance on the brine in a differential length of tube produces the following differential equation.

$$\dot{m}_b \, C_{p,b} \, \frac{dT_b}{dx} = \frac{\dot{q}_{b,x}}{L_t}$$ (2.3)

where $\dot{m}_b$ is the mass flow rate of brine through one tube, $C_{p,b}$ is the specific heat of the brine, T_b is the temperature of the brine, and $\dot{q}_{b,x}$ is the heat transfer rate as a function of x, the variable along the length of one tube, L_t.

Assuming that the conductance is constant along the length of the tube and the rate of sensible energy change of the storage media is small compared to the total heat transfer rate, the heat transfer rate between the storage media and the brine can be simplified to the following:

$$\dot{q}_{b,x} = UA \, (T_s - T_{b,x})$$ (2.4)

where UA is the conductance area product for a single tube between the brine and the the selected surface for the analysis, $T_{b,x}$ is the brine temperature at x, and T_s is the

temperature of the selected surface for the analysis and is assumed constant along the length of the tube. For example, T_s for the charging process is the temperature of the water in the tank. The temperature of the brine at any position can be determined by substituting Eq. (2.4) into Eq. (2.3) and integrating.

$$T_{b,x} = T_s + (T_{b,i} - T_s) \exp\left(\frac{-UA\,x}{\dot{m}_b C_{p,b}\, L_t}\right)$$

(2.5)

where $T_{b,i}$ is the inlet brine temperature. Assuming that the selected surface temperature is constant over the length of the tube and integrating the temperature of the brine over the length of the tube gives the average driving force for the heat transfer, also known as the log-mean-temperature difference.

$$\Delta T_{lm} = \frac{(T_{b,o} - T_s) - (T_{b,i} - T_s)}{\ln\left((T_{b,i} - T_s)/(T_{b,o} - T_s)\right)}$$

(2.6)

$T_{b,o}$ is the outlet brine temperature from the tank. Utilizing ΔT_{lm}, the heat transfer rate between the brine and the selected surface is the following:

$$\dot{Q}_b = UA\, N_{tube}\, \Delta T_{lm}$$

(2.7)

The above equations are the governing equations for both the charging and discharging periods of tank operation, any additional simplifications will be explained in section pertaining to the specific mode of tank operation.

2.2.2 Charging Model

The charging analysis will be split into three periods: 1) sensible charging, 2) unconstrained latent charging, and 3) constrained latent charging. Sensible charging is the process of reducing the tank water temperature to the freezing point. Whenever the

tank is discharged such that the water temperature is above the freezing point, the tank must be sensibly charged before ice will be built on the tubes. Unconstrained latent charging is the period when ice builds on the tubes, but the ice formations on adjacent tubes do not intersect. Once the formations touch, the area available for heat transfer is constrained, thus the name constrained latent charging. The constrained charging period is characterized as a sharp decrease in charging rate due to the reduced area for heat transfer and the increase in heat flow path length.

2.2.2.1 Assumptions

A computationally simple model was desired for ease and speed of calculations. The model is characterized by a long, horizontal tube with convection to both the inside and outside walls. The tubes are spaced on a square grid, and no heat transfer between adjacent tubes is considered. The ice growth is assumed to be uniform along the length of the tube; therefore, the conductance is assumed to be constant over the entire length of the tube.

2.2.2.2 Model inputs

The model requires both a geometric and a thermal description of the tank. The geometric description includes the tube inside and outside diameters, length, center-to-center spacing, and number. The thermal description includes the inlet brine temperature and volume flow rate, the initial water temperature, the initial latent storage percentage on the tubes, the desired final storage percentage, and the conductance-area product for the tank. The initial latent storage percentage on the tubes pertains to the amount of ice that has already been built on the tubes. The desired final storage percentage is the percentage of storage capacity when the charging period is to be stopped.

2.2.2.3 Sensible charging

The sensible charging period lowers the temperature of the water to the freezing temperature. It is assumed that no latent charging occurs in this period. During this period the charging rate is affected by the temperature of the water due to the decrease in driving force for heat transfer as the temperature of the tank decreases; therefore, in order to simulate the transient response of the tank the model must solve the governing differential equation (Eq. (2.1)) to determine the new water temperature. Since there is no ice building in this period, the governing differential equation simplifies to the following:

$$\dot{Q}_b + \dot{Q}_{gain} = m_w \, C_{v,w} \frac{dT_w}{dt} \qquad (2.8)$$

The heat transfer rate from the brine to the water, $\dot{Q}_b$, is negative because it is directed out of the system (water).

The overall conductance between the brine and the water based on the outside area of one tube, $A_{t,o}$, is given in the following equation:

$$U_{tot} = \left[\frac{A_{t,o}}{A_{t,i} \, h_b} + \frac{A_{t,o} \ln (D_{t,o}/D_{t,i})}{2 \, \pi \, k_t \, L_t} + \frac{1}{h_w} \right]^{-1} \qquad (2.9)$$

where $A_{t,i}$ is the inside surface area of one tube, $D_{t,i}$ and $D_{t,o}$ are the inside and outside tube diameters respectively, h_b and h_w are the heat transfer coefficients of the brine and water respectively, and k_t is the thermal conductivity of the tube. The first term in Eq. (2.9) represents the convective resistance inside the tube, the second term represents the resistance of the tube, and the third term is the convective resistance outside the tube.

The heat transfer coefficient inside the tube, h_b, was determined using the Dittus-Boelter [1] correlation for turbulent flow in a circular tube.

$$\overline{Nu}_D = 0.023\ Re_D^{4/5}\ Pr^{4/10} \tag{2.10}$$

where the average Nusselt number based on the inside diameter of the tube is defined as follows:

$$\overline{Nu}_D = \frac{h_b D}{k} \tag{2.11}$$

The heat transfer coefficient of the water, h_w, was determined using the Churchill and Chu [1] correlation for free convection from a long, horizontal tube. Flow inversion due to the water passing through its maximum density is neglected; however, the bulk thermal compressibility of water, β_w, is a function of the average water temperature and a decrease in performance will be realized at the maximum density.

$$\overline{Nu}_D = \left\{0.60 + \frac{0.387\ Ra_D^{1/6}}{\left[1 + (0.559/Pr)^{9/16}\right]^{8/27}}\right\}^2 \qquad 10^{-5} < Ra_D < 10^{12} \tag{2.12}$$

The mean Nusselt number is based on the outside diameter of the tube. The temperature, T_s, used in several of the governing equations is the average water temperature in the tank.

The method for solving the governing equations is as follows:

1) determine the total conductance between the brine and the water (Eq. (2.9)),

2) determine the outlet brine temperature (Eq. (2.5)),

3) determine the log-mean-temperature difference (Eq. (2.6)),

4) determine the heat transfer rate from the water to the brine (Eq. (2.7)),

5) determine the new average water temperature from the differential equation ((Eq. 2.8))

This process is repeated until the new estimate of the tank temperature is unchanged.

2.2.2.4 Unconstrained latent charging

During the unconstrained latent charging period, the charging rate is affected by the amount of ice on the tubes. In order to simulate a transient response of the ice tank, the governing differential equation (Eq. (2.1)) must be solved to determine the new ice thickness. The heat transfer is one-dimensional in cylindrical coordinates.
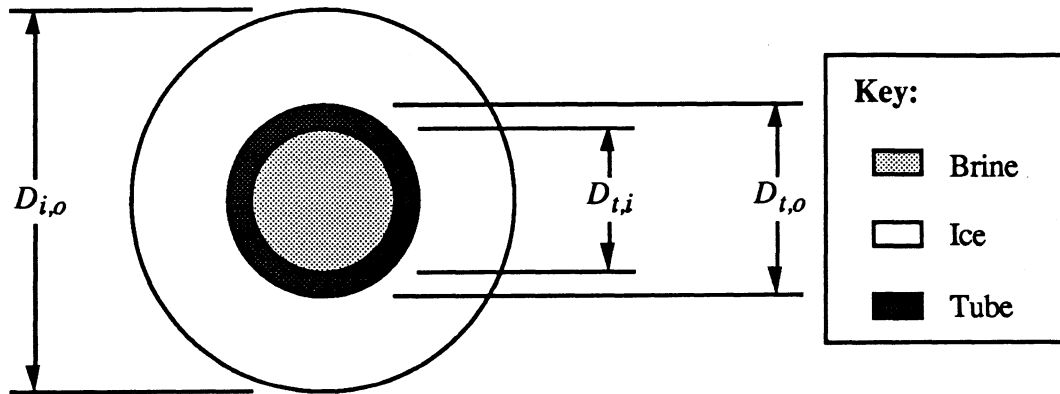
Fig. 2.1 Unconstrained charging geometry and nomenclature.

The governing differential equation can be simplified by showing that the internal energy changes of the water and the ice are small relative to the energy involved in the phase change. These internal energy changes are small due to the small temperature difference between the ice and the working fluid. For the ice tank considered ($m_i \approx 13,500$ lb), the sensible storage of the ice is less than 4% of the latent capacity if the ice is subcooled to 20 °F. In addition, since ice does not build on the tubes until the average water temperature is at the freezing point, the sensible energy change of the water is zero. Therefore, the simplified energy balance is

$$\dot{Q}_b + \dot{Q}_{gain} = - u_{i,f} \frac{dm_i}{dt} \qquad (2.13)$$

The overall conductance between the brine and the storage medium based on the outside area of the ice, $A_{i,o}$, is as follows,

$$U_{tot} = \left[\frac{A_{i,o}}{A_{t,i}\, h_b} + \frac{A_{i,o}\, \ln\left(D_{t,o}/D_{t,i}\right)}{2\, \pi\, k_t\, L_t} + \frac{A_{i,o}\, \ln\left(D_{i,o}/D_{t,o}\right)}{2\, \pi\, k_i\, L_t} + \frac{1}{h_w} \right]^{-1} \tag{2.14}$$

where $D_{i,o}$ is the outer diameter of the ice shown in Fig. 2.1, and k_i is the thermal conductivity of the ice. The second to last term in Eq. (2.14) is the resistance of the ice that is formed on the outside of the tubes. The heat transfer coefficients are calculated using the same correlations as in the sensible charging period (Eqs. (2.10) and (2.12)). The temperature, T_s, for the unconstrained latent charging period is the average temperature of the water, which is constant at 32 °F.

A new outside ice diameter can be determined explicitly by solving the governing differential equation for the differential change in mass of ice of the system,. Since the ice geometry is cylindrical, the new ice diameter can be found using the following equation

$$D_{i,o}^{(1)} = \sqrt{D_{i,o}^{(0)2} + 4\, \frac{dm_i}{dt}\, \Delta t \Big/ \left(\pi\, \rho_i\, L_t\, N_{tube}\right)} \tag{2.15}$$

where $D_{i,o}^{(0)}$ and $D_{i,o}^{(1)}$ are the old and new outside diameter of the ice respectively, Δt is the time step, and ρ_i is the density of the ice.

The governing equations are solved with the following method: 1) determine the total conductance between the brine and the water (Eq. (2.14)), 2) determine the outlet brine temperature (Eq. (2.5)), 3) determine the log-mean-temperature difference (Eq. (2.6)), 4) determine the heat transfer rate from the water to the brine (Eq. (2.7)), 5) determine the rate of change of the mass of ice from the differential equation

(Eq. (2.13)), 6) determine the new estimate for the outside ice diameter (Eq. (2.15)), and repeat steps 1 - 6 until the new estimate of the ice diameter is unchanged.

2.2.2.5 Constrained latent charging

The constrained latent charging period starts when the ice formation diameter is equal to the tube spacing. The center-to-center tube spacing will be referred to as the critical diameter. The heat transfer rate decreases because the heat transfer area decreases and the length that the heat must travel increases. These two factors are shown in Fig. 2.2.
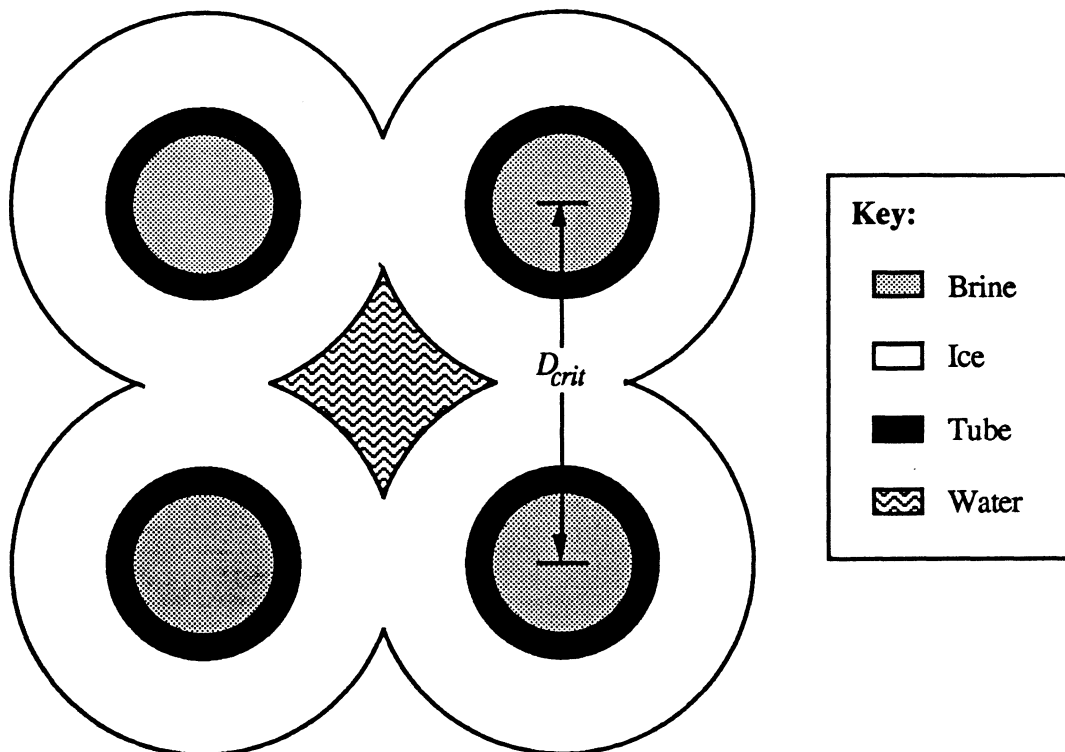
Fig. 2.2 Constrained charging geometry and nomenclature.

The heat transfer is no longer one dimensional and the boundary conditions are complicated; therefore, it cannot be solved analytically. Cummings [2] performed an

analysis to determine the thermal resistance for a specific geometry, but not for a range of geometries. In order to analyze this two-dimensional geometry, a finite element heat transfer program, FEHT [3], was used to numerically determine the heat transfer rates. The symmetry of the problem allows the model input to the program to be as shown in Fig. 2.3. Since the brine flowing through the adjacent tubes is assumed to be at the same temperature, the intersection of the ice formations are adiabatic.
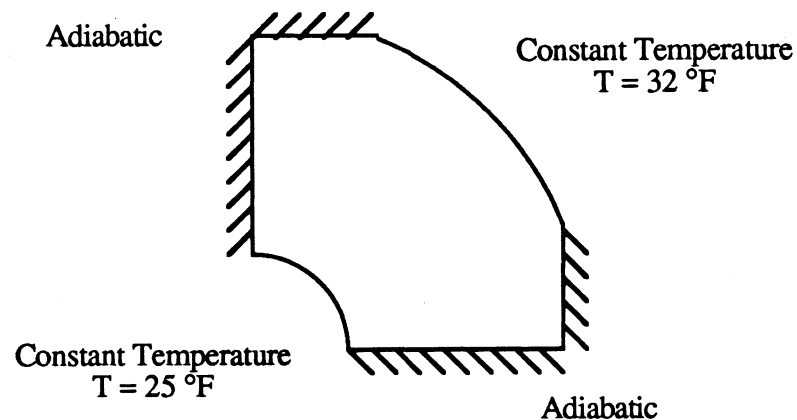
Fig. 2.3 Finite element model geometry and boundary conditions.

The heat transfer rate was determined for a range of tube diameter to tube spacing ratios of 0.1 to 0.8. From the results of the finite element analysis a correction factor was developed to correct the analytically obtainable one-dimensional heat transfer rate for the two-dimensional effects.

$$f = \frac{\dot{Q}_{act}}{\dot{Q}_{crit}}$$

(2.16)

$\dot{Q}_{act}$ is determined from the finite element analysis and $\dot{Q}_{crit}$ is determined from analytic solution in cylindrical coordinates at the critical diameter. A graph of the resulting correction factors is shown in Fig. 2.4.
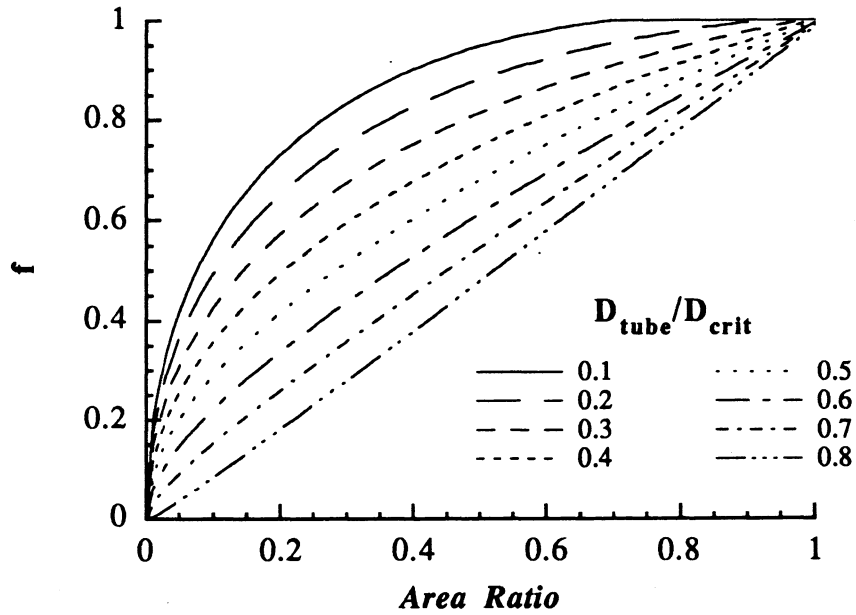
Fig. 2.4 Correction factor, f, as a function of the area ratio and the ratio of the outside tube diameter and the critical diameter.

These results were correlated with non-dimensional geometric variables to obtain the following equation.

$$f = -1.441\,AR + 2.455\,\sqrt{AR} + \frac{D_{t,o}}{D_{crit}}\,(3.116\,AR - 3.158\,\sqrt{AR}) \tag{2.17}$$

AR is the ratio of the actual heat transfer area to the area that would be available if the area were not constrained. An analysis of the geometry in Fig. 2.2 results in Eq. (2.18). The area ratio is a function of the ratio of the outside diameter of the ice formation to the critical diameter, $D_{i,o}/D_{crit}$ as shown in Fig. 2.5.

$$AR = 1 - \frac{4}{\pi}\cos^{-1}\left(\frac{D_{crit}}{D_{i,o}}\right) \tag{2.18}$$
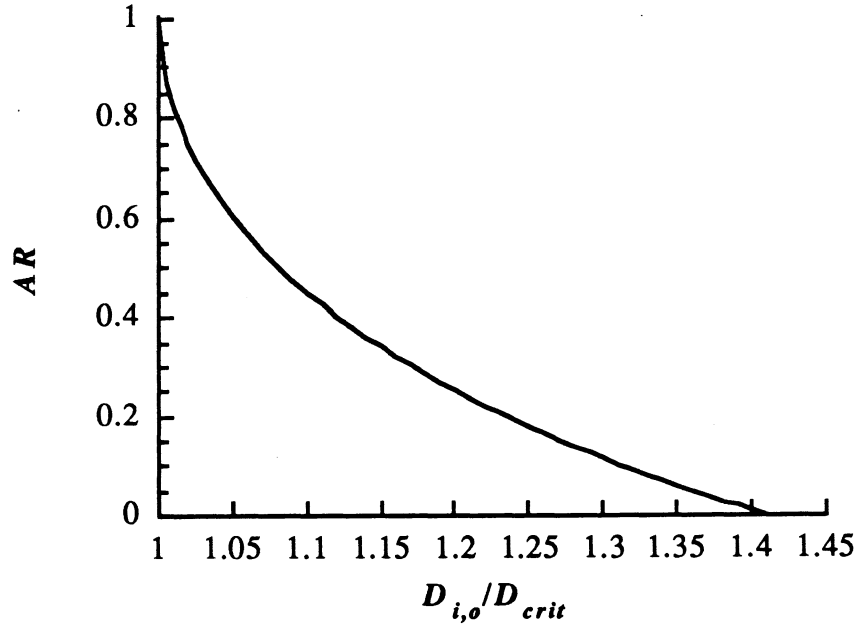
Fig. 2.5 Area ratio after heat transfer area is constrained.

The correction factor, **f**, is a function only of geometric quantities, and is used to modify the conductance of the ice at the critical diameter.

$$U_{tot} = \left[\frac{A_{i,o}}{A_{t,i}\, h_b} + \frac{A_{i,o}\, \ln\left(D_{t,o}/D_{t,i}\right)}{2\, \pi\, k_t\, L_t} + \frac{A_{i,o}\, \ln\left(D_{crit}/D_{t,o}\right)}{2\, \pi\, k_i\, L_t\, f} + \frac{1}{h_w} \right]^{-1}$$

(2.19)

where

$$A_{i,o} = \pi\, D_{i,o}\, L_t\, N_{tube}\, AR$$

(2.20)

The heat transfer coefficient of the brine is determined by using Eq. (2.10); however, the heat transfer coefficient of the water, h_w, is assumed constant at the value it has before the water formations intersect.

The governing differential equation is identical to that of the unconstrained latent charging rate, but the change in diameter is no longer explicit in the change in ice mass. Newton's method was employed to solve for the new ice diameter.

$$m_i = \rho_i \left(4 D_{crit} \sqrt{D_{i,o}^2 - D_{crit}^2} + \left(\frac{\pi}{4} - 2 \cos^{-1} \left(\frac{D_{crit}}{D_{i,o}} \right) \right) D_{i,o}^2 - \frac{\pi}{4} D_{t,o}^2 \right) \tag{2.21}$$

A graph of the ratio of actual ice mass to total ice mass versus the ratio of ice thickness and the maximum ice thickness is shown for several geometries in Fig. 2.6. A $D_{t,o}/D_{crit}$ ratio of zero corresponds to cylindrical growth an infinitely small tube, and a ratio of one corresponds to growth around tubes that are touching. The solution procedure for the constrained latent charging period is identical to the unconstrained latent charging period.
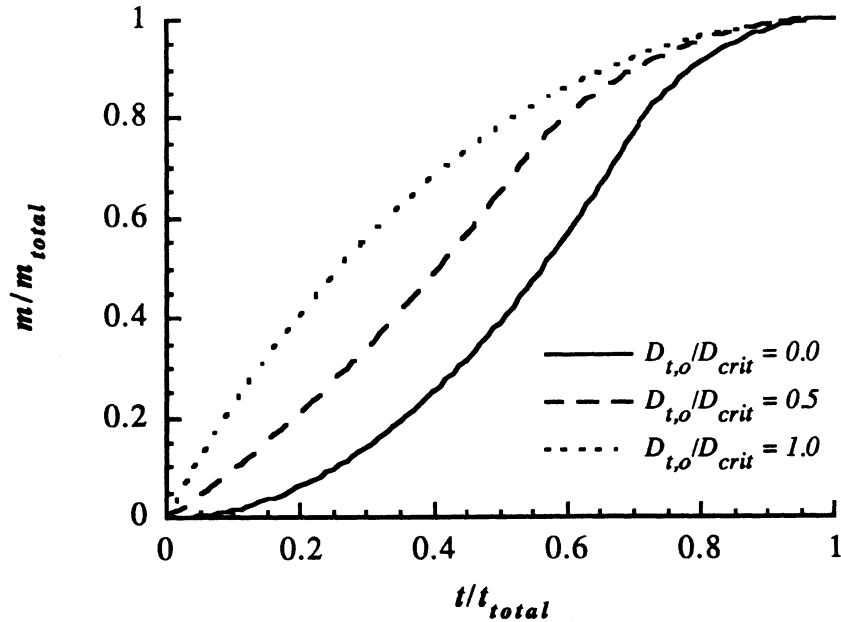
Fig. 2.6 Percentage of mass as a function of the thickness ratio.

2.2.3 Discharging model

During discharge, the space load is being fully or partially met by the ice-storage tank depending on the tank control strategy; therefore, an accurate account of discharging performance is needed to determined whether or not the storage tank is able to meet the load. The discharging period will be split into two periods: 1) Unconstrained latent discharging, and 2) Constrained latent and sensible discharging. The unconstrained latent discharging is characterized by the cylindrical melting of ice around the tubes. The unconstrained latent and sensible discharging is characterized by the melting of ice after the advancing water formations intersect and the sensible discharging of the water around the tubes.

2.2.3.1 Assumptions

As in the charge model, the discharge model assumes that the tube is long and horizontal with convection on the inside of the tube. On the outside of the tubes, the heat transfer through the water before adjacent formations intersect is assumed to be purely conduction, this is referred to the unconstrained discharging period. It is assumed that there is no convection due to the lack of density gradients and small area around the tubes. However, once the water formations intersect (constrained), the analysis becomes more complicated. The heat transfer from the working fluid is split between the melting of ice and the heating of the water around the tubes. The two discharging periods, that is constrained and unconstrained, are assumed be continuous at the point of transition; in other words, there is no jump discontinuity between the two, thus the total conductance just before and just after intersection are equal. During the constrained period, the geometry is complicated and there are no heat transfer coefficient correlations for the natural convection during this period. From the knowledge of the total conductance and

the water temperature at the time when the water formations intersect, the heat transfer coefficient that gives the same total conductance is calculated. This heat transfer coefficient is assumed to be constant over the remainder of the discharging period. The heat transfer coefficient between the water and the ice is determined from an energy balance just before the water formations intersect. The amount of heat transfer to the ice and the water temperature are used to determine the heat transfer coefficient.

2.2.3.2 Model inputs

The inputs of the discharging model are the full description of the geometry of the tank as in the charging model, the inlet brine temperature, the system flow rate of brine or the discharge rate, and the desired temperature to be delivered to the load (blended outlet temperature), TB.

2.2.3.3 Unconstrained latent discharging

The unconstrained latent discharging period is characterized by the cylindrical growth of water around the outside of the tubes. The governing differential equation can be simplified because the sensible internal energy change in the ice is zero since the ice stays at a constant temperature. However, the sensible internal energy change in the water is no longer negligible due to the increased temperature difference between the brine and the water. Equation (2.1) can be simplified to Eq. (2.22), where dm_w/dt is the rate of change of the mass of water.

$$\dot{Q}_b + \dot{Q}_{gain} = u_{i,f}\frac{dm_w}{dt} + m_w \, C_{v,w}\frac{dT_w}{dt} \qquad (2.22)$$

The heat transfer mechanism through the water is assumed to be conduction. However, when the discharge period starts there is no water around the tubes; therefore,

the heat transfer analysis is done assuming that the temperature on the outside of the tube is at the freezing point. The total conductance between the brine and the surface of the tube based on the outside area of the water formation, $A_{w,o}$, during this period is given in the following equation.

$$U_{tot} = \left[\frac{A_{w,o}}{A_{t,i} \, h_b} + \frac{A_{w,o} \ln \left(D_{t,o}/D_{t,i} \right)}{2 \, \pi \, k_t \, L_t} + \frac{A_{w,o} \ln \left(D_{w,o}/D_{t,o} \right)}{2 \, \pi \, k_w \, L_t} \right]^{-1}$$

(2.23)

The temperature of the surface of the ice is assumed to be constant at the freezing point. The heat transfer coefficient of the brine is difficult to determine because the Reynold's number of the flow through a single tube may be below the turbulent transition. However, if the laminar value of the Nusselt number is used the heat transfer rate is low and the performance of the tank is decreased significantly below the manufacturer's experimental performance. Therefore, a transition region was defined between Reynold's numbers of 700 and 1,300. Below 700 the flow was considered laminar, above 1,300 the flow was considered turbulent. Between the two, the Nusselt number was linearly interpolated between the turbulent and laminar values. The laminar Nusselt number was determined using the Heaton form (Eq. (2.24)) with constants for constant wall temperature [4] that takes into account developing thermal and hydrodynamic boundary layers, and the turbulent Nusselt number was determined using the Dittus-Boelter correlation (Eq. (2.10)).

$$\overline{Nu_D} = 3.66 + \frac{0.0534 \left(Re_D \, Pr \, D / L_t \right)^{1.15}}{1 + 0.0316 \left(Re_D \, Pr \, D / L_t \right)^{0.84}}$$

(2.24)

The sensible energy change of the water is determined from the change in average water temperature with time. Since the water formation is cylindrical the bulk average water temperature can be analytically determined.

$$\overline{T}_w = T_{w,o} - (T_{w,o} - T_{t,o}) \left[\frac{1}{2 \ln (D_{w,o}/D_{t,o})} - \frac{D_{t,o}^2}{D_{w,o}^2 - D_{t,o}^2} \right] \qquad (2.25)$$

where $T_{w,o}$ is the temperature of the ice-water boundary, assumed to be constant at the freezing point, and $T_{t,o}$ is the surface temperature of the tube. From the bulk average temperature, the derivative of the temperature with respect to time is approximated in finite difference form.

$$\frac{dT_w}{dt} = \frac{\overline{T}_w^{(1)} - \overline{T}_w^{(0)}}{\Delta t} \qquad (2.26)$$

The heat transfer rate is determined using the log-mean-temperature difference, where T_s in Eq. (2.6) is the temperature of the ice boundary (assumed to be 32°F).

The method for solving the governing equations is as follows:

1) determine the total conductance between the brine and the ice boundary (Eq. (2.23)),

2) determine the outlet brine temperature (Eq. (2.5)),

3) determine the log-mean-temperature difference (Eq. (2.6)),

4) determine the heat transfer rate from the brine to the water (Eq. (2.7)),

5) determine the bulk average water temperature and estimate the change in internal energy of the water,

6) determine the rate of change of the mass of water from the differential equation (Eq. (2.22)),

7) determine the new estimate for the outside water diameter.

Repeat steps 1 - 7 until the new estimate of the water diameter is unchanged.

2.2.3.4 Constrained latent and sensible discharging

After the water formations intersect, the heat transfer process is split into two parts: 1) brine to the water, and 2) water to the ice. The bulk average water temperature is no longer analytically obtainable due to the two-dimensional geometry, so the sensible heating of the water is harder to determine.

The heat transfer coefficients between the tube and the water and between the water and the ice are not known due to of the complicated geometry. However, the heat transfer rate just before and just after the water formations are assumed to be equal. The heat transfer coefficient between the tube and the water, $h_{t\text{-}w}$, was determined from the knowledge of the total heat transfer rate and water temperature just before the water formations intersect, and assumed constant during the remainder of the discharging period. The log-mean-temperature difference based on the average water temperature (as opposed to the ice surface temperature as in the unconstrained latent discharging period) is determined and used to determine the UA_{tot}. Both the conductance of the convection inside the tube and the tube itself remain constant; therefore, the conductance of the convection between the tube and water can be determined.

$$UA_{tot} = \frac{\dot{Q}_b + \dot{Q}_{gain}}{\Delta T_{lm}\left(T_w = \overline{T}_w\right)} \tag{2.27}$$

$$h_{t\text{-}w} = [A_{t,o}\,(1/UA_{tot} - 1/(A_{t,i}h_b) - \ln\,(D_{t,o}/D_{t,i})/(\,2\,k_t\,L_t))]^{-1} \tag{2.28}$$

ΔT_{lm} $(T_w = \overline{T}_w)$ means that the log-mean-temperature difference is determined using the bulk water temperature as the selected temperature, T_s.

The heat transfer coefficient between the ice and the water, $h_{w\text{-}i}$, is determined from the knowledge of the heat transfer rate to the ice and the water temperature. Both of the heat transfer coefficients are assumed to be constant over the remainder of the discharging period.

$$h_{w\text{-}i} = \frac{\dot{Q}_b + \dot{Q}_{gain} - m_w\, C_{v,w} \dfrac{dT_w}{dt}}{A_{w,o}\left(\overline{T}_w - T_{w,o}\right)}$$

(2.29)

A description of the solution method is as follows:

1) determine the heat transfer coefficients as described just before the water formations intersect,

2) determine the conductance between the brine and the water,

3) determine the outlet brine temperature,

4) determine the heat transfer rate from the brine to the water,

5) determine the heat transfer rate from the water to the ice,

6) compute the new estimate of the water temperature and the outside water diameter.

Repeat steps 1 - 6 until the water temperature and water diameter converge.

2.3 Tank characteristics and validation

The control strategies and the time dependent performance of the charging and discharging periods are presented in this section. The model performance is validated with manufacturer's performance data (Calmac model 1190). The working fluid is 25% ethylene glycol (brine). The nominal capacity of the ice-storage tank is 190 ton-hrs, which includes the latent capacity of the ice and sensible capacity of the water if is heated to a temperature of approximately 60°F.

2.3.1 Charging period

During the charging period the entire flow rate of brine is often circulated through the tank. The higher the flow rate of brine, the lower the required inlet temperature is to charge the tank in the given amount of time. For example, to charge a Calmac 1190 to full charge in 12 hours with 40 GPM the inlet temperature would have to be about 20°F; however, if 60 GPM was circulated through the tank the inlet temperature would only have to be about 23°F. If a lower inlet temperature is needed, the chiller will operate at a lower COP and thus require more power to charge the tank. Thus, since the parasitic pumping power is small relative to the chiller power, the optimum charging control is the highest flow rate that the chiller will still deliver the desired charging rate.

During the sensible charging period, the charging rate is dependent on both the log-mean temperature difference between the working fluid temperature and the average water temperature and the properties of the water. The sensible charging rate as a function of time for a specific situation is shown in Fig. 2.7. The local minimum that appears for $T_{b,i} = 30°F$ at time 0.4 hr in Fig. 2.7 is a result of the variation in properties of the water as it is passing through its maximum density. The sensible charging period is presented for completeness, it is not usually encountered in air-conditioning processes.

During the unconstrained latent charging period the charging rate is nearly constant, but the charging rate drops significantly in the constrained latent charging period. The latent charging rate as a function of the percent of latent capacity is shown in Fig. 2.8 for several inlet brine temperatures, and as a function of time in Fig. 2.9 for an inlet temperature of 20°F. The break in the curve corresponds to the point at which the adjacent ice formations touch. The charging rate is very dependent on the inlet brine

temperature because the increase in inlet temperature decreases the driving force (log-mean-temperature difference) for the heat transfer.

In order to validate the charging model, the geometry of the Calmac 1190 ice tank was input to the program. The simulated time dependent charging results are shown in the following pages. However, Calmac does not provide data for charging rate as a function of either state of charge or time; rather, they give average values for the charging rate over the entire charging period [5]. Therefore, the validation of this charging model is based on an average charging rate over the entire latent charging period. While this comparison is not ideal, it does allow an order of magnitude comparison of the instantaneous charging rates.
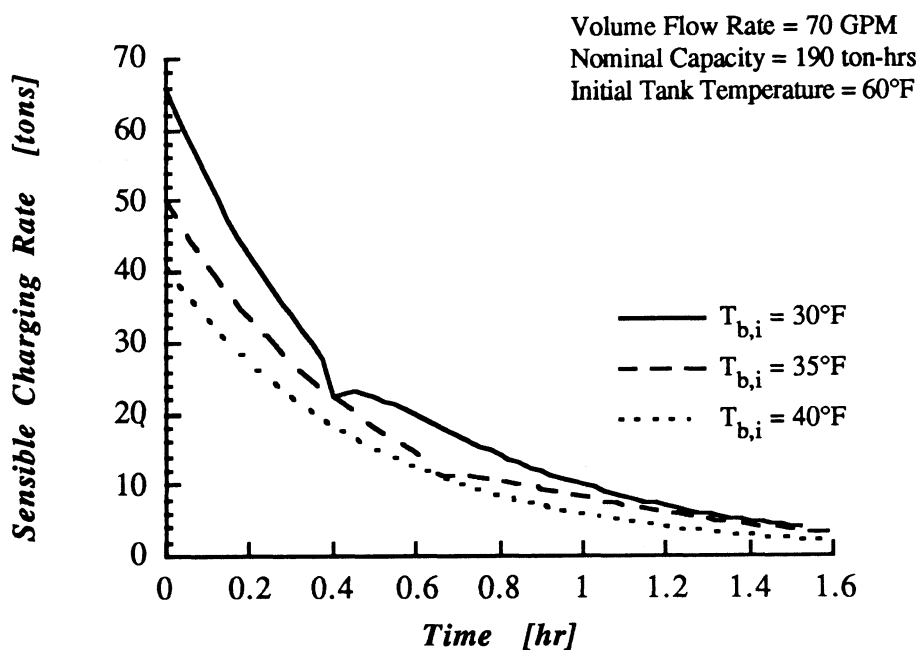
Fig. 2.7 Sensible charging rate as a function of time for several inlet temperatures.
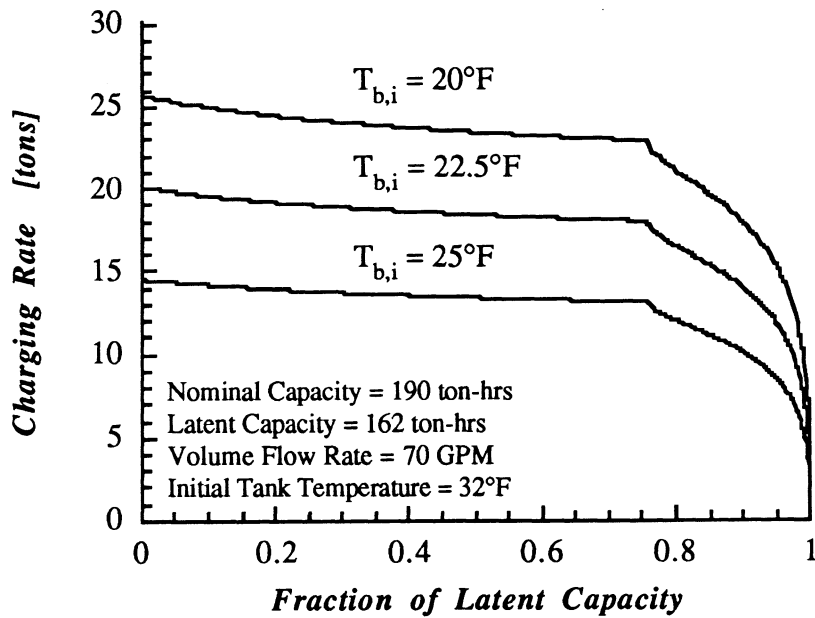
Fig. 2.8 Latent charging rate for several inlet brine temperatures.
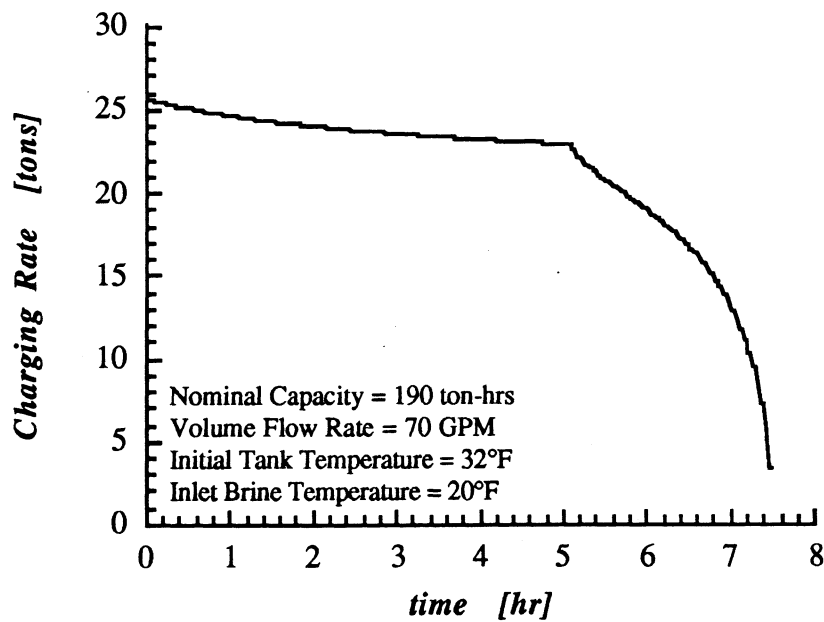
Fig. 2.9 Latent Charging rate as a function of time.

The performance map that the model generates is shown in Fig. 2.10. The charging rate is an average over the length of the latent charging period. The charging period is the time that it takes to freeze the entire tank when it is initially at a water temperature of 32°F. The latent charging rate is determined by dividing the total storage capacity by the time to charge the tank. The performance map also shows the average brine temperature rise through the tank. This is helpful in determining whether the chiller selection will be able to charge the tank.
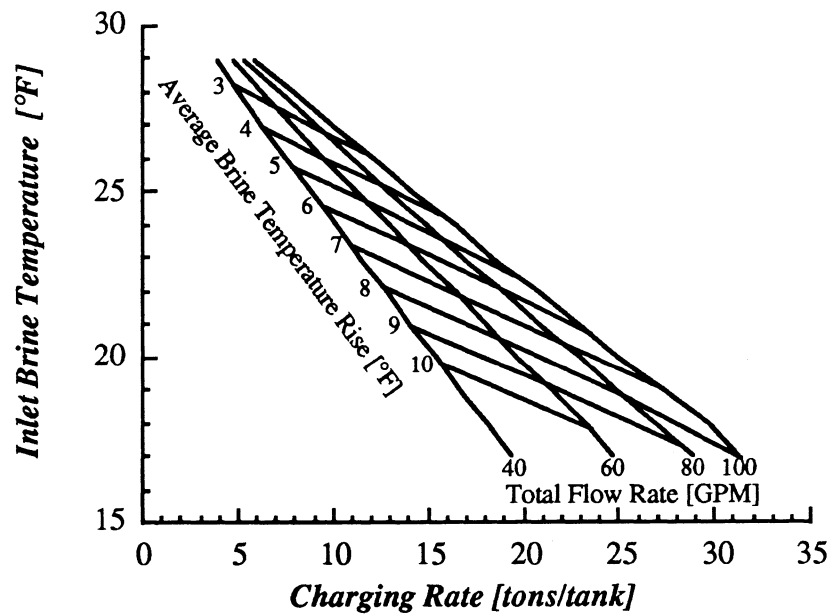
Fig. 2.10 Average charging rate and brine temperature rise given by ice-storage tank model.

The comparison of the model and Calmac data was done using the root mean square difference (*RMSD*) and the the mean bias difference (*MBD*).

$$RMSD = \left[\frac{1}{n} \sum_n \left(\overline{Q}_{Calmac} - \overline{Q}_{model}\right)^2\right]^{1/2}$$

(2.30)

$$MBD = \frac{1}{n} \sum_n \left(\overline{Q}_{Calmac} - \overline{Q}_{model}\right)$$

(2.31)

Determination of the severity of these differences is done by normalizing the differences with average value of the charging rate given by Calmac for the n runs [6].

$$NRMSD = \frac{RMSD}{\left(\sum_n \overline{Q}_{Calmac}\right)/n}$$

(2.32)

$$NMBD = \frac{MBD}{\left(\sum_n \overline{Q}_{Calmac}\right)/n}$$

(2.33)

The average charging rates given by the model were always less than the Calmac data. The values for the *RMSD, NRMSD, MBD, and NMBD* are given in Table 2.1. The *MBD* and the *RMSD* are approximately the same and positive because the model always underpredicts the average charging rate. The major reason for the discrepancy is the use of a constant inlet brine temperature in the model. In order to keep a constant charging rate, Calmac varies the inlet brine temperature and publishes a table of minimum entering brine temperatures [5] in order to achieve full charge as a function of the average inlet brine temperature and the average latent charging rate.

RMSD [tons]	*NRMSD*	*MBD* [tons]	*NMBD*
2.00	0.126	1.87	0.117

Table 2.1 Difference Analysis of average charging rate results.

RMSD [°F]	*NRMSD*	*MBD* [°F]	*NMBD*
1.07	0.045	1.04	0.044

Table 2.2 Difference Analysis of inlet temperature results.

The inlet brine temperature was within 2°F of the inlet brine temperature that would give the average latent charging rate that Calmac publishes. Table 2.2 gives the differences between the inlet temperature to give the same average charging rate as the Calmac data.

2.3.2 Discharging period

During the discharge period the load on the space is met by the tank; therefore, both the discharging rate and the temperature delivered are determined by the space load. The flow through the tank is varied in order to obtain the required temperature to meet the load. The blended outlet temperature, TB, is the temperature that is delivered to the load, and is obtained by the mixture of the brine outlet temperature, $T_{b,o}$, and the brine inlet temperature, $T_{b,i}$. Figure 2.11 shows the set up of the ice tank (chiller upstream).
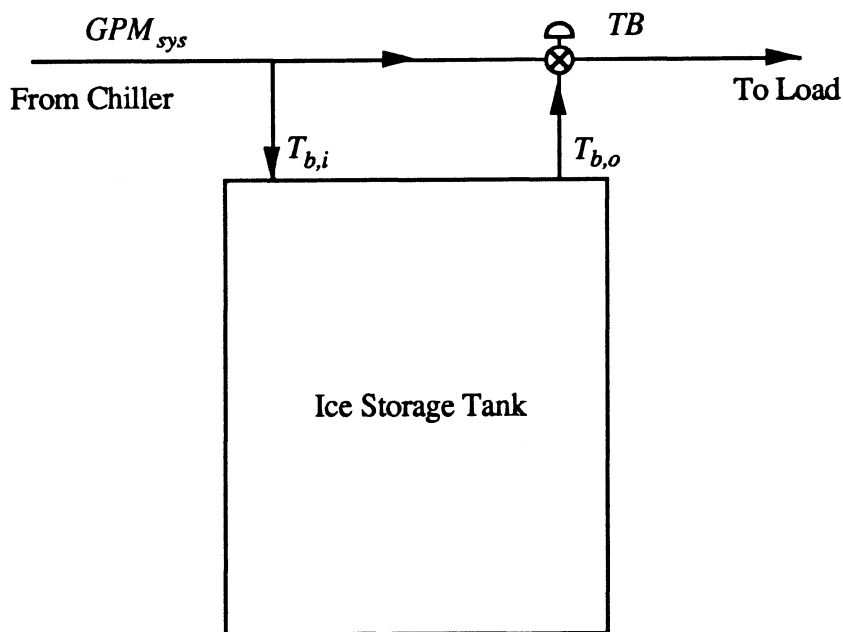
Fig. 2.11 Ice-storage tank configuration and nomenclature.

The tank water temperature and the minimum available outlet temperature from a tank subject to a constant load as a function of the fraction of nominal capacity of the tank is shown are Fig. 2.12.

Nominal Tank Capacity = 190 ton-hrs
Discharge Rate = 15.8 tons
$T_b = 50°F \quad T_{b,i} = 60°F$

$\overline{T}_w$

$T_{b,o}$

Fraction of Nominal Tank Capacity
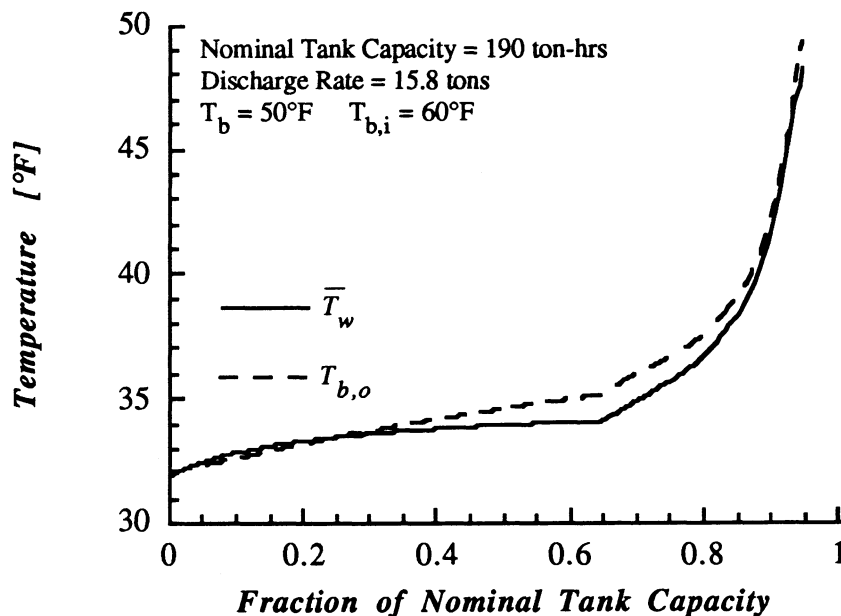
Fig. 2.12 Tank water temperature and minimum available outlet temperature as a function of fraction capacity.

Figure 2.12 shows that at some points during the unconstrained latent discharging period the outlet brine temperature is less than the water temperature: this behavior is due to the averaging of the water temperature over the entire length of the tube. The increased available minimum temperature during the unconstrained latent discharging period is primarily due to the decreased conductance as water builds around the tubes; the temperature of the ice boundary is assumed to be constant at the freezing temperature. The increase after the water formations intersect is due primarily to the increased water temperature in the tank.

The heat transfer rate for constant flow through the tank is shown in Fig. 2.13.

Figure 2.14 shows the tank outlet temperature for a constant flow rate through the tank and shows two different constant discharge rates and the blended outlet temperature. The important aspect of the figure is that the curve for the constant flow through the tank is the locus of all the discharge schedules with a system flow rate of 40 GPM. The final fraction of nominal capacity is nearly independent of tank history.
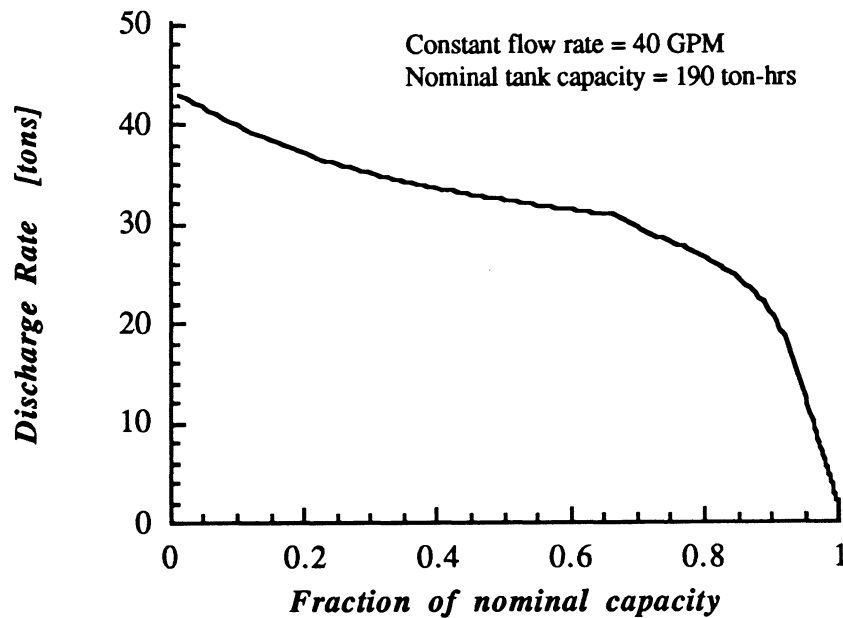
Fig. 2.13 Discharge rate with constant volume flow rate through tank.

The results from the model were compared with Calmac's discharging performance maps [5]. Calmac publishes the discharging rate of the tank as a function of the inlet brine temperature, the desired blended outlet temperature, and the fraction of nominal storage capacity. For a given discharge rate and inlet and blended outlet temperatures, the graph presents the fraction of nominal storage capacity at which the tank can no longer deliver the desired blended outlet temperature. This was determined

by inputting a constant discharge rate and blended outlet temperature and running the model until the blended outlet temperature could no longer be supplied. The discharge performance map given by the model is shown in Fig. 2.15.
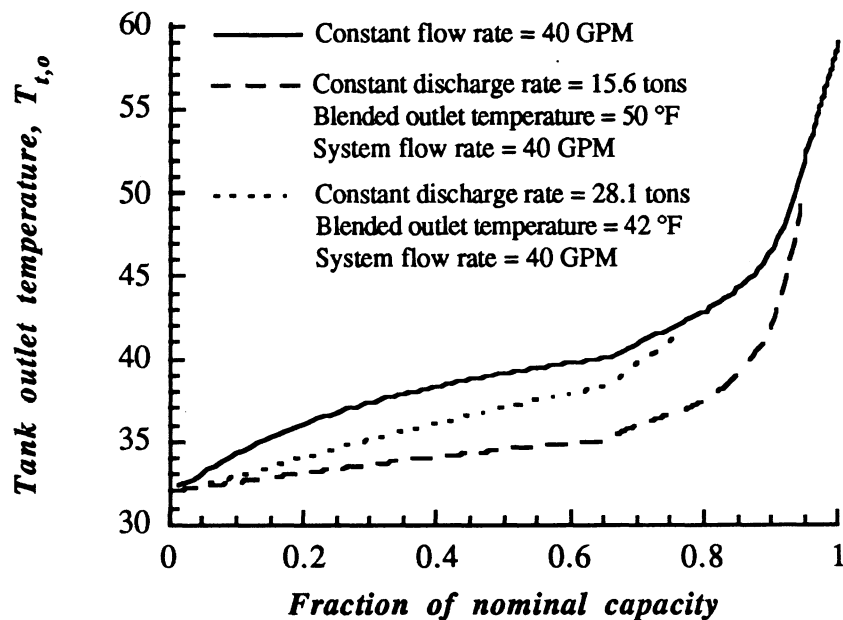
Fig. 2.14 Tank outlet temperature as a function of nominal tank capacity.

The model predicts high outlet temperatures and low discharge rates accurately. However, when the discharge rate is high, the model usually underpredicts the fraction at which the tank could no longer meet the load compared to Calmac's data. When the outlet temperature is low, the model usually overpredicts the fraction at which the tank could no longer meet the load. In addition, the model overpredicts tank performance near the end of the unconstrained discharge period (i.e. storage fractions between 0.5 and 0.65).
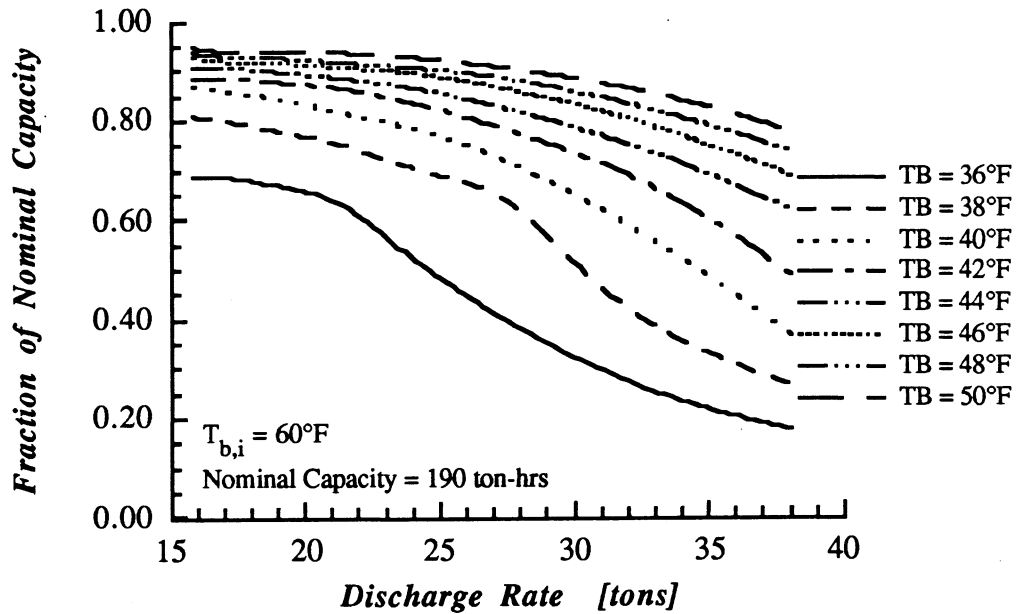
Fig. 2.15 Discharge performance map given by model.

The difference analysis was done between the fraction of nominal capacity that Calmac predicted the tank could no longer deliver that temperature given the load and the fraction that the model predicted. The results of the difference analysis are given in Table 2.3.

RMSD [ton-hrs]	NRMSD	MBD [ton-hrs]	NMBD
0.07	0.094	-0.02	-0.022

Table 2.3 Difference Analysis of fraction of nominal capacity results.

The negative *MBD* indicates that on the average the model was overpredicting the fraction of nominal capacity that the desired blended outlet temperature could still be met given the load.

2.3.3 Example of tank discharge performance with a varying load.

In a real application the tank is rarely subject to a constant load and desired blended outlet temperature over the entire discharging period. Therefore, it is of interest to see how the model predicts tank performance under varying load conditions. As an example the system sizing example in the Calmac performance literature [5] will be used along with Calmac's Levload computer program [6] to investigate the tank performance and compare it to the model prediction. The example utilizes a partial storage, series flow system with the chiller upstream from the ice tank. The cooling load profile for the design day is shown in Fig. 2.16. According to Calmac, the nominal chiller capacity is 478 tons. The remainder of the cooling load will be met with 23 Calmac model 1190 ice tanks. The volume flow rate of brine through the system is 1700 GPM (73.9 GPM/tank). The load profile on an individual tank is shown in Fig. 2.17.
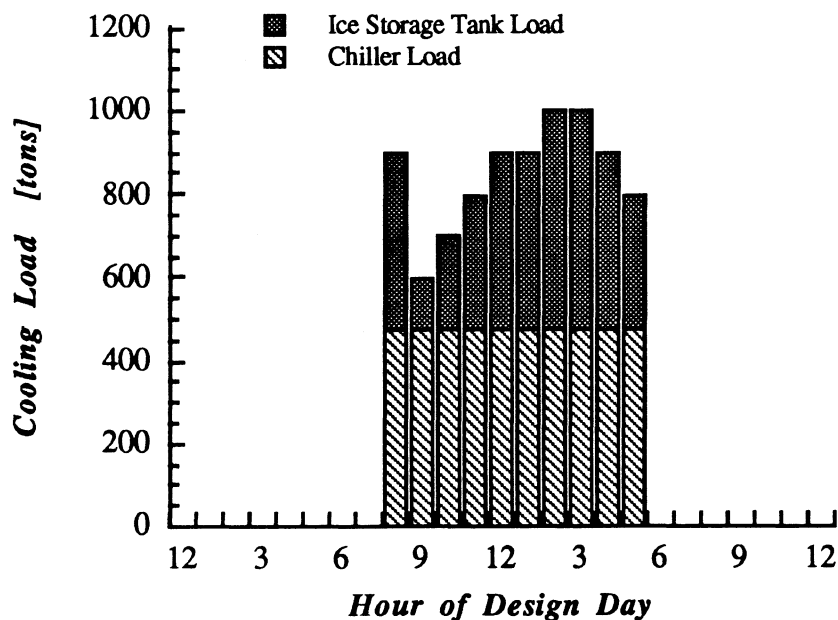
Fig. 2.16 Design Day Load Schedule.

The desired blended outlet temperature is constant at 45°F for the entire day. The inlet to the ice tank varies hourly due to the changing load. The volume flow rate through the tank is shown in Fig. 2.18. The points from Levload are assumed to be at the end of the hour. The Levload estimates for the flow through the tank are determined from the data that make up the performance map for the tank.
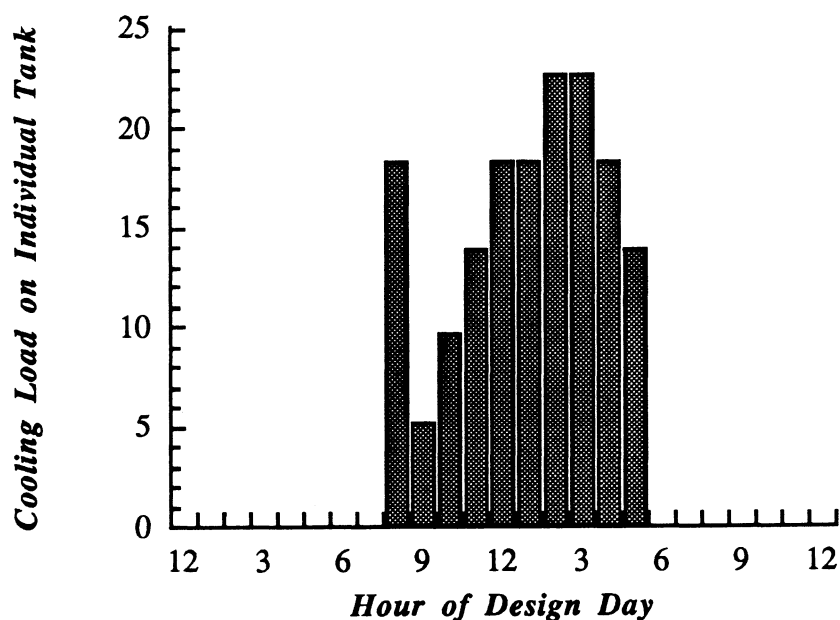
Fig. 2.17 Load schedule on individual ice tank.

During the first four hours of discharge (unconstrained discharging period), the model agrees well with Calmac's estimates of tank performance. Near the end of the unconstrained period the model overpredicts the discharge performance; the hours 5 through 7 demonstrate this behavior. The predicted flow through the tank is quite different from Calmac's estimate during the last three hours of discharge (which corresponds to the constrained discharging period). In this period, the flow through the

tank varies rapidly due to the increasing water temperature. A possible reason for the discrepancy in the performance is the strong dependence of the heat transfer rate on the water temperature during the constrained discharging period; the use of the average temperature of the water may overpredict the performance of the tank.

In addition to the ability to change the load on the tank, the model also allows the user to change the blended outlet temperature to the load. The varying of the blended outlet temperature will affect the temperature returning from the load, or the flow rate of the brine through the system.
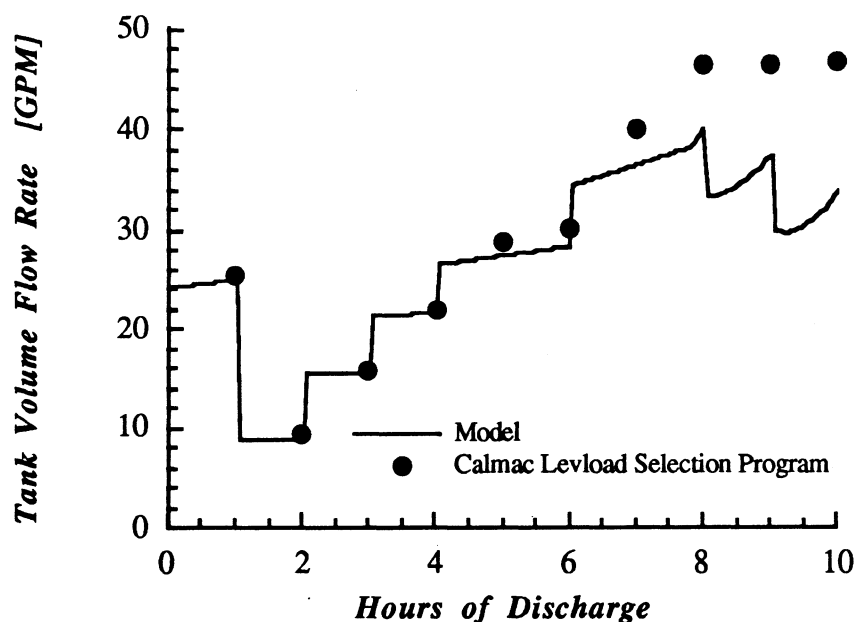
Fig. 2.18 Comparison of model and Levload predictions for flow through tank under varying load conditions.

2.4 Effectiveness of ice-storage tanks

The thermal effectiveness of a heat exchanger is defined as the ratio of the actual heat transfer rate to the maximum possible heat transfer rate. For both the charging and

discharging periods of an ice-storage tank, the maximum possible heat transfer rate is obtained when the outlet brine temperature from the tank is 32°F. Therefore, the effectiveness can be written as follows:

$$\varepsilon = \frac{\dot{m}_b \, C_{p,b} \, (T_{b,i} - T_{b,o})}{\dot{m}_b \, C_{p,b} \, (T_{b,i} - 32)}$$

(2.34)

Equation (2.34) can be simplified by cancelling the mass flow rate and specific heat terms. The actual heat transfer rate can be written as a function of the effectiveness:

$$\dot{Q}_b = \varepsilon \, \dot{m}_b \, N_{tube} \, C_{p,b} \, (T_{b,i} - 32)$$

(2.35)

For the latent charging period, the model was used to determine the effectiveness of the ice-storage tank as a function of the charged fraction of latent capacity. Figure 2.19 shows the dependence of the effectiveness on the the charged capacity and volume flow rate of brine through the tank for an inlet brine temperature of 25°F. The effectiveness decreases as the charged capacity and the volume flow rate of brine through the tank increase. The effectiveness for several inlet brine temperatures is shown in Fig. 2.20 for a volume flow rate of 70 GPM. The effectiveness is nearly independent of inlet brine temperature for the latent charging period.

For the discharge period, the model was run with constant inlet brine temperature and a constant flow rate through the tank in order to generate the effectiveness as a function of the discharged capacity. For reasons outlined later, the discharged capacity of the tank will be presented as a fraction of the maximum capacity obtainable with the given inlet brine temperature. The discharged capacity ratio is a function of the inlet brine temperature. The maximum capacity is determined using the following equation,

$$Maximum \ \ Capacity \ = m_i \left(u_{i,f} + C_{v,w} \, (T_{b,i} - 32) \right)$$

(2.36)

where the first term represents the latent capacity of the tank and the second term represents the sensible capacity of the tank if the storage media is raised from the freezing temperature to the inlet brine temperature.
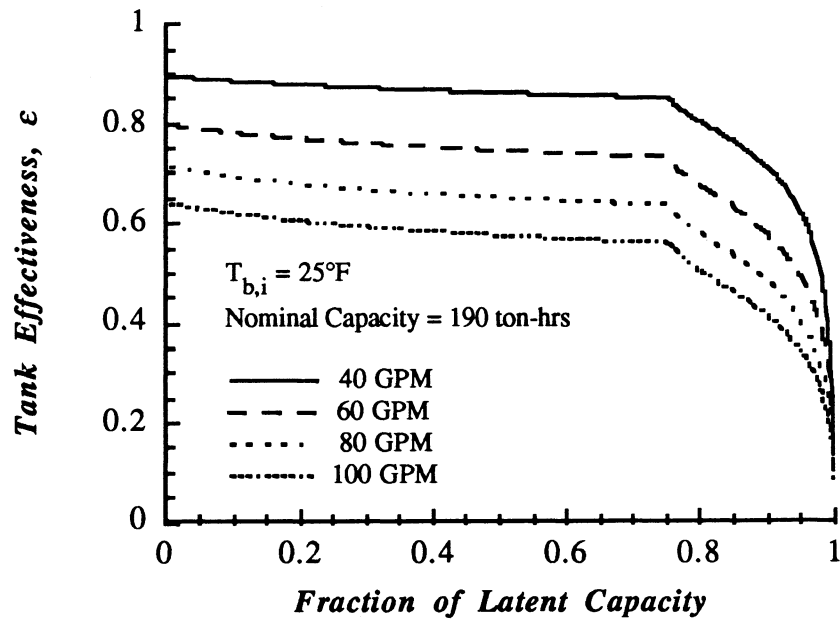
Fig. 2.19 Effectiveness for several volume flow rates of brine through the tank.

The effectiveness decreases with decreasing resident capacity and increasing mass flow rate through the tank. Figure 2.21 shows the dependence of the effectiveness on the mass flow rate of brine through the tank and the discharged capacity ratio for an inlet brine temperature of 60°F.

The effectiveness as a function of inlet brine temperature and discharged capacity ratio is shown in Figs. 2.22 through 2.26. With the discharged capacity ratio as the abscissa, the family of curves for different inlet brine temperatures coalesce; therefore, Fig 2.21 is sufficient to describe the tank effectiveness for a range of inlet brine temperatures.
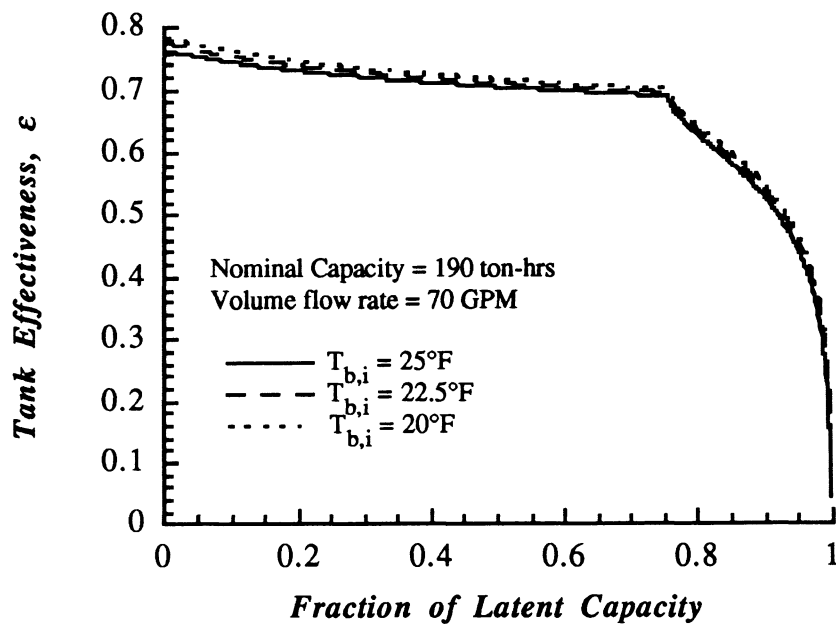
Fig. 2.20 Effectiveness as a function of inlet brine temperatures for 70 GPM.
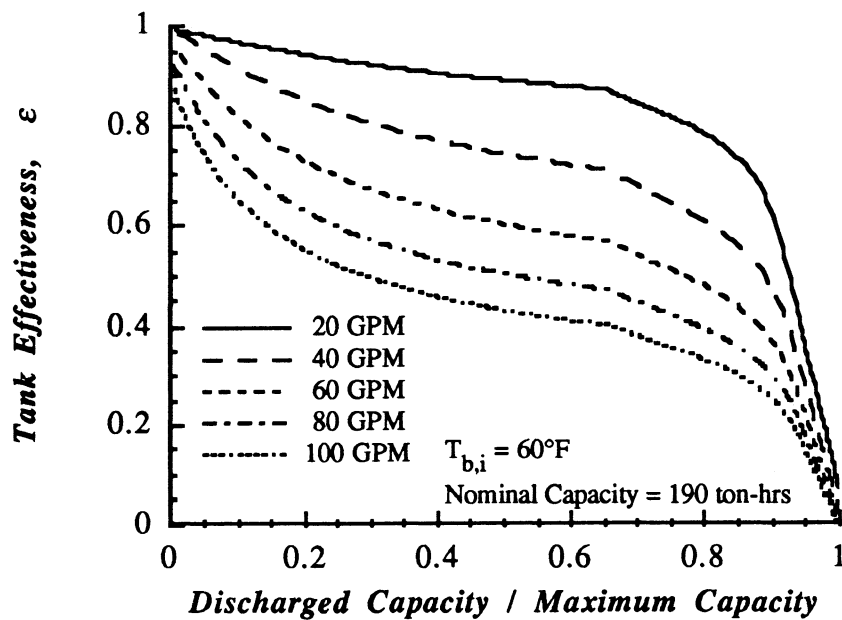
Fig. 2.21 Effectiveness of ice-storage tank for several flow rates through the tank.
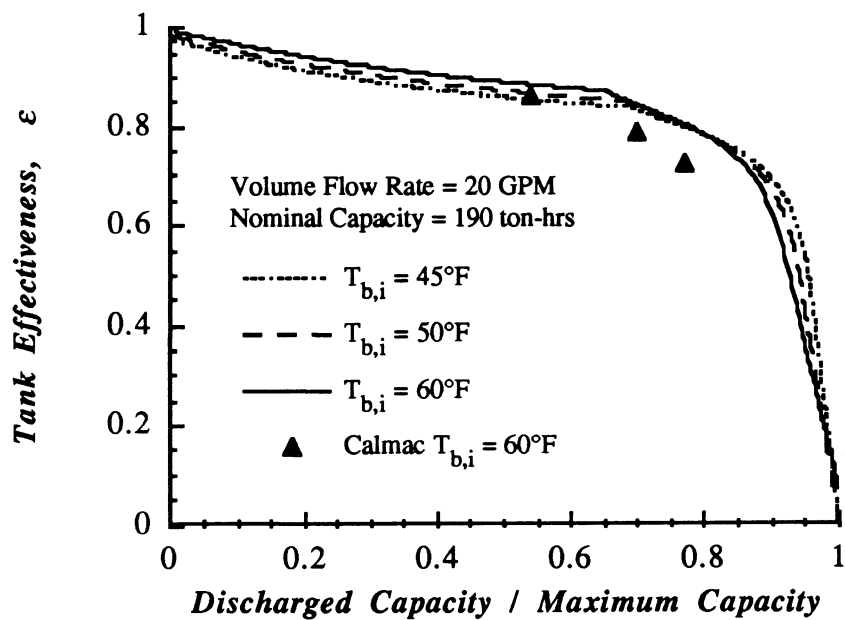
Fig. 2.22 Effectiveness as a function of the inlet brine temperature for 20 GPM.
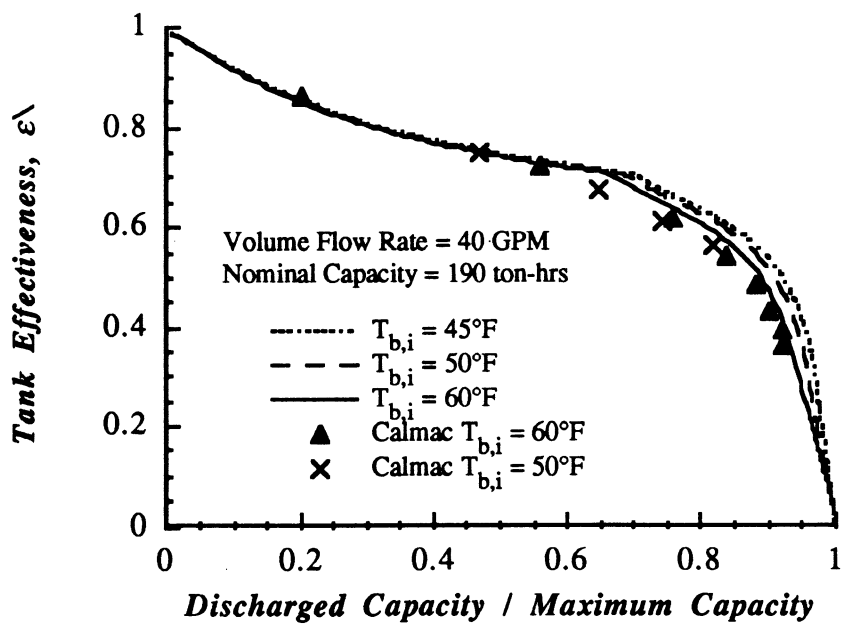
Fig. 2.23 Effectiveness as a function of the inlet brine temperature for 40 GPM.
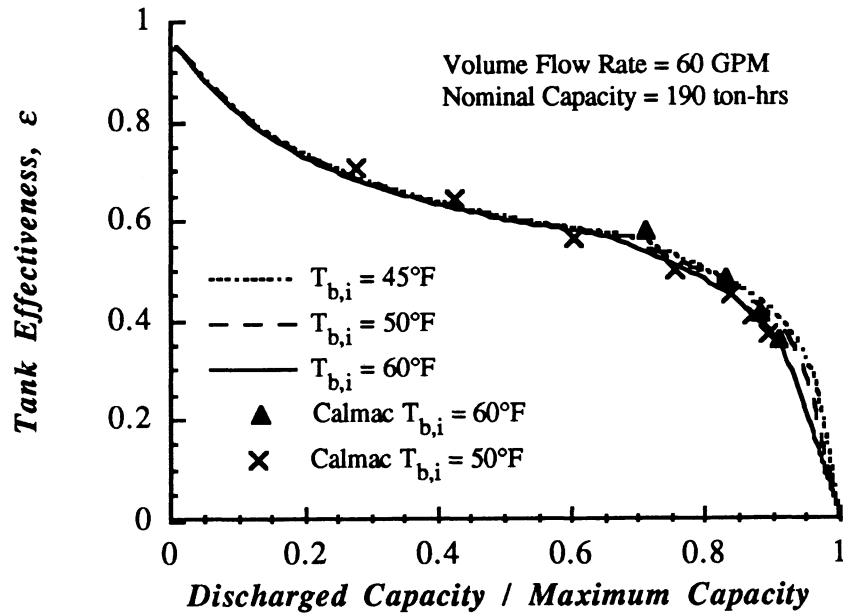
Fig. 2.24 Effectiveness as a function of the inlet brine temperature for 60 GPM.
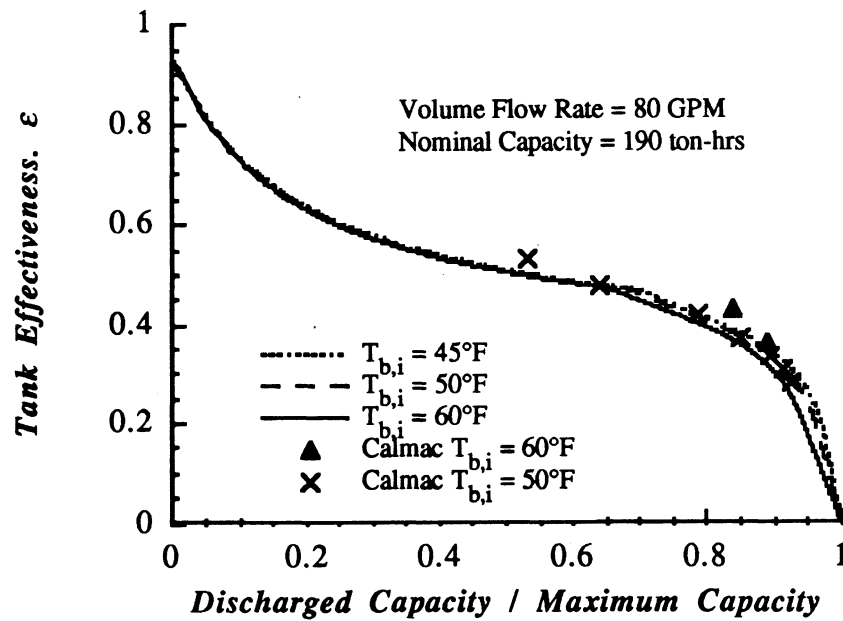
Fig. 2.25 Effectiveness as a function of the inlet brine temperature for 80 GPM.
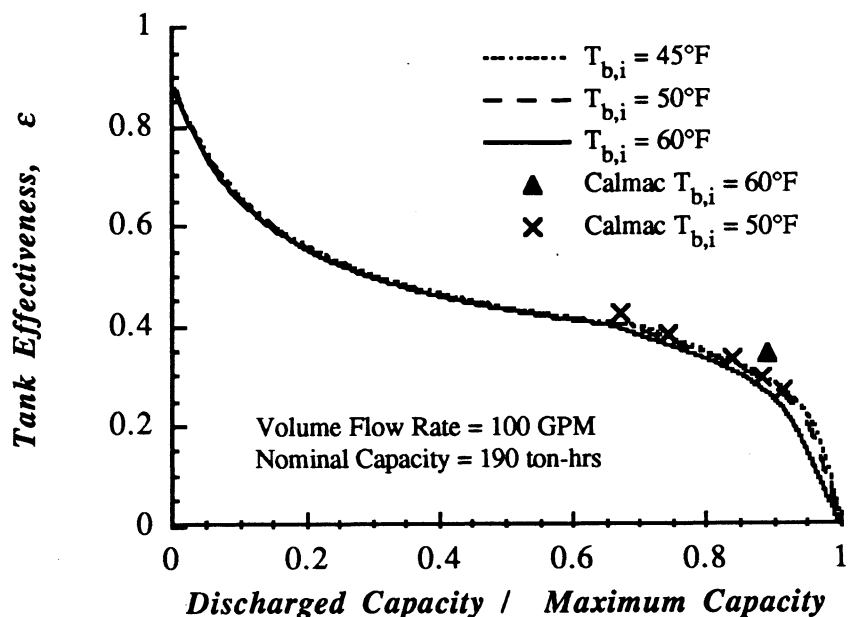
Fig. 2.26 Effectiveness as a function of the inlet brine temperature for 100 GPM.

Figures 2.22 through 2.26 also show the values that are calculated from Calmac's performance data for their model 1190. The agreement between the model simulation and the data is very good for both inlet temperatures of 50°F and 60°F for all volume flow rates through the tank.

The effectiveness concept is a simple model for the prediction of tank performance. For the latent charging period, the tank effectiveness can be determined from the knowledge of the charged fraction of latent capacity and the volume flow rate of the brine. The charging rate can be determined from the effectiveness and the inlet brine temperature. If the volume flow rate of brine is changed during the charging period the performance can be predicted by inspection of the effectiveness curve for that particular flow rate. For the discharge period, the tank effectiveness can be determined if both the discharged capacity ratio and the volume flow rate of brine through the tank are known.

The discharged capacity ratio depends on the maximum obtainable capacity for the given inlet brine temperature. The performance of the tank can be determined from the effectiveness and the inlet brine temperature. Different inlet brine temperatures and volume flow rates

2.5 Chapter summary

Both the charging and discharging periods of the ice-on-coil, internal melt ice-storage tank with brine as the working fluid were modeled and validated. The governing differential equations and the heat transfer analysis are outlined and the characteristics of the ice tank were discussed. The charging period is characterized by near constant performance before the ice formations intersect and rapidly decreasing performance after intersection. The charging model results were within 12% of Calmac's average charging data. During the discharging period, the discharged fraction at which the ice tank can no longer meet the required load is nearly independent of tank history. The discharging model results were within 10% of Calmac's discharging data. The effectiveness concept for both the latent charging and the discharging of ice-storage tanks was presented as a simple model for predicting tank performance.

References 2

1. Incropera, F. P., and D. P. DeWitt, *Introduction to Heat Transfer*, John Wiley & Sons, New York, 1985.

2. Cummings, M. S., "Modeling, Design, and Control of Partial Ice-Storage Air-Conditioning Systems," M.S.. Thesis, University of Wisconsin--Madison, 1989.

3. Klein, S. A., W. A. Beckman, and G. E. Myers, *FEHT Finite Element Heat Transfer Program*, F-Chart Software, Middleton, Wisconsin, Version 5.49, 1991.

4. Duffie, J. A., and W. A. Beckman, *Solar Engineering of Thermal Processes*, John Wiley & Sons, New York, 1980.

5. *Levload Ice Bank Performance Manual*, Product Literature, Calmac Manufacturing Corporation, Englewood, New Jersey, April 1987.

6. *Levload OPAC Cool Storage Selection Program*, Calmac Manufacturing Corporation, Englewood, New Jersey, 1990.

Chapter Three

Minimization of Air-Conditioner Cooling Load

Conventional constant air volume (CAV) systems usually require large amounts of reheat if both the sensible and latent loads on the space are to be met. The latent load usually limits the maximum operating temperature of the air-conditioner (A/C) coil. In other words, if the latent space load is met, there is a potential to meet or exceed the sensible space load. Therefore, the outlet from the air-conditioner coil is overcooled sensibly and reheat must be added to bring the air up to the required supply temperature. Although reheat is usually considered free because the heat is taken from the condenser of the chiller, the cost of initially overcooling the air is significant. Ideally, the coil should cool the air directly to the desired supply state, thereby minimizing the load on the coil. The minimum load on the coil is the sum of the load on the space and the load from the ventilation air. The reheat can be minimized by using some of the return air. This is accomplished by splitting the return air flow into two flows: one mixes with the fresh air and is cooled by the air-conditioner coil, and the other bypasses the coil and mixes with the coil outlet. Processing a smaller flow rate of air requires that the coil operating temperature be reduced in order to do the same amount of cooling. A reduction in coil load is achieved because the reheat is reduced. Although the chiller coefficient of

performance (COP) is decreased due to the lower operating temperatures, a reduction in chiller power can be realized.

3.1   Conventional and variable flow air-conditioning systems.

A typical CAV system is shown in Fig. 3.1. The conventional system usually requires reheating of the the air-conditioning coil outlet state because the sensible load is exceeded. The variable air volume (VAV) system is controlled such that the air flow rate through the system is varied in order to exactly meet the sensible load. The VAV system controls the space temperature but allows the space humidity ratio to fluctuate The CAV system with variable flow is shown in Fig 3.2. It uses some return air bypassing the coil, which provides some reheat in order to reduce the coil load. The CAV system with variable flow differs from the VAV system in that the amount of flow rate processed is controlled such that both the latent and sensible loads are met. The CAV system with variable flow controls both the space temperature and humidity.
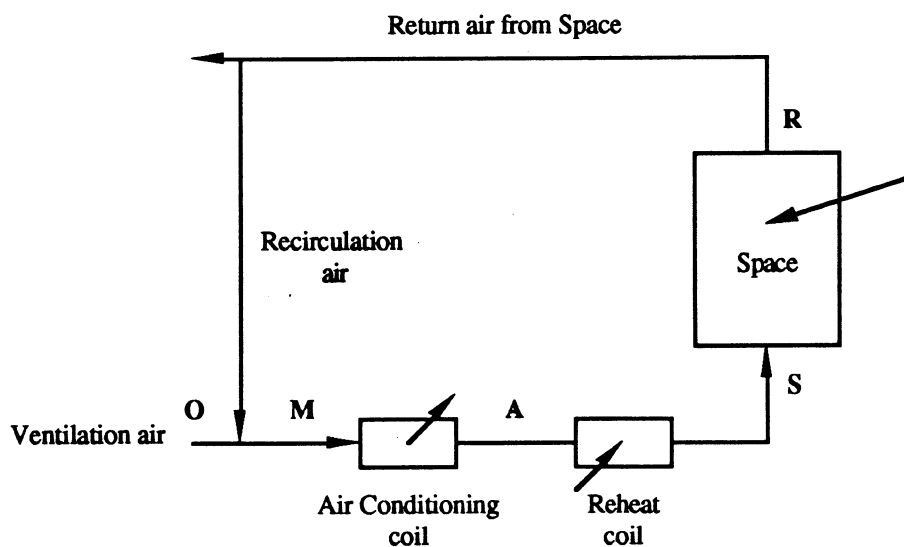
Fig. 3.1 The conventional CAV air-conditioning system.
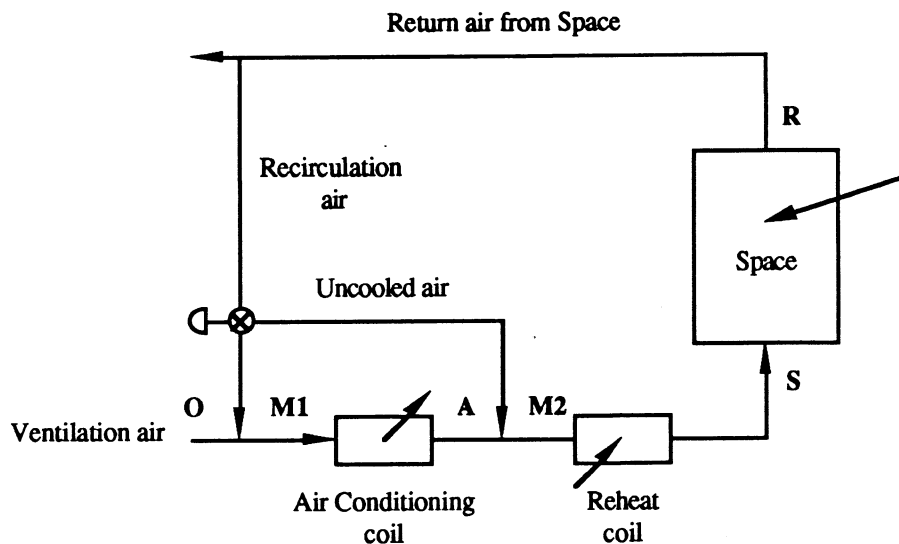
Fig. 3.2 The variable flow CAV air-conditioning system.
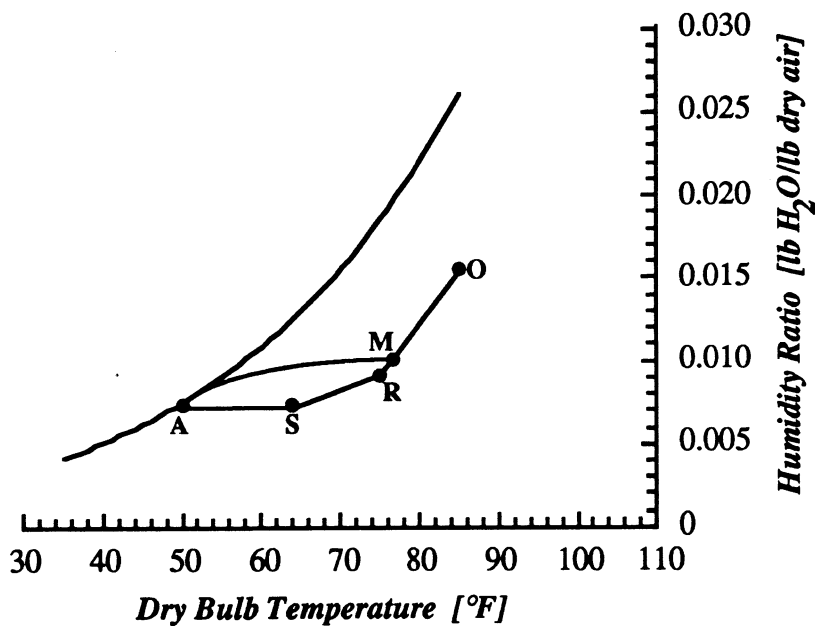
Fig. 3.3 Psychrometrics of conventional system.

3.1.1 Psychrometric analysis of conventional systems.

The process for the conventional system is shown on a psychrometric chart in Fig. 3.3. The line M - A is the cooling of the air flow through the air-conditioner coil.

The line **A - S** is the sensible reheat of the air to the supply state. The line **S - R** is the load line for the space. An energy balance on the entire system results in the following equation for the coil load

$$\dot{Q}_{A/C} = \dot{Q}_S + \dot{Q}_{RH} + \dot{m}_{vent}\left(i_o - i_i\right) \qquad (3.1)$$

where $\dot{Q}_S$ is the space load, $\dot{Q}_{RH}$ is the reheat, $\dot{m}_{vent}$ is the ventilation mass flow rate, and i_i and i_o are the enthalpies of the inlet (ventilation) air and the outlet (exhaust at space conditions) air respectively. The last term in Eq. (3.1) will be referred to as the ventilation load. Since the space load, ventilation mass flow rate, and ambient conditions are fixed, the reheat is the only quantity that can be controlled to reduce the coil load.

3.1.2 Psychrometric analysis of variable flow systems.

As described earlier, the return air from the space will be used to reduce the need for reheat of the air stream; thus the air-conditioner must operate at a lower temperature in order to obtain the required supply temperature and humidity. The coil outlet temperature is always lower than the temperature of the conventional system because the same amount of moisture must be removed from a smaller flow of air. If the outlet temperature from the air-conditioner coil is less than about 38°F, the coil surface begins to frost and a defrost cycle must be incorporated into the coil operation. Since defrosting the coil penalizes the coil performance, it would add to the power consumption of the air-conditioner. Therefore, two scenarios will be considered, 1) the space load allows total elimination of reheat with the outlet temperature greater than 38°F (as shown in Fig. 3.4), 2) the space load requires the outlet temperature to be less than 38°F for elimination of reheat, and the coil will be operated such that the outlet air temperature is 38°F and some reheat will be required (as shown in Fig. 3.5 process line **M2 - S**). Although the

process **M1** - **A** in Figs. 3.4 and 3.5 have larger enthalpy differences than the corresponding process **M** - **A**, for the conventional system (Fig. 3.3), there is less flow through the coil, resulting in a lower coil load.
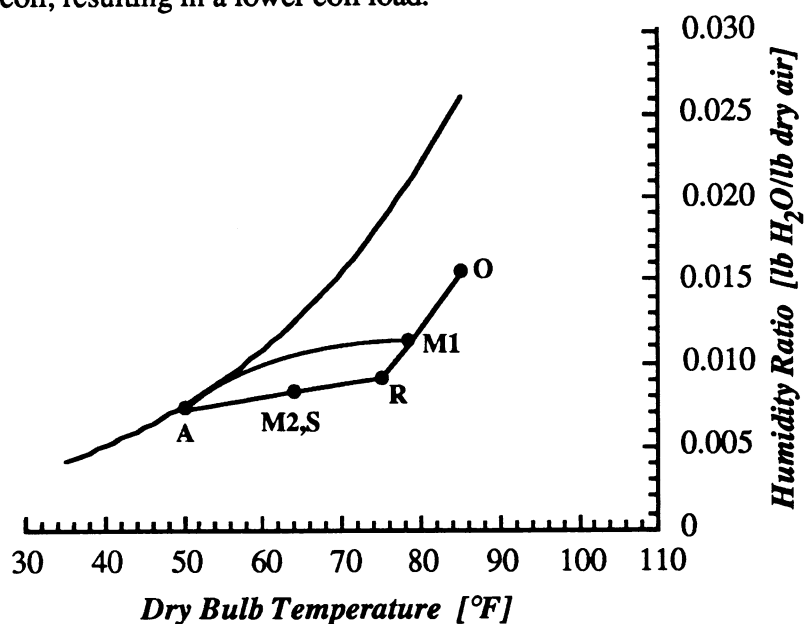
Fig. 3.4 Variable flow through air-conditioner coil with elimination of reheat.
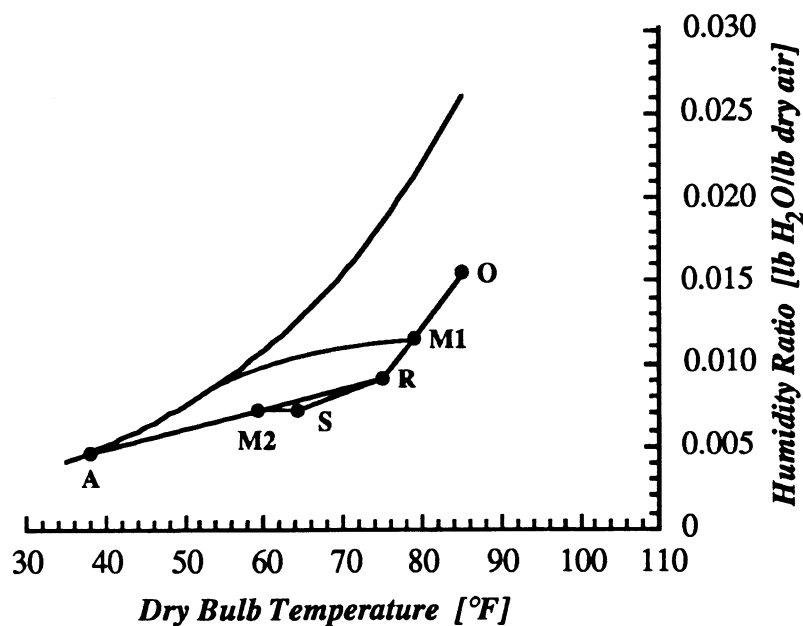
Fig. 3.5 Variable flow through cooling coil with minimum coil outlet temperature.

3.2 Simulation of variable flow through A/C coil

The variable flow system was modeled with TRNSYS [1]. Both the conventional and variable flow systems were modeled and a parametric study was done to determine the important factors for reducing the A/C coil load.

3.2.1 TRNSYS model

A TRNSYS deck was produced to model the power consumption of the variable flow air-conditioner system. The system is as shown in Fig. 3.2, with a specified volume flow rate, total space load and sensible heat ratio (SHR), and space set-point and ambient conditions. The sensible heat ratio is the ratio of the sensible load on the space to the total load on the space.

The air-conditioner coil model uses curve fits of manufacturer's performance data to determine the off-rated performance of a direct expansion coil based on rated performance [2]. The coil specific inputs to the coil model are shown in Table 3.1. The values in Table 3.1 are at ARI conditions: 67°F evaporator entering wet bulb temperature, 95°F condensing entering dry bulb temperature and 37.5 cfm/1000 Btu/hr cooling capacity.

Parameter Description	Value and Units
Rated Total Capacity	287,000 Btu/hr
Rated Coefficient of Performance	3.02
Rated Bypass fraction	0.18
Rated volume flow rate	11,000 cfm

Table 3.1 Coil specific inputs to air-conditioner model.

The rated bypass fraction is the fraction of the flow through the air-conditioner coil that passes through the coil uncooled. The air-conditioner model takes into account the following variations from ARI conditions: 1) the dependence of the coil capacity and COP on the entering wet bulb temperature to the evaporator and the entering dry bulb temperature to the condenser, 2) the dependence of the coil capacity and the COP on the fraction of rated flow through the system, 3) the dependence of the COP on the part load ratio, and 4) the dependence of the bypass factor on the fraction of rated flow through the system.

Parameter Description	Value and Units
Space set-point [Dry bulb temp / Relative Humidity]	72°F / 50% RH
Outdoor conditions [Dry bulb temp / Relative Humidity]	91°F / 45% RH
Sensible Load	70,000 Btu/hr
Latent Load	30,000 Btu/hr
Circulation flow rate	8,000 cfm
Return air fraction	0.85

Table 3.2 Nominal design for TRNSYS model.

The nominal design of the system is shown in Table 3.2. Unless otherwise stated, all graphs are at the nominal design conditions.

3.2.2 Parametric analysis

The TRNSYS model was used to do a parametric analysis on the variable flow system. The flow rate of air was varied between 4,000 and 10,000 cfm for a total space load of 100,000 Btu/hr. The fraction of ventilation flow was varied between 5 and 25%

of the total flow rate of air. The sensible heat ratio of the total load was varied between 0.4 and 0.9. The space set-points considered were 75°F / 40% RH and 72°F / 50% RH. The fraction of the total flow sent through the coil was varied in order to see the effect on the coil load.

3.2.2.1 Ratio of total volume flow to total space load

The ratio of the total volume flow rate to the total space load is a measure of the length of the load line of the space. The total flow is inversely proportional to the length of the load line; in other words, for the same space load, doubling the flow halves the load line. This is shown by an energy balance on the space

$$i_R - i_S = \frac{\dot{Q}_S}{\dot{m}}$$

(3.2)

where i_R and i_S are the enthalpies of the room and supply states respectively.

In the simulation, the fraction of the total flow through the A/C coil is varied for a constant space and ventilation (i.e. the mass flow rate of the ventilation air is constant) loads and ambient conditions. The operating temperature of the coil is the same for any length of load line given a constant space set-point and SHR (see Fig. 3.4) because a change in the length of the load line only moves the supply state to the space along the load line extended. Figure 3.6 verifies this behavior because the power for different flow rates coincide. Figure 3.7 shows the power of the air-conditioner for several volume flow rates with the total load fixed. For Figs. 3.6 and 3.7 the mass flow rate of the ventilation air is constant for all flow rates.
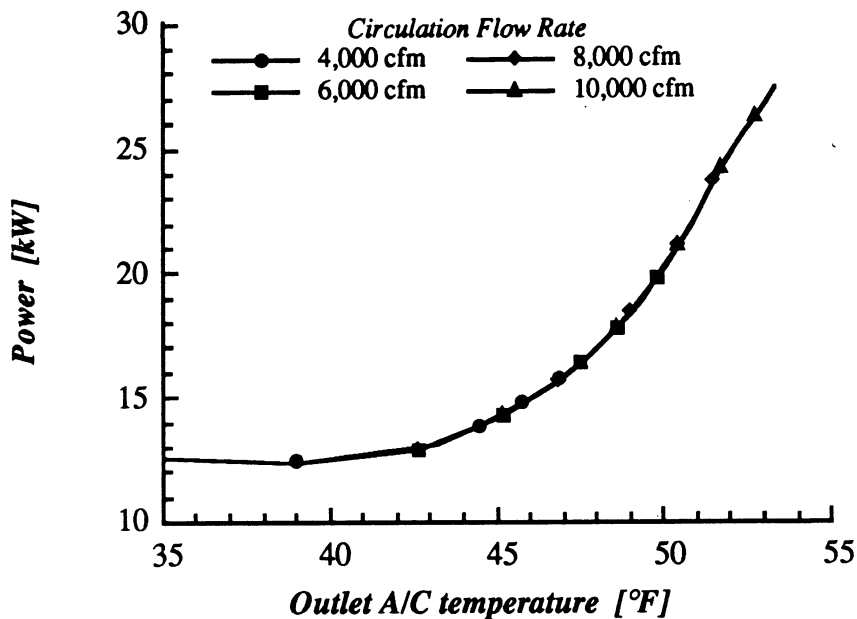
Fig. 3.6 Power versus the outlet air-conditioner coil temperature and circulation flow rate.
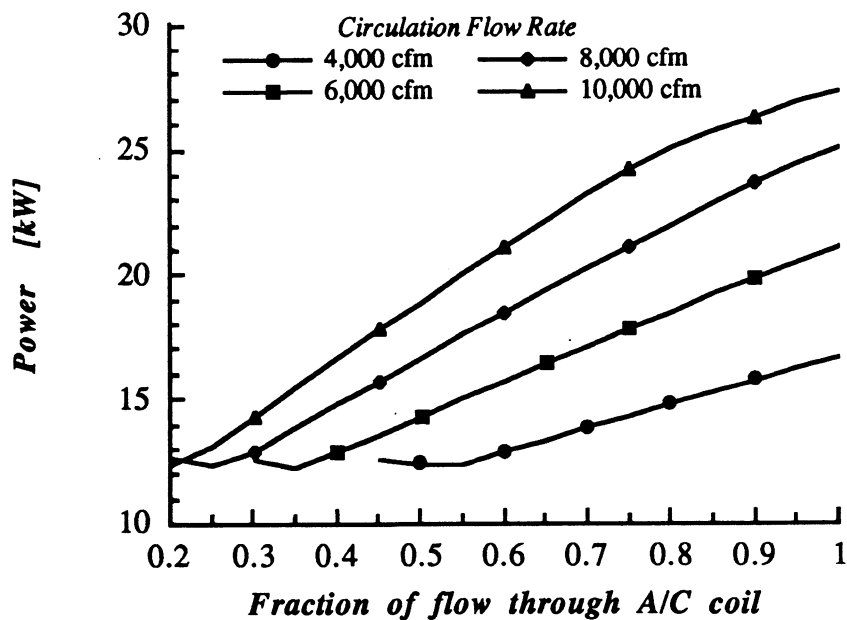
Fig. 3.7 Power as a function of fraction of flow through coil and circulation flow rate.

If too much flow is sent through the coil the power is increased because the latent load is limiting the operating temperature of the coil and some sensible reheat (Fig. 3.8 line M2 - S) is required in order to obtain the correct supply temperature.

Legend
A - A/C outlet state
M1 - Mixture of outdoor
       and return air
M2 - Mixture of A/C outlet
       and return air
R - Desired room state
S - Desired supply state

— — — A/C Operating temperature
            such that reheat is eliminated

Humidity Ratio [lb H_2O/lb dry air]

Dry Bulb Temperature [°F]
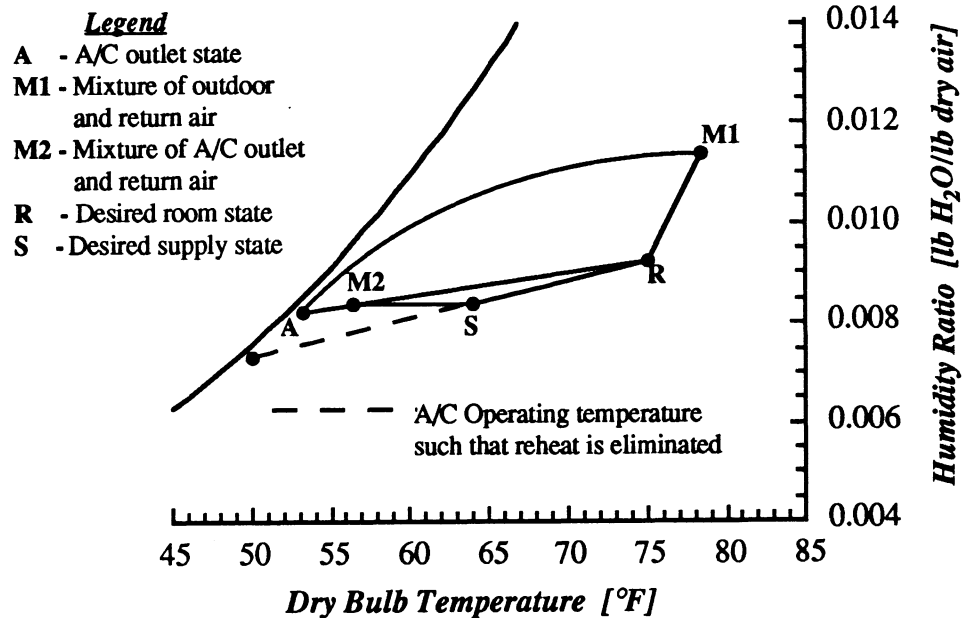
Fig. 3.8 System operation with too much flow through A/C coil.

If too little flow is sent through the coil the power is increased because the sensible load is limiting the operating temperature of the coil and the supply state is too dry (Fig. 3.9 point M2). The power shown in the figure when too little flow is sent through the coil assumes that the space humidity ratio stays constant despite the lower supply humidity; in reality the humidity ratio would decrease slightly (Fig. 3.9 R2).

Theoretically, there is a minimum coil load where the reheat is eliminated, this corresponds to both the sensible and latent load being exactly met. With zero reheat, the coil load is equal to the sum of the space load and the ventilation load (Eq. (2.1)).

However, for low SHRs (large latent loads) the reheat cannot be eliminated because of the load line does not intersect the saturation line on the psychrometric chart.
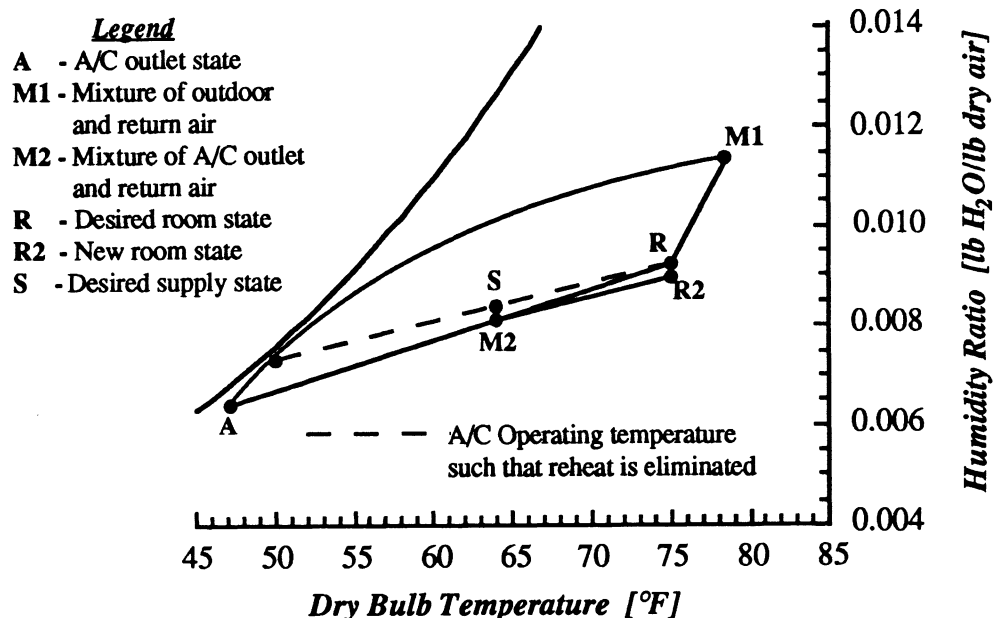
Fig. 3.9 System operation with too little flow through A/C coil.

3.2.2.2 Ventilation flow rate

The A/C coil model takes into consideration the effect of the inlet wet bulb temperature on the performance of the air-conditioner [2]. The COP of the A/C coil decreases for increasing inlet wet bulb temperatures. Figure 3.10 shows that the inlet state does not cause the optimum fraction of flow to change significantly and the ventilation flow rate for the variable flow system only changes the power consumption of the air-conditioner. The reason that the fraction does not change is that the air bypassing the coil is always at the return state, independent of the ventilation flow rate. Therefore, the optimum fraction of air flow through the air-conditioner coil is basically independent

of the ventilation flow rate given that the return air flow rate is sufficient to achieve the outlet A/C state that corresponds to the minimum A/C power.
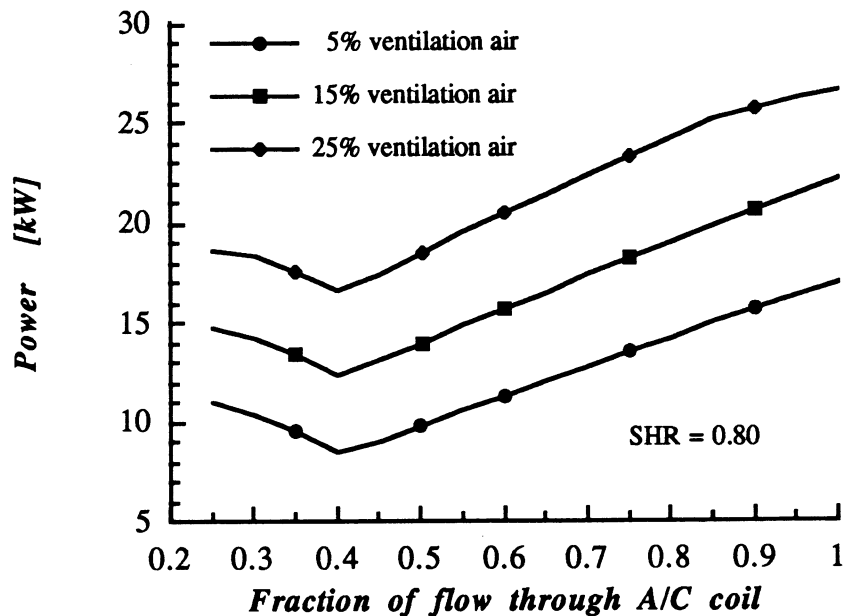
Fig. 3.10 Power versus fraction of circulation flow through air-conditioner coil and ventilation flow rate.

3.2.2.3   Sensible heat ratio

The sensible heat ratio has a large effect the fraction of total flow through the coil that corresponds to minimum power consumption. The SHR is the slope of the load line; therefore, it determines the temperature at which the air-conditioner coil should operate. It also determines whether or not the reheat can be totally eliminated or if the coil will have to be run at the lowest temperature without requiring defrost. Figure 3.11 shows the shift in the optimum fraction for several SHRs. Since the A/C power for SHRs of 0.60, 0.65 and 0.70 in Fig. 3.11 do not reach a minimum for outlet temperatures greater than 38°F (Fig. 3.12), the outlet A/C temperature would be 38°F and some reheat would

be needed in order to obtain the desired supply state. Figure 3.11 also shows that the air-conditioner power decreases with the latent load (increasing SHR) for the conventional system (fraction through the coil equals 1) but the minimum power stays approximately the same because the total space and ventilation loads are identical and the reheat is eliminated thus requiring that the A/C coil loads are identical (Eq. (3.1)).
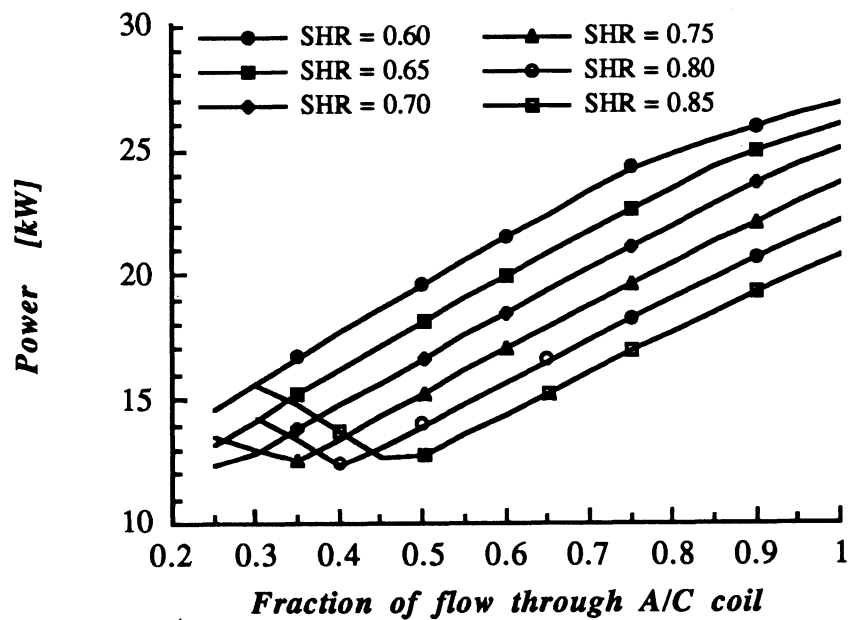
Fig 3.11 Power versus fraction though air-conditioner coil and SHR.

Figure 3.12 demonstrates that the operating temperature in order to minimize the A/C power decreases with the SHR. The power data in Figs. 3.11 and 3.12 are restricted to outlet air temperatures greater than 35°F because the coil defrost cycles that would be required were not modeled.
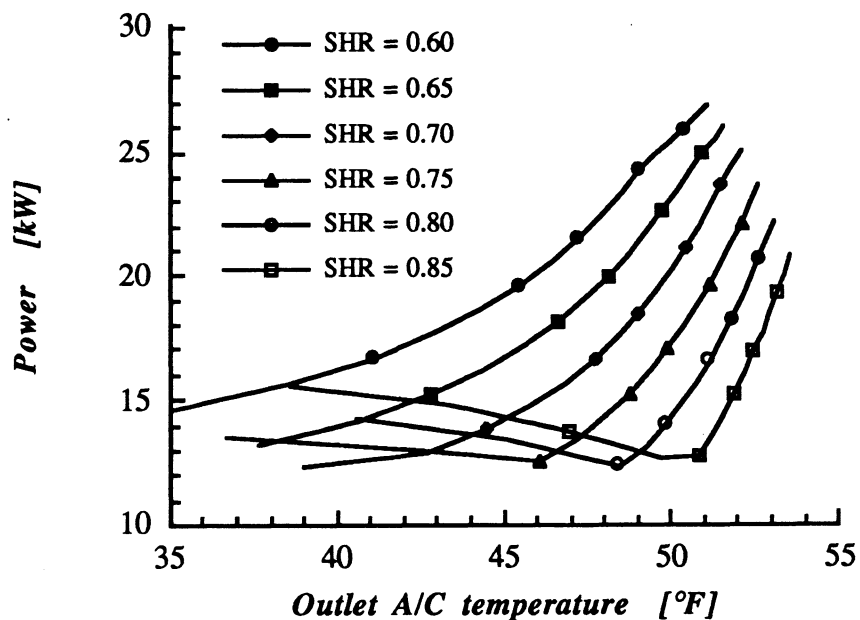
Fig 3.12 Power versus outlet air-conditioner temperature and SHR.

3.2.2.4 Ambient conditions

The ambient conditions, similar to the ventilation flow rate, only affect the amount of power consumed by the air-conditioner and not the optimum fraction through the coil. The power curves for several ambient conditions are shown in Fig. 3.13.

3.2.2.5 Space set-point

The space set-point will affect the power of the A/C coil because the both the ventilation load and the operating temperature of the A/C coil are affected by the set-point. The operating temperature of the coil is affected by the set-point because the load line (with slope equal to the SHR) intersects the saturation line on the psychrometric chart at a different point due to the different starting point (set-point). Figure 3.14 shows that both

the A/C coil power and the fraction of total flow that corresponds to the minimum power change for changing zone set-point.
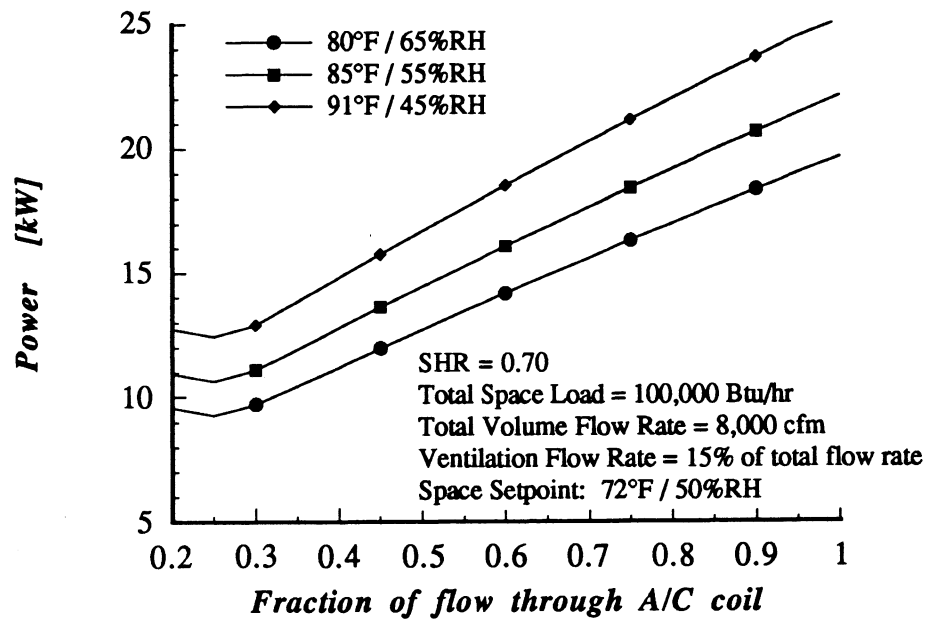
Fig. 3.13 Power versus fraction of circulation flow through A/C coil and ambient conditions.

3.2.2.6 Results of parametric analysis

The fraction of the total flow through the coil that gives the minimum air-conditioner power is dependent only on the space set-point, the total circulation flow, and the SHR of the space load. The ambient conditions and fraction of ventilation mass flow affect the power of the A/C coil, but do not affect the operating temperature or fraction of total flow through coil to obtain minimum power.
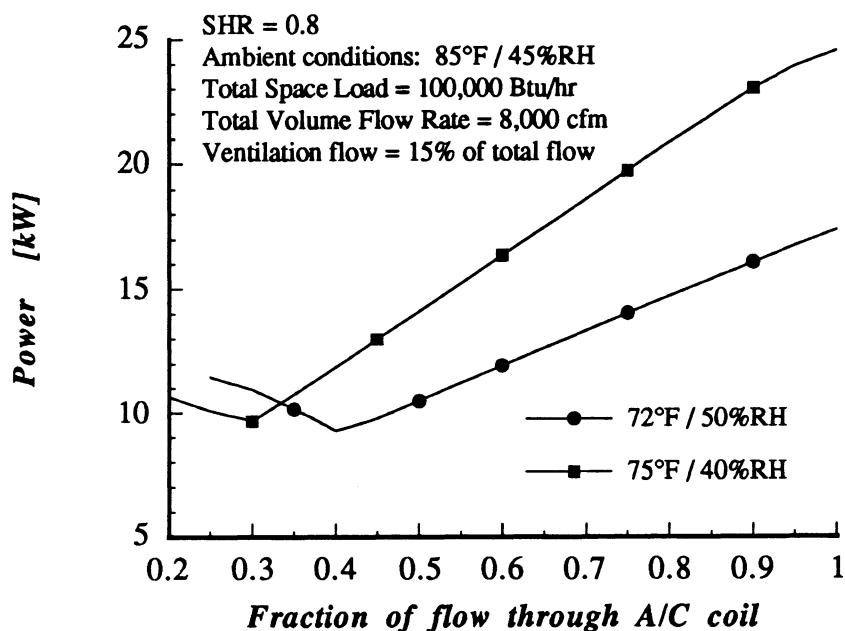
Fig. 3.14 Power versus fraction of flow through A/C coil and space set-point.

3.2.3 Ideal optimum flow through coil

The fraction of total flow through the A/C coil that produces the minimum air-conditioner power is deemed the optimum fraction of flow through the coil. When the required operating temperature is above 38°F, the minimum A/C power occurs when the sensible and latent space loads are met exactly; however, if the space loads require an operating temperature below 38°F, the latent load is met exactly and the outlet state of the A/C is reheated to obtain the required supply temperature. The ideal optimum flow is determined by assuming that the A/C outlet state is saturated. Figure 3.15 shows the ideal optimum flow through the coil as a function of SHR at the nominal design space set-point and load description. For the nominal design SHR of 0.7 and for the SHR of 0.8 the optimum fractions of total flow through the coil are approximately 0.25 and 0.38 respectively, which compares well with the fractions shown in Fig. 3.11. Figure 3.11

was prepared with TRNSYS results that took into consideration a bypass fraction
through the coil that resulted in an outlet state that was not saturated.
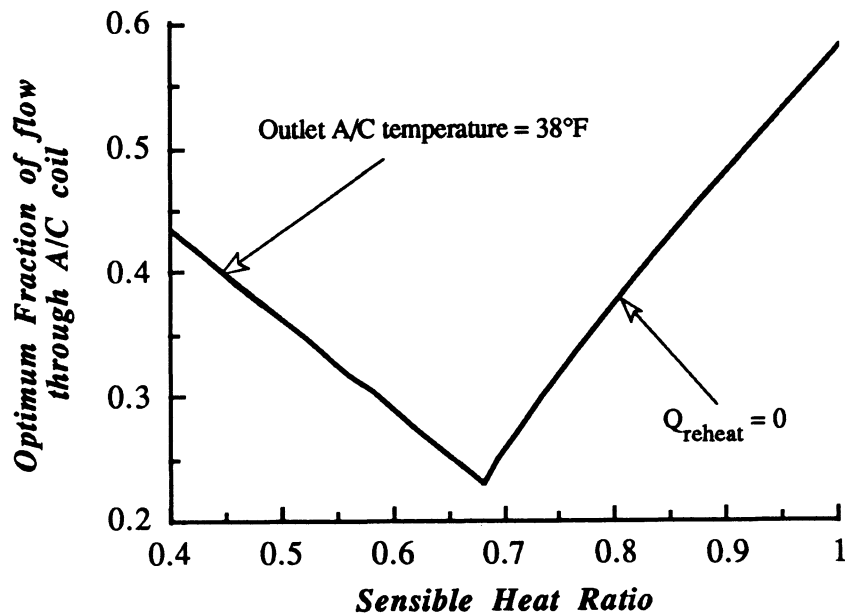
Fig. 3.15 Optimum fraction through the air-conditioner coil for the nominal design.

Figure 3.16 shows the optimum fraction for several different flow rates for the
nominal space set-point. As the flow rate delivered to the space increases, the fraction
though the coil decreases because the supply state moves toward the set-point. The point
on the line for 4,000 cfm when the optimum fraction equals one corresponds to a supply
state at saturated conditions.

3.2.4 Variable flow controller

A controller that determines either the optimum fraction of flow to be sent through
the coil, or the fraction given a constant coil outlet temperature when subject to changing
loads was developed.
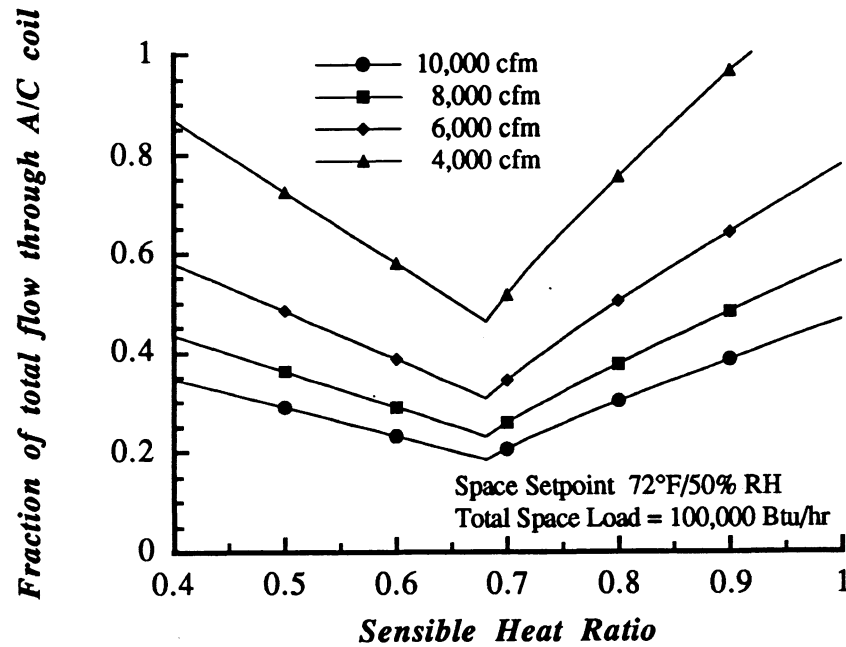
Fig. 3.16 Optimum fraction through coil for several circulation flow rates at nominal space set-point and load.

Rather than curve fitting the results shown in Fig. 3.16, a more fundamental approach was taken in developing the controller. A curve fit of the saturation line on the psychrometric chart (enthalpy and humidity ratio), the space set-point temperature and humidity, and the SHR are used with Newton's method to predict the saturation temperature at which the load line intersects the saturation line. The optimum fraction of flow rate through the coil is calculated using the saturation temperature and humidity ratio (coil outlet state), set-point temperature and humidity ratio, and the circulation flow rate of air through the system. The curve fits for the enthalpy and humidity ratio of the saturation line are as follows:

$$i_{sat} = -2.8065 + 0.5541\,T_{sat} - 0.0055\,T_{sat}^2 + 7.2874\times10^{-5}\,T_{sat}^3 \qquad (3.3)$$

$$\omega_{sat} = 10^{-4}\left(1.2626 + 1.1614\,T_{sat} - 0.0014\,T_{sat}^2 + 4.1348\text{x}10^{-4}\,T_{sat}^3\right) \tag{3.4}$$

where i_{sat} is the enthalpy [Btu/lbm dry air], ω_{sat} is the humidity ratio [lbm water/lbm dry air], and T_{sat} is the saturation temperature [°F]. In addition, the changes in temperature and humidity ratio as a result of sensible and latent loads are simplified as follows:

$$\Delta T = Q_S / 0.24 \tag{3.5}$$

$$\Delta\omega = Q_L / 1061 \tag{3.6}$$

where 0.24 is the specific heat of dry air and 1061 is the heat of vaporization of water.

The inputs the the controller are the space set-point temperature, humidity ratio, and enthalpy, the space load and sensible heat ratio, and the circulation flow rate. Also, if the performance with a constant coil operating temperature is desired, the outlet coil temperature must be input, and if the optimum performance is desired, the convergence tolerance used in Newton's method must be input. The coil outlet state was assumed to be saturated at the outlet temperature because in order to take into account the bypass fraction the inlet state of the A/C coil is needed and this significantly complicates the calculations. Output from the controller is the fraction of the total flow that should be sent through the coil and the temperature of the outlet air from the air-conditioner coil. A flow chart of the controller is shown in Fig. 3.17.

BEGIN

INPUTS
MODE,LOAD,SHR,
MF_TOT,T_SET,W_SET,
H_SET,FRN_VENT

MODE (Opt. Control = 1, Set A/C temp. = 2)
LOAD = Space Load [Btu/hr]
SHR = Sensible Heat Ratio of Space Load
MF_TOT = Circulation mass flow [lbm/hr]
T_SET = Setpoint temperature [°F]
W_SET = Setpoint humidity ratio
         [lbm H2O/lbm dry air]
H_SET = Setpoint enthalpy [Btu/lbm dry air]
FRN_VENT = Fraction of ventilation air

MODE = 1   False   INPUT T_ACO

True

INPUT TOL

T_ACO = Desired constant Outlet A/C temperature [°F]

TOL = Convergence tolerance for optimal controller

MODE = 1   False   T_SAT = T_ACO

True

INITIAL GUESS FOR T_SAT

T_SAT = Outlet A/C temperature

CALCULATE W_SAT

W_SAT = Outlet A/C humidity Ratio

NEWTON'S METHOD TO DETERMINE CORRECT T_SAT

DETERMINE X1 TO MEET SENSIBLE LOAD

DETERMINE X2 TO MEET LATENT LOAD

X = MAX(X1,X2)

X = Fraction of total flow through A/C coil

T_SAT>38°F   False   T_SAT = 38°F

True

DETERMINE X TO GIVE CORRECT SUPPLY STATE

DETERMINE X TO MEET LATENT LOAD

X >1   False   X<FRN_VENT   False

True   True

X = 1   X = FRN_VENT

OUTPUT X, T_SAT

END

Fig. 3.17 Flow chart for optimal controller.

3.2.5 Example of A/C flow control for a varying load

The total space load profile for the design day in the example is shown in Fig. 3.18. The latent load is assumed to be constant at 20,000 Btu/hr and the outdoor and set-point conditions are assumed to be constant at 91°F / 45% RH and 72°F / 50% RH respectively. The constant outdoor conditions will not affect the optimum fraction of the total flow through the coil, but it will affect the air-conditioner power. The air-conditioner coil parameters given in Table 3.1 and the nominal design parameters given in Table 3.2 will be used.
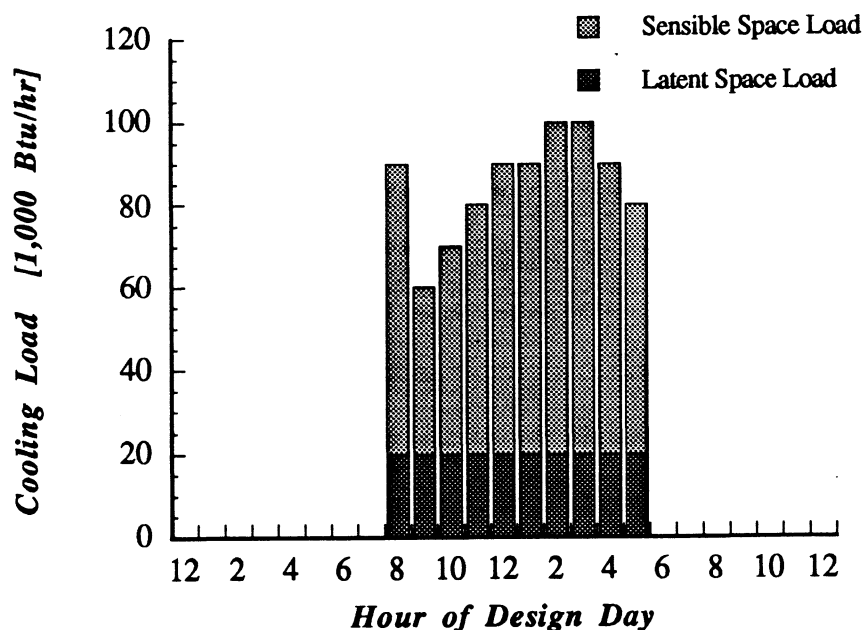
Fig. 3.18 Design day load schedule for variable flow example.

For the conventional system the latent load on the space is the limiting load for the A/C coil. Since the ambient and set-point conditions and the latent load are constant, the load on the coil will be constant because the outlet A/C humidity must be the same in order to meet the latent load. Since the A/C load, ambient conditions and set-point conditions are

constant, the reheat changes as the sensible space load changes. As the sensible space load decreases the supply temperature increases thus increasing the amount of sensible reheat needed. Figure 3.19 shows that the A/C power for the conventional system is constant. The power for the variable flow system varies with the space load because the reheat is eliminated or minimized. This example demonstrates a savings of about 50%.
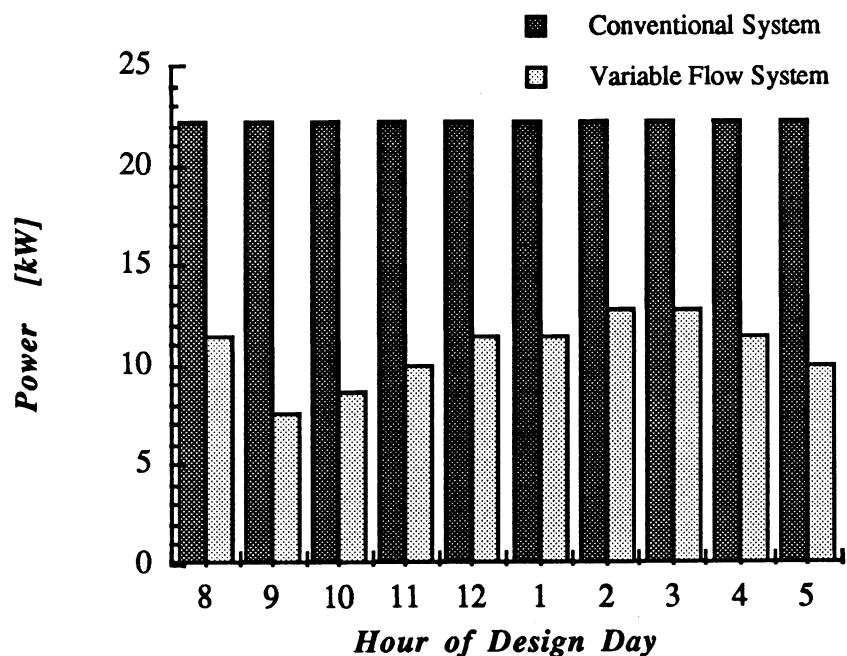
Fig. 3.19 Power of conventional and variable flow systems for variable space load.

3.2.6   Design considerations

The size of the A/C coil is smaller than for the conventional system because the reheat is smaller. The design day loads and ambient conditions determine the size of the A/C coil. In the example in the previous section, the rated capacity of the A/C coil sized for the conventional system was 287,000 Btu/hr based on the maximum A/C coil load of about 237,000 Btu/hr. The maximum A/C coil load for the variable flow system is

decreased to about 161,000 Btu/hr, which is approximately 30% less than the conventional system.

An alternative configuration would be to process less air and mix room air with the supply stream just before the diffuser to increase the supply temperature. This would allow the designer to decrease the duct size and fan power due to the lower flow rates through the system. This configuration is essentially the same as a cold air distribution system except that the amount of air processed is a function of the loads and the total flow of air needed.

3.3 Chapter summary

A variable flow system that minimizes the A/C coil load while meeting both the sensible and latent space loads was presented. The amount of air flow that should be cooled by the A/C coil is a function of the SHR of the space load, the space set-point conditions, and the total flow through the system. The ambient conditions and ventilation flow rate did not affect the amount of flow that should be cooled in order to minimize the A/C coil load. A variable flow rate controller was developed that determines the amount of air flow that should be cooled in order to minimize the A/C coil load. Although the A/C coil must operate at a lower temperature and thus a lower COP, a decrease in power consumption can still be realized because of the decreased load on the coil.

References 3

1. Klein S. A., et al., *TRNSYS: A Transient Simulation Program,* University of Wisconsin - Madison, Engineering Experiment Station Report 38-12, Version 13.1, 1988.

2. Urban, R. E., "The Performance of Conventional and Humid-Climate Vapor-Compression Supermarket Air-Conditioning Systems," M.S. Thesis, University of Wisconsin - Madison, 1988.

Chapter Four

System Comparison and Results

The purpose of this chapter is to compare the following systems with respect to design day energy consumption: 1) conventional CAV system, 2) CAV system with ice-storage, 3) variable flow system, and 4) variable flow system with ice-storage. The amount of energy used during the design day, nominal chiller size and the required amount of storage will be compared.

4.1 Description of systems

The conventional CAV system is shown in Fig. 4.1. The cooling is done by a reciprocating chiller with brine as the working fluid. The sensible reheat is assumed to be free (from the condenser of the chiller); however, the amount of reheat does effect the load on the chiller. For the systems with ice-storage tanks (Fig. 4.2), the chiller is upstream and connected in series. During the day, the chiller operates at its maximum available capacity (i.e. chiller priority) and the tank meets the remainder of the air-conditioning load. The variable flow systems are identical to Figs. 4.1 and 4.2 except that a fraction of the return air flow rate is used to reheat the outlet A/C state.

The space set-point, circulation flow rate, and ambient conditions are identical for all systems. The circulation flow rate is 10,000 cfm and 15% of the circulation flow rate

is ventilation air. The space set-point is 72°F and 50% relative humidity. The ambient

conditions are 91°F and 45% relative humidity.
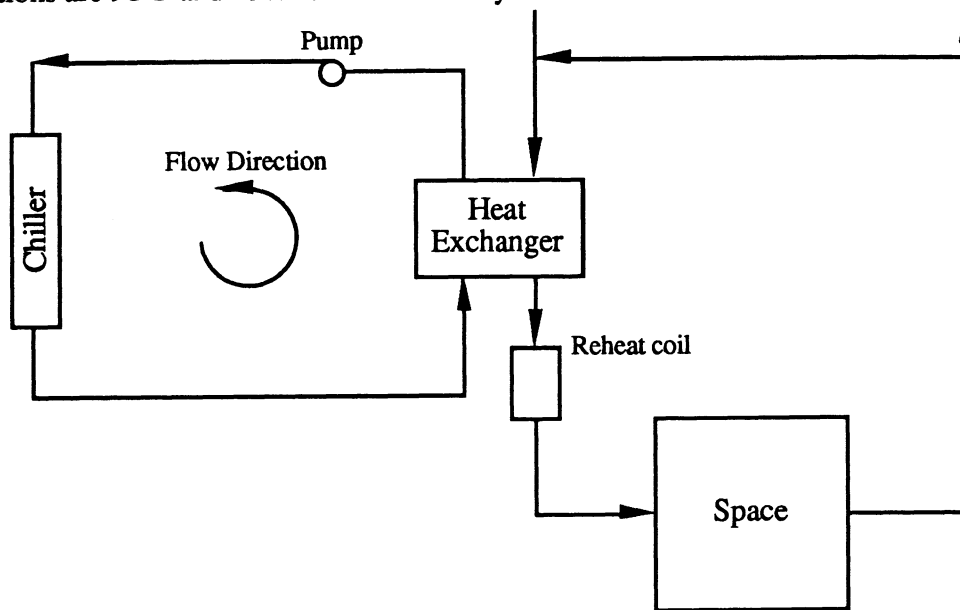
Fig. 4.1 Conventional system configuration.
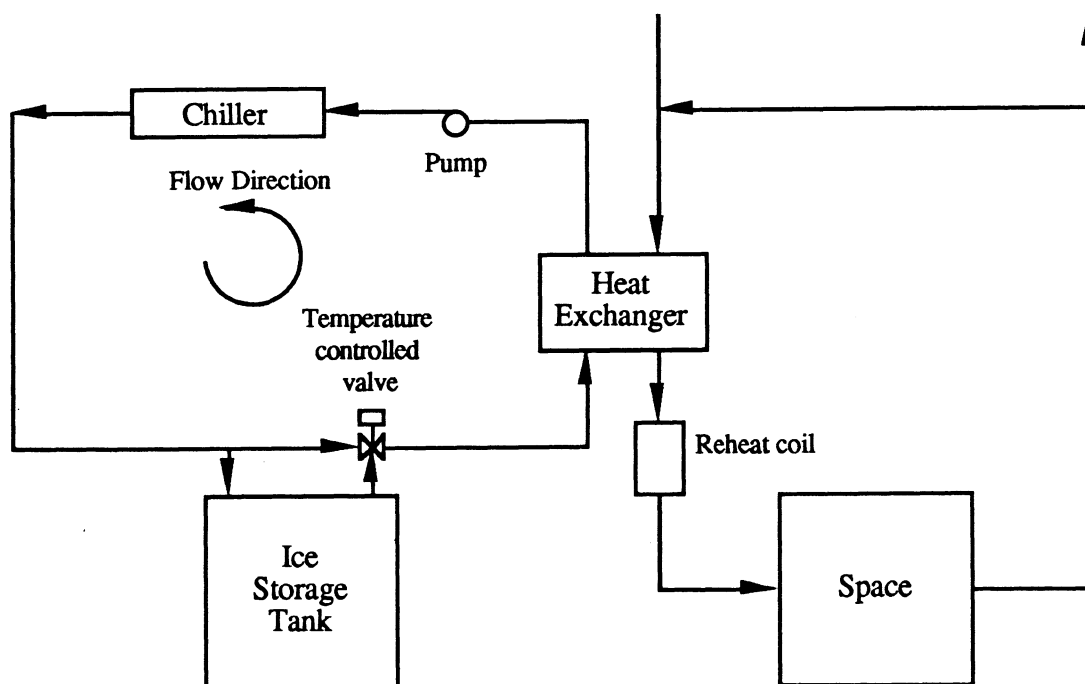
Fig. 4.2 Conventional system with ice-storage configuration.

4.2 System components

The chiller loop is assumed to operate with a constant brine flow rate. The capacity and COP of the chiller are assumed to be linear functions of the chilled brine set temperature (the outlet brine temperature of the cooling coil) [1]. The COP is assumed to have a value of 4 at a chilled brine set temperature of 45°F and 3 at 30°F. The fraction of the nominal chiller capacity is assumed to be 1 at a chiller brine set temperature of 55°F and 0.65 at 25°F.

The heat exchanger between the brine and the air is modeled using the effectiveness model for cooling coils developed by Braun [2]. The required inputs are the number of transfer units on both the air and brine sides of the heat exchanger, the inlet air temperature and humidity ratio, the outlet air temperature and humidity ratio, and the flow rate of brine. The outputs are the required inlet and outlet brine temperatures to the heat exchanger. This heat exchanger model will be used to determine the inlet brine temperature required to obtain the desired outlet air temperature. The same heat exchanger size is used for each system; both the air and brine sides of the heat exchanger are assumed to have $Ntu = 4$.

The ice-storage tank delivers the fraction of the cooling load that the chiller cannot meet. The ice tank is assumed to be the Calmac 1190 model for sizing purposes. The ice-storage tank model will be used to verify that the required loads can be met over the course of the design day.

4.3 Calculation of air-conditioning loads

The total load on the air-conditioner is the sum of the space load, ventilation load, and reheat (Eq. (3.1)). The space load has two components: sensible and latent. These

components determine the outlet air state from the air-conditioner and thus determine the chilled brine set temperature. The space loads are shown in Fig. 4.3. The maximum load is 225,000 Btu/hr. The design latent load of 45,000 Btu/hr is assumed to be constant during the day.
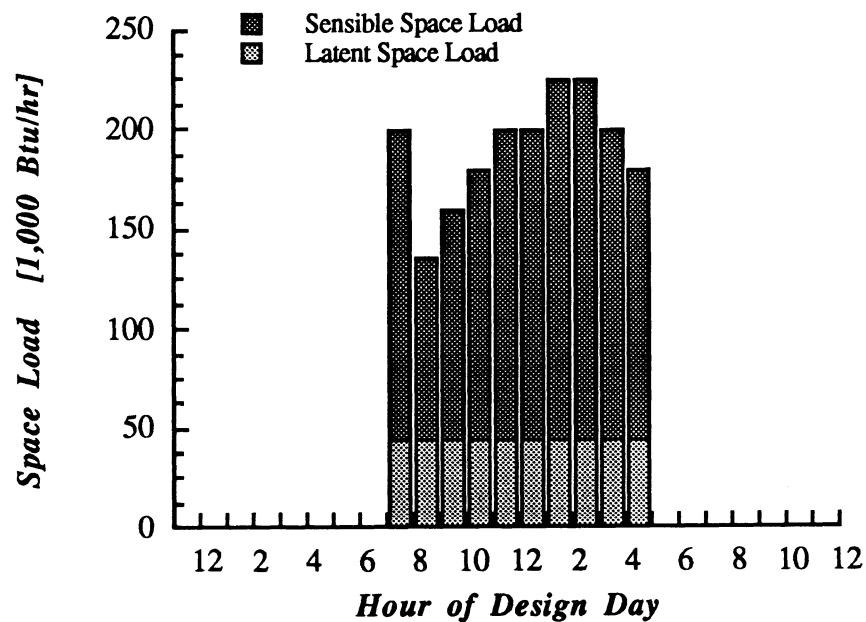
Fig. 4.3 Sensible and latent space loads on design day.

The ventilation load is calculated assuming that the design day ambient temperature and humidity ratio are constant over the course of the day and the ventilation mass flow rate is 15% of the circulation flow rate. Since the ambient conditions and the ventilation mass flow rate are constant the ventilation load is constant at 73,240 Btu/hr.

The sensible reheat is determined from the knowledge of the outlet cooling coil temperature and the supply temperature. The supply temperature is determined from the sensible load on the space and the space set-point temperature. The supply temperature

for the maximum load and a circulation flow rate of 10,000 cfm is about 55°F. The reheat for the conventional system on the design day is shown in Fig. 4.4.
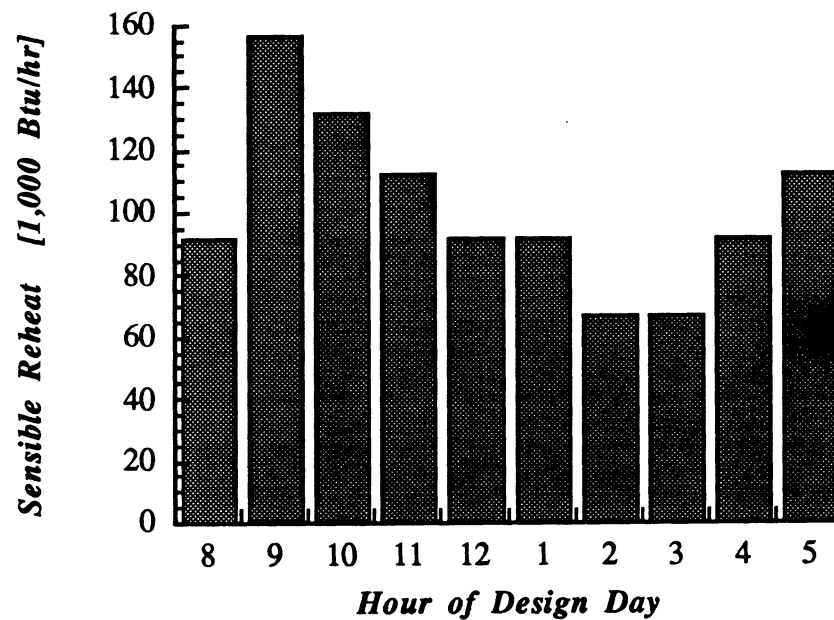
Fig. 4.4 Sensible reheat for the conventional system on design day.

The sensible reheat for the variable flow system is zero except for 6,650 Btu/hr at 9:00 am since the small sensible heat ratio would require an outlet temperature less than 38°F in order to eliminate the reheat.

The total load on the air-conditioner is shown in Fig. 4.5 for the conventional system. The total load on the air-conditioner is shown in Fig. 4.6 for the variable flow system. The integrated load over the design day is 3,652,320 Btu/hr for the conventional system and 2,644,010 Btu/hr for the variable flow system, a reduction of almost 30%.
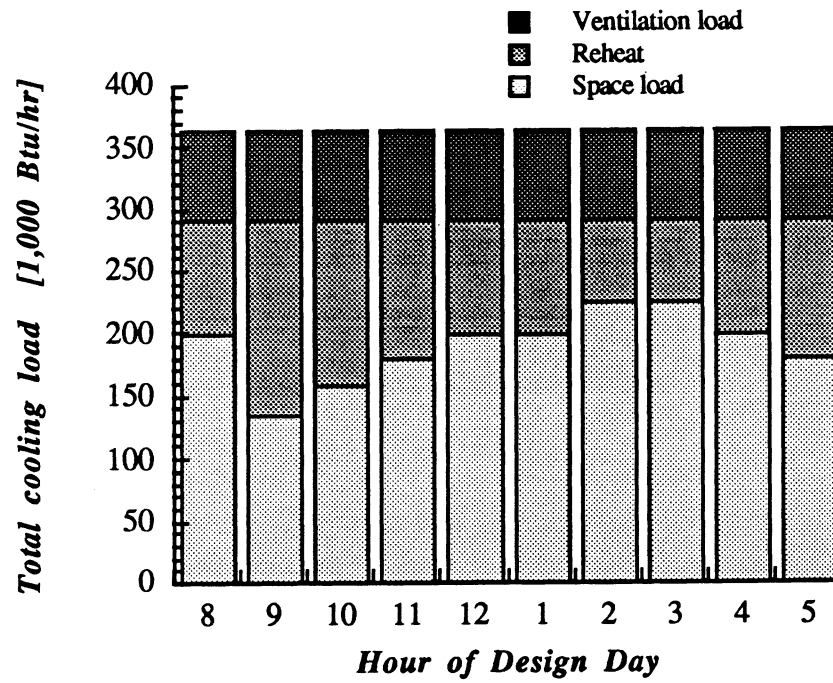
Fig. 4.5 Total cooling load for the conventional system.
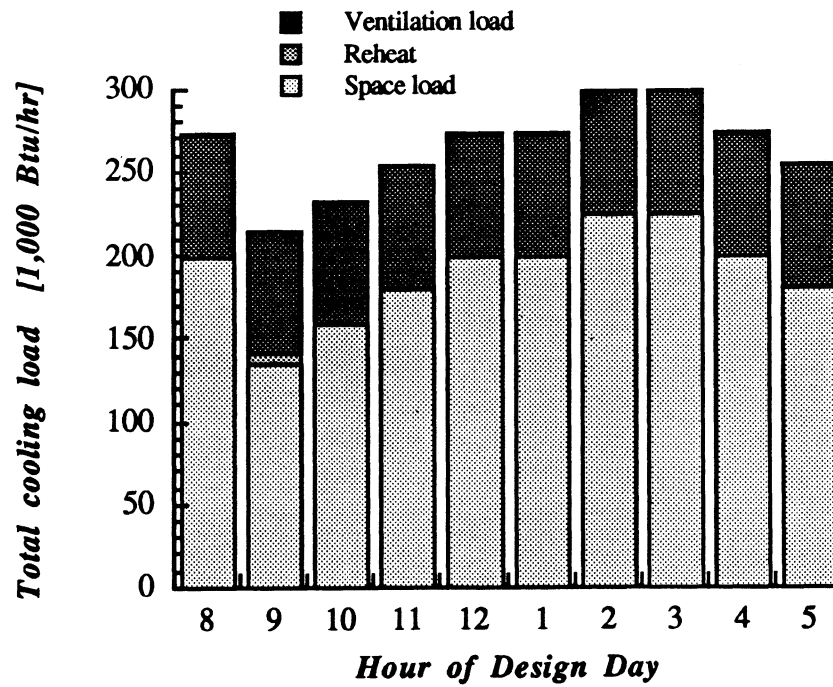
Fig. 4.6 Total cooling load for the variable flow system.

4.4 Sizing of chillers and ice-storage tanks

The nominal chiller size for the conventional system was calculated from the maximum design day load and fraction of nominal capacity at the chilled water set temperature required to meet the space supply state.

The nominal chiller size for the variable flow system was calculated in the same manner; however, the lower chilled brine set temperatures necessitated that at every hour during the design day the available chiller capacity be checked to ensure that the chiller capacity was not exceeded. For this example, the maximum design day load was the load which determined the nominal chiller size.

The chiller for the ice-storage systems must not only deliver part of the load during the day but also charge the ice-storage tank at night. The sizing of the chiller is more complex than for systems without storage. The integrated space loads can be represented as a function of the nominal chiller capacity (NCC),

$$Q_{space} = NCC \left(f_{load} N_{load} + f_{ice} N_{ice} \right) \qquad (4.1)$$

where f_{load} is the fraction of nominal chiller capacity at the chilled brine temperature necessary to meet the load, and f_{ice} is the fraction at the chilled brine temperature necessary to charge the ice-storage tank, N_{load} is the number of hours that the chiller is subject to the load, and N_{ice} is the number of hours that the chiller is charging the tank. The chillers were allotted 11 hours to charge the ice-storage tank.

The ice-storage tanks are sized based on the amount of storage required and the blended outlet temperature from the tank. The fraction of nominal tank capacity that could be discharged is estimated based on the average load on the tank, the inlet temperature to the tank, and the blended outlet temperature (Fig. 2.15). In order to obtain

the number of ice-storage tanks, the required amount of storage is divided by the fraction of nominal tank capacity.

4.5 Comparison of system sizing and design day power consumption

A comparison of the systems is shown in Table 4.1. The parasitic power for the fans is assumed constant for all the designs. The pumping power for the brine loop was conservatively estimated to be less than 5% of the chiller power and therefore was neglected. Therefore, the total design day energy consumption is only the energy required to operate the chiller. The brine flow rate was determined by specifying that the chilled brine set temperature was 43°F at the maximum design day space load; the brine flow rate was approximately 60 GPM for all systems.

	Nominal chiller size [tons]	Amount of storage [ton-hrs]	Peak Daytime [kW]	Daytime energy [kWh]	Total design day energy [kWh]
Constant	36		29.4	293.7	293.7
Constant + ice-storage	19	130.5	15.5	154.5	321.4
Variable	29.5		24.0	216	216.0
Variable + ice-storage	13.5	98.8	11.1	110.9	232.8

Table 4.1 System component and power consumption comparison.

The ice-storage systems required more energy than the corresponding systems without storage due to the reduced COP of the chiller under ice-making conditions; however, the both the peak power and total energy consumption during the daytime were decreased 40 to 50%. Due to variable rate structures and demand charges that increase cost per kWh and kW during peak times respectively, the daytime peak power and total energy consumption are important ways to compare ice-storage systems. The variable flow systems, despite the penalties associated with requiring a lower brine temperature, still reduced the energy consumption for the same air-conditioning loads by 25 to 30%. In addition to the lower energy consumption for the variable flow systems, the nominal chiller capacity was reduced by 18% and 28% for the systems without and with storage respectively. For systems with storage, the required amount of storage was decreased by 24%, but the number of ice-storage tanks was unchanged due to the large nominal capacity.

The loads on the chiller and the ice-storage tank for the design day are shown in Figs. 4.7 and 4.8. The hours with no loads are due to the assumption that the ice-storage tank is charged in 11 hours. The ice-storage tank model verified that the tank can deliver the required cooling at the temperatures required for the variable flow system.

The results from this example can be generalized. If the space loads, brine flow rate, and circulation air flow rate were increased by a factor of 10 the results presented in Table 4.1 would be ten times larger. However, since the ice-storage tanks are in increments of 190 ton-hrs, the flow rate of brine for each tank may be different and an analysis of tank performance would have to be done to insure that the tank can meet the required loads.
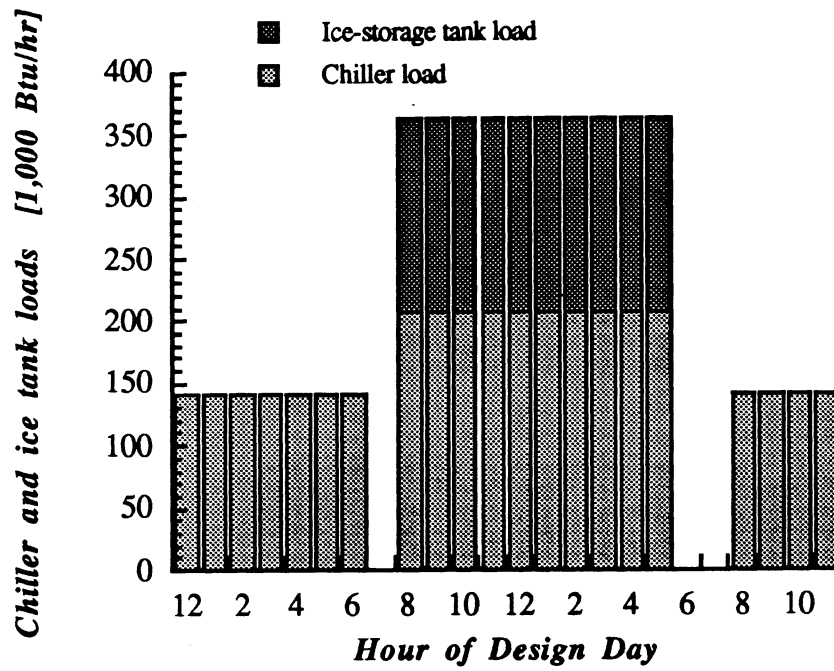
Fig. 4.7 Conventional system loads on the chiller and ice-storage tank.
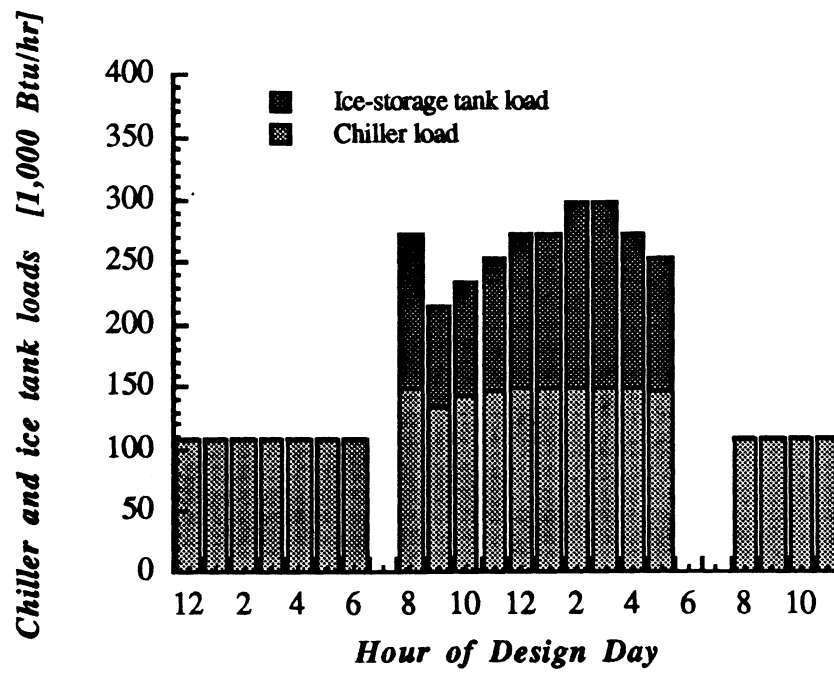
Fig. 4.8 Variable flow system loads on the chiller and ice-storage tank.

4.7 Chapter summary

In this chapter, an example of an air-conditioning system was used to show the trends in design for conventional and variable flow systems with and without ice-storage. In general, systems with ice-storage required smaller chillers than for the corresponding systems without storage and the variable flow systems required less total energy and smaller chillers for the corresponding conventional systems.

References 4

1. Cummings, M. S., "Modeling, Design, and Control of Partial Ice-Storage Air-Conditioning Systems," M.S. Thesis, University of Wisconsin - Madison, 1989.

2. Braun, J. E., "Methodologies for the Design and Control of Central Cooling Plants," Ph.D. Thesis, University of Wisconsin - Madison, 1988.

Chapter Five

Conclusions and Recommendations

This chapter presents the results of this work and cites areas for future research. The results are divided into two sections: ice-storage tank modeling and minimization of air-conditioning load.

5.1 Modeling of ice-storage tanks

A mechanistic model for a static ice-on-coil ice-storage tank with a finite capacitance working fluid was developed. The charging period of tank operation was compared with Calmac's model 1190 with very good results. The model was within 12% of Calmac's average charging rates.

The discharging period of tank operation was modeled and compared with Calmac's performance data for model 1190. The model was within 10% of Calmac's fraction of capacity at which the tank could no longer meet the required load and outlet temperature.

An effectiveness method for both the latent charging and discharging period of tank operation was presented. For the latent charging period, the effectiveness is a function of the volume flow rate of brine through the tank and the charged fraction of latent capacity. For the discharging period, it was deterined that if the resident capacity of

the tank was presented as a ratio of the capacity and the maximum obtainable capacity with the given inlet brine temperature the curves for different inlet temperatures coalesce. The effectiveness of the ice-storage tank for the discharging period is a function of the flow rate of brine through the tank and the ratio of resident to maximum obtainable capacity.

5.2 Minimization of air-conditioning load

The minimization of air-conditioning load was accomplished by reducing the sensible reheat required by the system. A fraction of the relatively warm return air flow rate was mixed with the air-conditioner coil outlet in order to reduce the reheat. The amount of return air that bypasses the cooling coil is a function of the total space load, the sensible heat ratio of the space load, the space setpoint, and the circulation flow rate of air. In order to meet both the sensible and latent loads on the space, the air-conditioner must operate at a lower temperature and therefore a lower coefficient of performance. Despite the decrease in performance, the power requirements of the variable flow system are reduced. Depending on the amount of reheat of the conventional system, the power reduction can be as high as 50%.

A flow rate controller was developed that predicts the fraction of the total air that should be processed by the air-conditioner coil and the required outlet air-condtioner temperature.

5.3 Recommendations for further work

The recommendations for further work are as follows:

- Investigation of the effect that different tube spacings and diameters have on the charging and discharging characteristics of a constrained-area ice-storage tank.

- A year long simulation using the ice-storage tank model to investigate the the design of ice-storage tanks to minimize energy and demand.

- A simulation using the methods of minimization of the air-conditioning load and a comparison to the conventional system.

- Investigate the savings if the air-conditioner is operated at a constant temperature rather than the optimum temperature. Is there an optimum constant temperature?

- Minimization of air-conditioning load with a two-coil, or humid climate, system. The two-coil system has an additional air-conditioning coil in the return air duct that sensible cools the return air.

Appendices

Charge model program listing

```
      program charge
c*********************************************
c*                                          *
c*           Ice-Storage Tank Model         *
c*           ==========================     *
c*           CALMAC Ice-on-Coil Tank        *
c*                                          *
c*     This program simulates the charging period of ice- *
c* storage tank operation.  The inputs are:                *
c*          Tti         Initial tank temperature [F]       *
c*          Tbi         Inlet brine temperature  [F]       *
c*          time_end    Ending time             [hr]       *
c*          dO          Time step               [hr]       *
c*          Flow        Brine flow rate         [GPM]*
c*          Tmin        Minimum allowable outlet          *
c*                      temperature            [F]         *
c*          Perstore    Initial capacity of tank          *
c*                      on tubes              [%]          *
c*                                                          *
c*                              Todd Jekel     *
c*                              5 - 17 - 91    *
c*                                            *
c*********************************************

c----Variable Declaration-------------------------------
```

```
      implicit none

      real*8 A_crit,A_o,Acs_tube,alpha_b,AR
      real*8 B_w,Bw
      real*8 Cap_nom,Capacity,CF,Cp_b,Cp_w,Cv_b,Cv_i,Cv_w
      real*8 D_crit,D_i_tube,D_max,D_o,D_o_temp,D_o_tube,
     &       dm_i,dO,dT,dT_lm,dTdO,dTT
      real*8 eff
      real*8 F,Flow
      real*8 g,Gr_w
      real*8 h_b,h_if,h_w
      real*8 k_b,k_i,k_tube,k_w,kv_b,kv_w,kvb,kvw
      real*8 L_tube,Lat_cap
      real*8 m_i,m_w,mf_tot,mf_tube,mm
      real*8 Ntu,Nu_b,Nu_w
      real*8 Old_dm,Old_T
      real*8 Per_store,pi,Pr_b,Pr_w,Prw
      real*8 Q_gain,Q_net,Q_tot,Q_tube
      real*8 Re_b,rho_b,rho_i,rho_w,Ra_w,RR
      real*8 T_amb,T_bbar,T_bi,T_bo,t_crit,T_film,T_frz,
     &       T_min,T_t,T_ti,T_tank,Tb_i,time,
     &       time_end,Thick,tol,tol2,Ts_avg,TT
      real*8 U_tot,U_tube,UA,UA_tank
      real*8 v
      integer N_tube

      parameter (pi = 3.14159)
      parameter (g = 32.2)        !c [ft/s^2]

c----Statement functions for properties-------------------------

      kv_b(T_bbar) = 0.1416 - 0.005158*(T_bbar-32.)/1.8 + 0.0001097*
     &           ((T_bbar-32.)/1.8)**2.
      B_w(T_film) = abs((-0.279 + 0.00854*T_film - 0.0000411*
     &           T_film**2.)/1000.)
      kv_w(T_film) = (12.24 - 0.2047*T_film + 0.001223*T_film**
     &           2.)/100.        !c [ft^2/hr]
      Pr_w(T_film) = 25.17 - 0.4577*T_film + 0.002843*T_film**2.

c----CALMAC tank-----------------------------------------------

c--------Geometry data----------------------------------------

      open(unit=10,status='old')
      read(10,*)D_i_tube,D_o_tube,t_crit
      read(10,*)L_tube,N_tube
      read(10,*)Cap_nom,UA_tank
      close(10)
```

```
D_i_tube = D_i_tube/12.
D_o_tube = D_o_tube/12.
t_crit = t_crit/12.

D_crit = D_o_tube + 2.*t_crit
A_crit = pi*D_crit*L_tube
D_max = D_crit*sqrt(2.)

c--------Thermal data-------------------------------------------

T_amb = 70.                   !c [F]
k_tube = 0.30                 !c [Btu/hr-ft-F]
m_w = 13527.                  !c [lbm]

c----Brine Properties--------------------------------------------

alpha_b = 0.00489
Cp_b = 0.90                   !c [Btu/lbm-F]
k_b = 0.303                   !c [Btu/hr-ft-F]
rho_b = 64.93                 !c [lbm/ft^3]

c----Water/Ice Properties----------------------------------------

Cp_w = 1.01                   !c [Btu/lbm-F]
Cv_w = 1.01                   !c [Btu/lbm-F]
rho_w = 62.4                  !c [lbm/ft^3]
T_frz = 32.                   !c [F]

Cv_i = 0.487                  !c [Btu/lbm-F]
k_i = 1.09                    !c [Btu/hr-ft-F]
rho_i = rho_w
c    rho_i = 57.5             !c [lbm/ft^3]
h_if = 144.0                  !c [Btu/lbm]

c----Convergence tolerances--------------------------------------

tol = 1.E-8
tol2 = 1.E-3

c----Read in system variables------------------------------------

print*,'Enter the initial tank temperature [F]:'
read*,T_tank
print*,'Enter the average entering brine Temperature [F]:'
read*,T_bi
print*,'Enter the time to charge, and timestep:'
read*,time_end,dO
print*,'Enter the total brine flow rate [GPM]:'
```

```
      read*,Flow
      print*,'Enter the minimum allowable outlet temperature [F]:'
      read*,T_min
      print*,'Enter the initial capacity of tank [%]:'
      read*,Per_store

c----Determine relavent constants-------------------------------

      Acs_tube = pi*D_i_tube**2./4.
      U_tube = log(D_o_tube/D_i_tube)/k_tube
      Lat_cap = m_w*h_if
      mf_tot = 36455.5*Flow/70.              !c [lbm/hr]
      mf_tube = mf_tot/N_tube
      v = mf_tube/(rho_b*Acs_tube)


c---------------------------------------------------------------
c----Charging Analysis------------------------------------------
c---------------------------------------------------------------

c----Estimate brine outlet temperature and tube/ice surface temp-

      T_bo = T_bi + 0.75*(T_ti-T_bi)
      Ts_avg = T_bi - (T_bi - (T_bo+T_bi)/2.)/2.

c----Set initial conditions-------------------------------

      Capacity = 0.
      dTT = 0.
      Old_T = T_tank
      T_t = T_tank
      time = 0.0
      CF = 1.
      dm_i = 0.
      m_i = Per_store*m_w*(rho_i/rho_w)
      D_o = sqrt(D_o_tube**2+4.*m_i/(rho_i*pi*L_tube*N_tube))
      if (D_o .gt. D_crit) then
           call dia(D_crit,D_o,D_o_tube,dm_i,L_tube,m_i,N_tube,rho_i)
      end if
      D_o_temp = D_o

c----Time loop-------------------------------------------

      do while (D_o .le. D_max)

c----Determine heat transfer coeff. inside tube------------------

100   T_bbar = (T_bi+T_bo)/2.
      kvb = kv_b(T_bbar)
      Re_b = v*D_i_tube/kvb
```

```
      Pr_b = kvb/alpha_b
      Nu_b = 0.023*Re_b**0.8*Pr_b**0.4
      h_b = Nu_b*k_b/D_i_tube

c----Determine heat transfer coeff. outside tube/ice surface----

      if (D_o .le. D_crit) then
        T_film = (Ts_avg + T_tank)/2.
        dT = abs(Ts_avg - T_tank)
        kvw = kv_w(T_film)
        Prw = Pr_w(T_film)
        Bw = B_w(T_film)
        Bw = dmax1(dble(5.e-6),Bw)
        Gr_w = g*D_o**3.*Bw*dT/(kvw/3600.)**2.
        Ra_w = Gr_w*Prw
        Nu_w = (0.6 + 0.387*Ra_w**(1./6.)*(1+(0.559/Prw)**
     &        (9./16.))**(-8./27.))**2.
        k_w = kvw*rho_w*Cp_w/Prw      !c [Btu/hr-ft-F]
        h_w = Nu_w*k_w/D_o
      else
c----h_w is constant at the value it had at D_o = D_crit--------
      end if

c----Determine the total conductance--------------------------

      if (D_o .le. D_crit) then
        A_o = pi*D_o*L_tube
        U_tot = 1./(D_o/(h_b*D_i_tube)+D_o*U_tube/2.+
     &        D_o*log(D_o/D_o_tube)/(2.*k_i)+1./h_w)
        UA = U_tot*A_o
      else if ((D_o .gt. D_crit) .and.
     &        (D_o .lt. D_max)) then
        A_o = D_o*(pi - 4.*acos(D_crit/D_o))*L_tube
        AR = A_o/A_crit
        RR = D_o_tube/D_crit
        CF = F(RR,AR)
        U_tot = 1./(A_o/(h_b*pi*D_i_tube*L_tube)+A_o*U_tube/(
     &        2.*pi*L_tube)+A_o*log(D_crit/D_o_tube)/(2.*pi*k_i*
     &        CF*L_tube)+1./h_w)
        UA = U_tot*A_o
      else
        A_o = 0.
        time = time-dO
        goto 200
      end if

      Ntu = UA/(mf_tube*Cp_b)
      T_bo = T_tank + (T_bi-T_tank)*exp(-Ntu)
      dT_lm = ((T_tank-T_bo)-(T_tank-T_bi))/log((T_tank-T_bo)/
```

```
   &        (T_tank-T_bi))
         Q_tube = abs(UA*dT_lm)
         Q_tot = N_tube*Q_tube
   if (time .eq. 0.) then
   print*,time,Q_tot/12000.
   end if
         eff = Q_tot/(mf_tot*Cp_b*(T_tank-T_bi))
         Q_gain = UA_tank*(T_amb - T_tank)
         Q_net = Q_tot-Q_gain
         if (Q_net .lt. 0.) then
           time = time-dO
           goto 200
         end if
         Ts_avg = T_tank - Q_net/(h_w*N_tube*A_o)

         if (T_tank .gt. T_frz) then
           dTdO = Q_net/(m_w*Cv_w)
           T_tank = T_t - dO*dTdO
         else
           T_tank = T_frz
           if (D_o .lt. D_crit) then
             dm_i = Q_net*dO/h_if
             D_o = dsqrt(D_o_temp**2.+4.*dm_i/(rho_i*pi*L_tube*
   &                N_tube))
           else
             dm_i = Q_net*dO/h_if
           call dia(D_crit,D_o,D_o_tube,dm_i,L_tube,m_i,
   &            N_tube,rho_i)
           end if
         end if

         mm = abs(dm_i-Old_dm)
         TT = abs(T_tank-Old_T)

         if ((mm .gt. tol) .or. (TT .gt. tol2)) then
           Old_dm = dm_i
           Old_T = T_tank
           goto 100
         else
           m_i = m_i+dm_i
           Per_store = m_i/(m_w*rho_i/rho_w)
           T_t = T_tank
           Thick = (D_o - D_o_tube)/2.
           D_o_temp = D_o
c          if (T_t .gt. T_frz) then
c            write(7,111)time,0.,eff,0.,Q_net/12000.,T_bo
c          else
             write(7,111)time,Per_store,T_t,Thick,Q_net/12000.,
   &                (T_bo-T_bi)/(T_t-T_bi)
```

```
c       end if
        end if

        Capacity = Capacity+Q_net*dO/12000.
        dTT = dTT+(T_bo-T_bi)*dO
        if (T_bo .lt. T_min) goto 200
        if (time+dO .gt. time_end) goto 200
        time = time + dO

      end do

200 write(*,1000)T_bi,Flow,time,Per_store,dTT/time,Capacity/time

111 format(1x,f7.4,f9.4,4f13.5)
1000 format(1x,2F8.1,4F10.4)

      STOP
      end

      subroutine dia(D_crit,D_o,D_o_tube,dm_i,L_tube,m_i,
     &          N_tube,rho_i)

      implicit none

      real*8 D_crit,D_o,D_o_tube,dm_i,L_tube,m_i,rho_i
      real*8 dMdD,f,M,mass,pi,tol
      integer i,N,N_tube

      parameter (pi = 3.14159)

      mass = (m_i+dm_i)/N_tube
      tol = 1.E-8
      N = 50

      do 10, i = 1,N
       M = rho_i*(D_crit*L_tube*(D_o**2.-
     &     D_crit**2.)**0.5 + (pi/4.-acos(D_crit/D_o))*
     &     L_tube*D_o**2. - pi*D_o_tube**2.*L_tube/4.)
       dMdD = rho_i*(pi*D_o*L_tube/2. -
     &     2*D_o*L_tube*acos(D_crit/D_o))
       f = D_o - (M-mass)/dMdD
       if ((f-D_o) .lt. tol) then
          return
       else
          D_o = f
       end if
10 continue
     write(7,*)'Method failed after 50 iterations!'
     stop
```

```
end

function f(RR,AR)

real*8 AR,CF,F,max

max = 1.

sqrtAR = dsqrt(AR)
CF = -1.44066*AR+2.45495*sqrtAR+RR*(3.1164*AR-3.1518*sqrtAR)

F = dmin1(CF,max)

end
```

Appendix B

Discharge model program listing

```
      program discharge
c******************************************
c*                                        *
c*          Ice-storage Tank Model        *
c*          =====================         *
c*          CALMAC Ice-on-Coil Tank       *
c*                                        *
c*     This program simulates the discharging period of ice-*
c* storage tank operation. The inputs are:              *
c*          nhd          Number of hours of discharge*
c*          Tbi          Inlet brine temperature  [F]   *
c*          time_step    time step            [hr]  *
c*          TBO          Blended outlet brine        *
c*                       temperature          [F]   *
c*          Q or Flow    Discharge rate or volume    *
c*                       flow rate of brine through   *
c*                       the tank        [tons or GPM]*
c*                                        *
c*                                Todd Jekel   *
c*                                5 - 17 - 91  *
c*                                        *
c******************************************

c----Variable Declaration---------------------------------

      implicit none

      real*8 A_crit,A_o,A_ice,Acs_tube,alpha_b,AR
      real*8 B_w,Bw,Bw_min
      real*8 Cap_nom,Capacity,CF,Cp_b,Cp_w,Cv_b,Cv_i,Cv_w
      real*8 D_crit,D_i_tube,D_max,D_o,D_o_temp,D_o_tube,ddm,
     &       dD_o_tempdO,dD_odO,dm_w,dO,dT,dT_lm,dTbdO_w,dTdO,
     &       dU_w,dTT,dTlm
      real*8 f,ff,Flow,fract
      real*8 g,Gr_w
      real*8 h_b,h_if,h_w,h_wi,h_w1
      real*8 k_b,K_crit,k_i,k_tube,k_w,kv_b,kv_w,kvb,kvw
      real*8 L_tube,Lat_cap
      real*8 m_w,m_w_crit,m_w_tot,mf_tot,mf_tube,mf_tank
      real*8 Ntu,Nu_b,Nu_w,Nu_b1,Nu_b2
      real*8 Old_dm,Old_T,one
      real*8 Per_store,pi,Pr_b,Pr_w,Prw
```

```
      real*8 Q_des,Q_gain,Q_ice,Q_net,Q_tot,Q_tube
      real*8 Re_b,rho_b,rho_i,rho_w,Ra_w,RR,RePrDL
      real*8 stp_hr
      real*8 T_amb,T_bbar,T_bi,T_bo,t_crit,T_des,T_film,T_frz,
     &     T_wi,T_wo,T_min,T_t,T_ti,T_tank,T_temp,Tb,Tb_w,time,
     &     time_end,Thick,tol,Ts_avg,TT,T_b_diff
      real*8 U_b,U_t,U_tot,U_tube,U_w,UA,UA_tank,U_tott
      real*8 v,x
      real*8 zero
      integer N_tube,mode,step,nhd,nhdstep

      common /H2O_PROP/Bw,k_w,kvw,Prw
      common /TANK_GEOM/D_o_tube,L_tube

      parameter (pi = 3.14159)
      parameter (g = 32.2)        !c [ft/s^2]
      parameter (one = 1.)
      parameter (zero = 0.)
      parameter (Bw_min = 5.e-6)

c----Statement functions for properties-------------------------

      kv_b(T_bbar) = 0.1416 - 0.005158*(T_bbar-32.)/1.8 + 0.0001097*
     &          ((T_bbar-32.)/1.8)**2.
      B_w(T_film) = abs((-0.279 + 0.00854*(T_film+1.) - 0.0000411*
     &          (T_film+1.)**2.)/1000.)
      kv_w(T_film) = (12.24 - 0.2047*T_film + 0.001223*T_film**
     &          2.)/100.        !c [ft^2/hr]
      Pr_w(T_film) = 25.17 - 0.4577*T_film + 0.002843*T_film**2.

c----CALMAC tank-------------------------------------------------

c--------Geometry data-------------------------------------------

      open(unit=10,status='old')
      read(10,*)D_i_tube,D_o_tube,t_crit
      read(10,*)L_tube,N_tube
      read(10,*)Cap_nom,UA_tank
      close(10)
      D_i_tube = D_i_tube/12.   !c [ft]
      D_o_tube = D_o_tube/12.        !c [ft]
      t_crit = t_crit/12.   !c [ft]
      D_crit = D_o_tube + 2.*t_crit
      K_crit = N_tube*144.*62.4*pi*L_tube*(D_crit**2-D_o_tube**
     &      2)/(4.*Cap_nom*12000.)
      A_crit = pi*D_crit*L_tube
      D_max = D_crit*sqrt(2.)

c--------Thermal data--------------------------------------------
```

```
      T_amb = 70.              !c [F]
      k_tube = 0.30            !c [Btu/hr-ft-F]
      m_w_tot = 13527.                !c [lbm]

c----Brine Properties-------------------------------------------

      alpha_b = 0.00489
      Cp_b = 0.9               !c [Btu/lbm-F]
      k_b = 0.303              !c [Btu/hr-ft-F]
      rho_b = 64.93            !c [lbm/ft^3]

c----Water/Ice Properties---------------------------------------

      Cp_w = 1.01              !c [Btu/lbm-F]
      Cv_w = 1.01              !c [Btu/lbm-F]
      rho_w = 62.4             !c [lbm/ft^3]
      T_frz = 32.              !c [F]

      Cv_i = 0.487             !c [Btu/lbm-F]
      k_i = 1.09               !c [Btu/hr-ft-F]
      rho_i = 62.4             !c [lbm/ft^3]
      h_if = 144.0             !c [Btu/lbm]

c----Determine relavent constants-------------------------------

      Acs_tube = pi*D_i_tube**2./4.
      U_tube = log(D_o_tube/D_i_tube)/k_tube
      Lat_cap = m_w_tot*h_if
      m_w_crit = rho_w*pi*(D_crit**2-D_o_tube**2)*N_tube*L_tube/4.

c----Read in system variables-----------------------------------

      T_ti = 32.              !c [F]
      print*,'Enter the number of hours to discharge:'
      read*,nhd
      print*,'Enter the average entering brine Temperature [F]:'
      read*,T_bi
      print*,'Enter the timestep:'
      read*,dO
      print*,'Enter the desired blended outlet temperature [F]:'
      read*,T_des
      print*,'Enter mode:  1 = Q_des. 2 = GPM'
      read*,mode
      if (mode .eq. 1) then
        print*,'Enter the desired discharge rate [tons]:'
        read*,Q_des
        Flow = 25.5*Q_des/(T_bi-T_des)
      else
```

```
      print*,'Enter the system flow rate [GPM]:'
      read*,Flow
   end if
   mf_tot = 36455.5*Flow/70.            !c [lbm/hr]


c-----------------------------------------------------------
c----Discharging Analysis--------------------------------
c-----------------------------------------------------------


   Capacity = 0.
   dTT = 0.
   mf_tank = mf_tot*(T_bi-T_des)/(T_bi-32.)
   mf_tube = mf_tank/N_tube
   v = mf_tube/(rho_b*Acs_tube)

c----Estimate brine outlet temperature and tube/ice surface temp-

   T_bo = T_bi + 0.75*(T_ti-T_bi)
   Ts_avg = T_bi - (T_bi - (T_bo+T_bi)/2.)/2.

c----Set initial conditions----------------------------

   step = 0
   nhdstep = 1
   T_tank = T_ti
   D_o = D_o_tube
   D_o_temp = D_o
   Old_T = 32.
   time = 0.0
   time_end = time_end+dO
   tol = 1.E-4
   m_w = 0.
   dm_w = 0.
   stp_hr = 1.

c----Time loop----------------------------------------------

   do while (Capacity .le. Cap_nom)

c----Determine heat transfer coeff. inside tube-----------------

100  T_bbar = (T_bi+T_bo)/2.
     kvb = kv_b(T_bbar)
     Re_b = v*D_i_tube/kvb
     Pr_b = kvb/alpha_b
     RePrDL = (D_i_tube/L_tube)*Re_b*Pr_b
     Nu_b1 = 3.66+(0.0534*(RePrDL)**(1.15))/(
&         1.+0.0335*(RePrDL)**(0.82))
     Nu_b2 = 0.023*Re_b**0.8*Pr_b**0.4
```

```
      if (Re_b .lt. 700.) then
        Nu_b = Nu_b1
      else if (Re_b .gt. 1300.) then
        Nu_b = Nu_b2
      else
        Nu_b = (Nu_b1*(1300.-Re_b)+Nu_b2*(Re_b-700.))/(1300.-700.)
      end if
      h_b = Nu_b*k_b/D_i_tube


c----Determine the properties of the water----------------------

      T_film = (Ts_avg + T_tank)/2.
      kvw = kv_w(T_film)
      Prw = Pr_w(T_film)
      k_w = kvw*rho_w*Cp_w/(Prw)
      Bw = dmax1(Bw_min,B_w(T_film))


c----Determine the effective thermal conductivity---------------

      if (m_w .lt. m_w_crit) then

c----Determine the total conductance---------------------------

      A_o = pi*D_o_temp*L_tube
      U_b = D_o_temp/(h_b*D_i_tube)
      U_t = U_tube*D_o_temp/2.
      U_w = D_o_temp*log(D_o_temp/D_o_tube)/(2.*k_w)
      U_tot = 1./(U_b+U_t+U_w)
      UA = U_tot*A_o
      Ntu = UA/(mf_tube*Cp_b)

      T_bo = T_frz + (T_bi-T_frz)*exp(-Ntu)
      dT_lm = ((T_frz-T_bo)-(T_frz-T_bi))/log((T_frz-T_bo)/
     &        (T_frz-T_bi))
      Q_tube = abs(UA*dT_lm)
      Q_tot = N_tube*Q_tube
      Q_gain = UA_tank*(T_amb - T_frz)
      Q_net = Q_tot+Q_gain
      if (m_w .ne. 0.) then
      T_wi = T_frz + Q_tube/(1./(log(D_o_temp/D_o_tube)
     &        /(2.*pi*k_w*L_tube)))
        T_wo = T_frz
        T_tank = T_wo - (T_wo-T_wi)*(1./(2.*log(D_o_temp/
     &        D_o_tube)) - D_o_tube**2/(D_o_temp**2-
     &           D_o_tube**2))
        dTbdO_w = abs(T_temp - T_tank)/dO
        Ts_avg = T_wi
      else
        Ts_avg = T_frz
```

```
            dTbdO_w = 0.
            end if
            dU_w = m_w*Cp_w*dTbdO_w
            Q_ice = Q_net-dU_w
            dm_w = (Q_net-dU_w)*dO/(h_if)    !c +Cp_w*(T_tank-T_frz))
            D_o_temp = dsqrt(D_o**2+4.*dm_w/(rho_w*pi*L_tube*
     &            N_tube))
            if (m_w .gt. (m_w_crit-200.)) then
              h_wi = (Q_net-dU_w)/(N_tube*A_o*(T_tank-T_frz))
              T_t = T_tank
              dTlm = ((T_t-T_bo)-(T_t-T_bi))/log(abs((T_t-T_bo)/
     &          (T_t-T_bi)))
              U_tott = Q_tot/abs(pi*D_o_tube*L_tube*N_tube*dTlm)
              h_w = 1./(1./U_tott-D_o_tube/(h_b*D_i_tube)-D_o_tube*
     &            U_tube/2.)
            end if

          else if (m_w .gt. m_w_crit) then

            if (m_w .gt. m_w_tot) m_w = m_w_tot
c           Gr_w = abs((g*Bw*dT*D_o_tube**3)/(kvw/3600.)
c    &            **2)
c           Ra_w = Gr_w*Prw
c           Nu_w = (0.6+0.387*Ra_w**(1./6.)*(1.+(0.559/Prw)**
c    &            (9./16.))**(-8./27.))**2
c           h_w = ff*Nu_w*k_w/D_o_tube

c----Determine the total conductance---------------------------

            A_o = pi*D_o_tube*L_tube
            U_tot = 1./(D_o_tube/(h_b*D_i_tube)+D_o_tube*U_tube/2.+
     &        1./h_w)

            UA = U_tot*A_o
            Ntu = UA/(mf_tube*Cp_b)

            T_bo = T_tank + (T_bi-T_tank)*exp(-Ntu)
            dT_lm = ((T_tank-T_bo)-(T_tank-T_bi))/log((T_tank-T_bo)/
     &        (T_tank-T_bi))
            Q_tube = abs(UA*dT_lm)
            Q_tot = N_tube*Q_tube
            Q_gain = UA_tank*(T_amb - T_tank)
            Q_net = Q_tot+Q_gain
            Ts_avg = T_tank+(Q_net/N_tube)/(h_w*A_o)

            if (m_w .ge. m_w_tot) then
              m_w = m_w_tot
              dm_w = 0.
              dTdO = Q_net/(m_w*Cv_w)
```

```
      T_tank = T_temp + dO*dTdO
      else
      A_ice = dmax1(zero,D_o_temp*(pi-4.*acos(D_crit/D_o_temp)
     &        )*L_tube)
      Q_ice = h_wi*N_tube*A_ice*(T_tank-T_frz)
      dm_w = Q_ice*dO/(h_if+Cp_w*(T_tank-T_frz))
      dTdO = (Q_net-Q_ice)/(m_w*Cv_w)
      T_tank = T_temp + dO*dTdO
      call dia(D_crit,D_o_temp,D_o_tube,dm_w,L_tube,m_w,
     &        N_tube,rho_w)
      end if
      end if

      ddm = abs(dm_w-Old_dm)
      if (m_w .lt. m_w_crit) then
        TT = 0.
      else
        TT = abs(T_tank-Old_T)
      end if
      Tb = (mf_tank*T_bo+(mf_tot-mf_tank)*T_bi)/mf_tot
      T_b_diff = abs(Tb-T_des)
      if ((ddm .gt. tol) .or. (TT .gt. .01) .or. (T_b_diff
     &    .gt. 0.01)) then
        Old_dm = dm_w
        Old_T = T_tank
        fract = (T_bi-T_des)/(T_bi-Tb)
        mf_tank = mf_tank*fract
        mf_tube = mf_tank/N_tube
        v = mf_tube/(rho_b*Acs_tube)
        step = step+1
        if (step .eq. 1000) then
          print*,'Enter guess value'
          print*,K_crit,Capacity/Cap_nom,mf_tank/mf_tot
      read*,x
          mf_tank = x*mf_tot
        mf_tube = mf_tank/N_tube
        v = mf_tube/(rho_b*Acs_tube)
          step = 0
        end if
        goto 100
      else
110   m_w = m_w+dm_w
      D_o = D_o_temp
      Thick = (D_o - D_o_tube)/2
      T_temp = T_tank
      step = 0
      if (mf_tank/mf_tot .gt. 1.) goto 200
      end if
```

```fortran
      Capacity = Capacity+Q_net*dO/12000.
      dTT = dTT+(Tb-T_bi)*dO
      write(9,111)time,T_tank,mf_tank*70./36455.5,mf_tank/mf_tot,
     &         Capacity/Cap_nom,m_w/m_w_tot*0.85
      write(11,111)time,T_tank,T_bi,T_bo,dT_lm
      if ((time+0.8*dO .gt. stp_hr) .and. (time-dO .lt. stp_hr)) then
        print*
        print*,time,Capacity/Cap_nom,mf_tank/mf_tot
      if (nhdstep .eq. nhd) goto 200
        print*
        print*,'Enter the average entering brine Temperature [F]:'
        read*,T_bi
        print*,'Enter the desired blended outlet temperature [F]:'
        read*,T_des
        print*,'Enter mode:  1 = Q_des. 2 = GPM'
        read*,mode
        if (mode .eq. 1) then
      print*,'Enter the desired discharge rate [tons]:'
      read*,Q_des
      Flow = 25.5*Q_des/(T_bi-T_des)
        else
      print*,'Enter the system flow rate [GPM]:'
        read*,Flow
        end if
      mf_tot = 36455.5*Flow/70.            !c [lbm/hr] about 70 GPM
        stp_hr = stp_hr+1.
      nhdstep = nhdstep + 1
        end if
        time = time + dO
    dT = Ts_avg-T_tank
  end do

 111 format(1x,f7.4,5f15.5)
 112 format(1x,f7.4,3e15.5,f15.5)
 200 write(*,1000)time,dTT/time,Capacity/time,Capacity/Cap_nom
1000 format(1x,4F15.4)
    STOP
    end

    subroutine dia(D_crit,D_o_temp,D_o_tube,dm_i,L_tube,m_i,
   &         N_tube,rho_i)

    implicit none

    real*8 D_crit,D_o_temp,D_o_tube,dm_i,L_tube,m_i,rho_i
    real*8 dMdD,f,M,mass,pi,tol
    integer i,N,N_tube

    parameter (pi = 3.14159)
```

```fortran
      mass = (m_i+dm_i)/N_tube
      tol = 1.E-8
      N = 50

      do 10, i = 1,N
      M = rho_i*(D_crit*L_tube*(D_o_temp**2-
     &    D_crit**2)**0.5 + (pi/4.-acos(D_crit/D_o_temp))*
     &    L_tube*D_o_temp**2 - pi*D_o_tube**2*L_tube/4.)
      dMdD = rho_i*(pi*D_o_temp*L_tube/2. -
     &    2*D_o_temp*L_tube*acos(D_crit/D_o_temp))
      f = D_o_temp - (M-mass)/dMdD
      if ((f-D_o_temp) .lt. tol) then
          return
      else
          D_o_temp = f
      end if
10    continue
      write(7,*)'Method failed after 50 iterations!'
      stop
      end
```

Appendix C

TRNSYS deck for parametric study of the variable flow system

```
*This deck runs a conventional system and varies the fraction
*of flow through the coil to find the minimum power point.
*1 - 2 - 1991
*
NOLIST
SIMULATION 0 17 1
TOLERANCE 0.00001 0.00001
WIDTH 132
************************
EQUATIONS 18
* Outside dry bulb temperature [F] and relative humidity [%]
    TDBOUT = 91
    RHOUT = 45
* Space dry bulb temperature [F] and relative humidity [%]
    TDBROOM = 72
    RHROOM = 50
* Fractions of return and ventilation flow rates
    FRN_RET = 0.85
    FRN_VENT = 0.15
* Determine the mass flow rates of return and ventilation
    MF_CIRC = 8000.*60.*[2,5]
    MF_RTT = FRN_RET*MF_CIRC
    MF_VENT = FRN_VENT*MF_CIRC
* Bypass fraction and mass flow rates
    X = [40,1]
    MF_BP = (1.-X)*MF_CIRC
    MF_RET = MF_RTT-MF_BP
* Building Load
    SHR = 0.7
    Q_TOT = 100000.
    Q_SENS = Q_TOT*SHR
    Q_LAT = Q_TOT*(1.-SHR)
    Q_REHE = [5,3]*0.24*([45,1]-[5,1])
    Q_ACT = [4,8]+[4,9]
************************
UNIT 45 TYPE 15 Algebraic operation to determine T_sup
************************
PARAMETERS 8
0 0 2 0 2 7 0 3
INPUTS 4
```

```
Q_SENS MF_CIRC 0,0 TDBROOM
8.E4   35000.  0.24  72.
*************************
UNIT 1 TYPE 33 Psychrometric properties of outside air
*************************
PARAMETERS 5
* Mode I_units P_atm WBmode Emode
   2    2   1.0  1    2
INPUTS 2
* T_db   RH
  0,0    0,0
  TDBOUT  RHOUT
*OUTPUTS
*  1   2   3   4   5   6
*  w  Twb   h  rmix rair Status
*************************
UNIT 2 TYPE 33 Psychrometric properties of space set-point
*************************
PARAMETERS 5
* Mode I_units P_atm WBmode Emode
   2    2   1.0  1    2
INPUTS 2
*  T_db   RH
   0,0    0,0
  TDBROOM  RHROOM
*OUTPUTS
*  1   2   3   4   5   6
*  w  Twb   h  rmix rair Status
*************************
UNIT 40 TYPE 14  Fraction of flow through coil
*************************
PARAMETERS 68
  0 1.00  1 1.00  1 0.95  2 0.95  2 0.90  3 0.90  3 0.85
  4 0.85  4 0.80  5 0.80  5 0.75  6 0.75  6 0.70  7 0.70
  7 0.65  8 0.65  8 0.60  9 0.60  9 0.55 10 0.55 10 0.50
 11 0.50 11 0.45 12 0.45 12 0.40 13 0.40 13 0.35 14 0.35
 14 0.30 15 0.30 15 0.25 16 0.25 16 0.20 17 0.20
*************************
UNIT 3 TYPE 11 Mixing box for return and fresh air
*************************
PARAMETERS 1
* Mode
  6
INPUTS 6
* Tdb_out w_out mf_vent Tdb_ret w_ret mf_ret
   0,0   1,1  MF_VENT  0,0   2,1  MF_RET
   TDBOUT 0.01  5.E3   TDBROOM 0.01  2.2E4
*OUTPUTS
*  1   2   3
```

```
*  To   wo   mfo
*************************
UNIT 4 TYPE 7 A/C coil
*************************
PARAMETERS 7
* AC2on CAPrat EIRrat BFrat CFMrat  Tset   wset
   0   287000. 3.024 0.18   11000.  TDBROOM 0.00834
INPUTS 9
* Tdb_in  w_in  mf_in  T_cond  T_ret  w_ret  mf_2  Q_sens  Q_lat
  3,1   3,2   3,3   0,0    0,0  2,1   0,0  Q_SENS  Q_LAT
  76.5 0.011 2.8E4  TDBOUT TDBROOM 0.01  0.    6.E4   4.E4
*OUTPUTS
*  1   2   3   4   5   6   7   8   9   10   11
*  To   wo   mf  Power Qs   Ql   plr   Qs   Ql   Texon  ac1on
*************************
UNIT 5 TYPE 11 Mixing box for A/C outlet and bypass
*************************
PARAMETERS 1
6
INPUTS 6
* Tdb_aco  w_aco  mf_ac   Tdb_ret  w_ret  mf_bp
  4,1   4,2   3,3    0,0    2,1   MF_BP
  50.   0.001  2.8E4   TDBROOM 0.01   0.
*OUTPUTS
*  1   2   3
*  To   wo   mfo
*************************
UNIT 6 TYPE 33 Psychrometric properties of coil+bypass output
*************************
PARAMETERS 5
* Mode I_units P_atm WBmode Emode
   4    2   1.0   1    2
INPUTS 2
*  T_db    w
   5,1    5,2
   60.   0.001
*OUTPUTS
*  1   2   3   4   5   6
* RH   Twb   h  rmix rair Status
*************************
UNIT 10 TYPE 28 Printer for power, etc.
*************************
PARAMETERS 21
1 0 17 10 2  0 -4 0 -4 0 -4 0 -4 0 -4 0 -4 0 -4 0 -4
INPUTS 8
X  4,1   4,4  Q_REHE  Q_TOT   Q_ACT 4,7  SHR
LABELS 8
X TACO POWER QREHEA LOAD QACTOT PLR SHR
END
```

Appendix D

Variable flow controller for air-conditoning load reduction

```
      subroutine TYPE18(time,xin,out,t,dtdt,par,info)
c**********************************************************
c*                                                        *
c*      This TRNSYS type is a flow controller that calculates the   *
c*  percentage of flow that should pass through the A/C coil in      *
c*  order to minimize the sensible reheat in the system.  The A/C    *
c*  coil outlet temperature is constrained to above 38 F so that     *
c*  frosting of the coil is not encountered.                         *
c*                                                        *
c*                              ---Todd B. Jekel  12-4-90  *
c*                                                        *
c*      PARAMETERS 2                                       *
c*                  Mode                                   *
c*                  1     Optimal controller               *
c*                        Convergence tolerance            *
c*                  2     Set A/C temperature              *
c*                        Temperature                      *
c*                                                        *
c*      INPUTS 7                                           *
c*                  Load [Btu/hr]                          *
c*                  SHR [sensible load/total load]         *
c*                  mf_tot [lbm/hr]                        *
c*                  T_set [F]                              *
c*                  w_set [lbm H2O/lbm air]                *
c*                  h_set [Btu/lbm]                        *
c*                  fm_vent [mf_vent/mf_tot]               *
c*                                                        *
c*      OUTPUTS 1                                          *
c*                  x [mf_ac/mf_tot]                       *
c*                  T_sat [F]                              *
c*                                                        *
c**********************************************************

      implicit none

      real dh_load          !c Total enthalpy change of the
c                              load [Btu/lbm]
      real dwdT_s           !c Derivative of saturation
c                              humidity ratio wrt saturation
c                              temperature
```

```
      real  f                          !c  New estimate of T_sat as given
c                                           by Newtons method
      real  frn_vent                   !c  Fraction of ventilation mass flow
      real  h_s                        !c  Curve fit for saturation enthalpy
      real  Load                       !c  Total load on space [Btu/hr]
      real  mode                       !c  Set A/C temperature or optimum
      real  mf_tot                     !c  Total mass flow rate of
c                                           air through system [lbm/hr]
      real  SHR                        !c  Sensible Heat Ratio of
c                                           space load
      real  T_aco                      !c  Desired outlet A/C coil temp.
      real  T_sat,w_sat,h_sat          !c  Saturation temperature,
c                                           humidity ratio, and
c                                           enthalpy (assumed A/C
.c                                          outlet state
      real  T_set,w_set,h_set          !c  Set-point temperature,
c                                           humidity ratio, and
c                                           enthalpy
      real  tol                        !c  Convergence tolerance
      real  x1                         !c  Fraction of flow that meets the
c                                           sensible portion in mode 2
      real  x2                         !c  Fraction of flow that meets the
c                                           latent portion in mode 2
      real  x                          !c  Fraction of total mass
c                                           flow of system that should
c                                           flow through the A/C coil
      real  w_s                        !c  Curve fit for saturation
c                                           humidity ratio as a function
c                                           of saturation temperature

c NOTE:  Time has no effect on the output of this controller, only the
c        inputs effect the outputs.

      real time,xin,out,t,dtdt,par
      integer info
      dimension xin(7),out(2),info(10),par(2)

c -----Curve fits for saturation humidity ratio, enthalpy, and the
c derivative of saturation humidity ratio wrt saturation temperature

      w_s(T_sat) = 1.E-4*(1.2626+1.1614*T_sat-1.393E-2*T_sat**2+
     &            4.1348E-4*T_sat**3)

      dwdT_s(T_sat) = 1.E-4*(1.1614-2.*1.393E-2*T_sat+3.*4.1348E-4*
     &               T_sat**2)

      h_s(T_sat) = -2.8065+0.55408*T_sat-0.00549*T_sat**2+7.28738E-5*
     &               T_sat**3
```

```
c  Set TRNSYS inputs to subroutine nomenclature

      mode = nint(par(1))
      if (par(1) .eq. 1) then
          tol = par(2)
      else
          T_aco = par(2)
      end if
      Load = xin(1)
      SHR = xin(2)
      mf_tot = xin(3)
      T_set = xin(4)
      w_set = xin(5)
      h_set = xin(6)
      frn_vent = xin(7)

c  On first call to type do usual TRNSYS checking

      if (info(7) .eq. -1) then
          call typeck(1,info,7,2,0)
          info(6) = 2                      !c  two output
          info(9) = 0                      !c  output depends only on
c                                              inputs, not time
      end if

c  Determine the "length" of the load line

      dh_load = Load/mf_tot

c  Initial guess for saturated state (assumed A/C outlet state)

      T_sat = 50.
      w_sat = w_s(T_sat)

      if (par(1) .eq. 1) then

100   f = T_sat-(1./SHR-1.-1061.*(w_set-w_sat)/(0.24*(T_set-T_sat)))/
    &     (-1061.*(-dwdT_s(T_sat)*(T_set-T_sat)+(w_set-w_sat))/(0.24*
    &     (T_set-T_sat)**2))
          if (abs(f-T_sat) .gt. tol) then
            T_sat = f
            w_sat = w_s(T_sat)
            goto 100
          else

c  Due to defrost constraints the exiting temperature from the A/C
c  should not be less than 38 F.

          if (T_sat .lt. 38.) then
```

```
            T_sat = 38.
            w_sat = w_s(T_sat)

c Determine the fraction through the A/C coil such that the latent
c portion of the load is met.  The sensible portion will be more than
c met and reheat will be needed in order to keep the space at the
c desired set-point.

            x = ((1.-SHR)*dh_load/1061.)/(w_set-w_sat)
          else
            h_sat = h_s(T_sat)

c Determine the fraction through the A/C coil such that both the
c latent and sensible load are exactly met.  No reheat is required;
c therefore, the A/C coil load is minimized.

            x = dh_load/(h_set-h_sat)
          end if
      end if
    else
      T_sat = T_aco
          x1 = (SHR*dh_load/0.24)/(T_set-T_sat)
          w_sat = w_s(T_sat)
          x2 = ((1.-SHR)*dh_load/1061.)/(w_set-w_sat)
          x = max(x1,x2)
    end if

    if (x .gt. 1.) then
        x = 1.
    end if
    if (x .lt. frn_vent) then
        x = frn_vent
    end if

c Set the fraction, x, to the TRNSYS output variable

    out(1) = x
    out(2) = T_sat
    return
    end
```

Bibliography

ASHRAE Handbook, Fundamentals Volume, American Society of Heating, Refrigerating and Air-Condioning Engineers, Incorporated, Atlanta, Georgia, 1985.

Braun, J. E., "Methodologies for the Design and Control of Central Cooling Plants," Ph.D. Thesis, University of Wisconsin - Madison, 1988.

Calmac Manufacturing Corporation, *Levload Ice Bank Performance Manual*, Product Literature, Calmac Manufacturing Corporation, Englewood, New Jersey, April 1987.

Calmac Manufacturing Corporation, *Levload OPAC Cool Storage Selection Program*, Calmac Manufacturing Corporation, Englewood, New Jersey, 1990.

Cummings, M. S., "Modeling, Design, and Control of Partial Ice-Storage Air-Conditioning Systems," M.S.. Thesis, University of Wisconsin--Madison, 1989.

Duffie, J. A., and W. A. Beckman, *Solar Engineering of Thermal Processes*, John Wiley & Sons, New York, 1980.

Incropera, F. P., and D. P. DeWitt, *Introduction to Heat Transfer*, John Wiley & Sons, New York, 1985.

Klein S. A., et al., *TRNSYS: A Transient Simulation Program*, University of Wisconsin - Madison, Engineering Experiment Station Report 38-12, Version 13.1, 1988.

Klein S. A., et al., *TRNSYS User's Manual*, University of Wisconsin - Madison, Engineering Experiment Station Report 38-12, 1988.

Klein, S. A., W. A. Beckman, and G. E. Myers, *FEHT Finite Element Heat Transfer Program*, F-Chart Software, Middleton, Wisconsin, Version 5.49, 1991.

Mitchell, J. W., *Energy Engineering*, John Wiley & Sons, New York, 1983.

Stoecker, W. F., and J. W. Jones, *Refrigeration and Air Conditioning*, Second Edition, Mac-Graw Hill Book Company, New York, 1982.

Urban, R. E., "The Performance of Conventional and Humid-Climate Vapor-Compression Supermarket Air-Conditioning Systems," M.S. Thesis, University of Wisconsin - Madison, 1988.